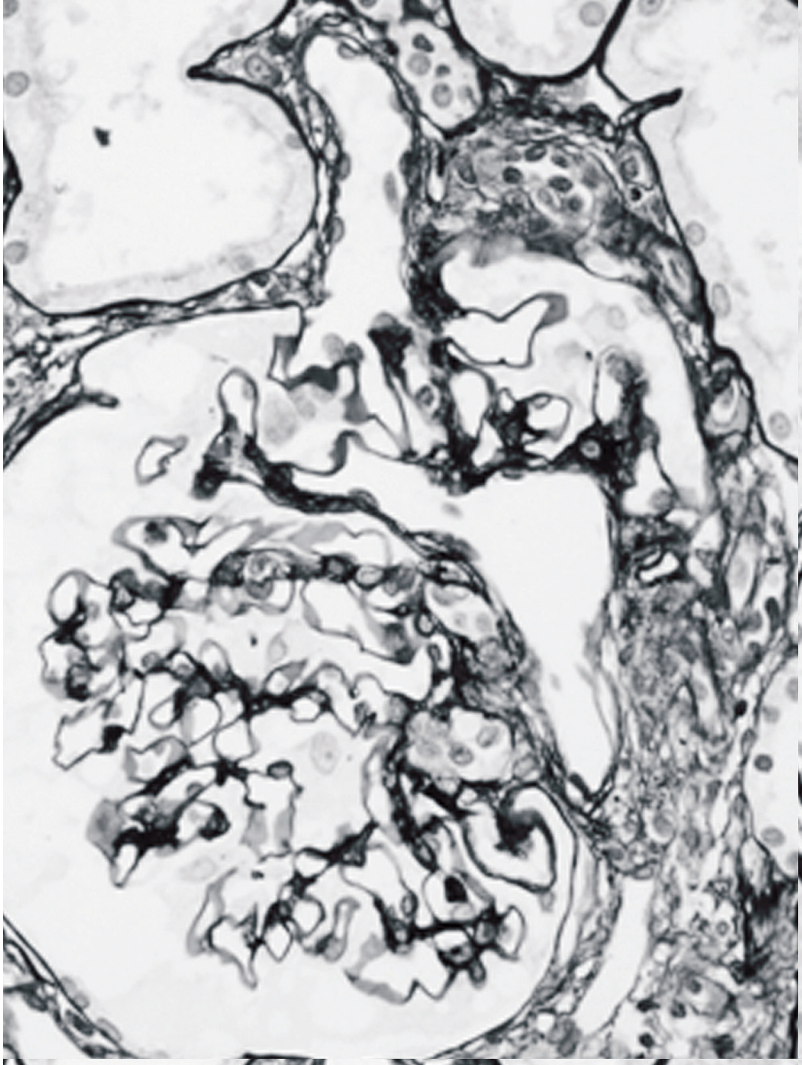

JPTM

Journal of Pathology and Translational Medicine

May 2016
Vol. 50 / No. 3
jpatholtm.org
pISSN: 2383-7837
eISSN: 2383-7845

Pathologic Evaluation of Breast Cancer after Neoadjuvant Therapy

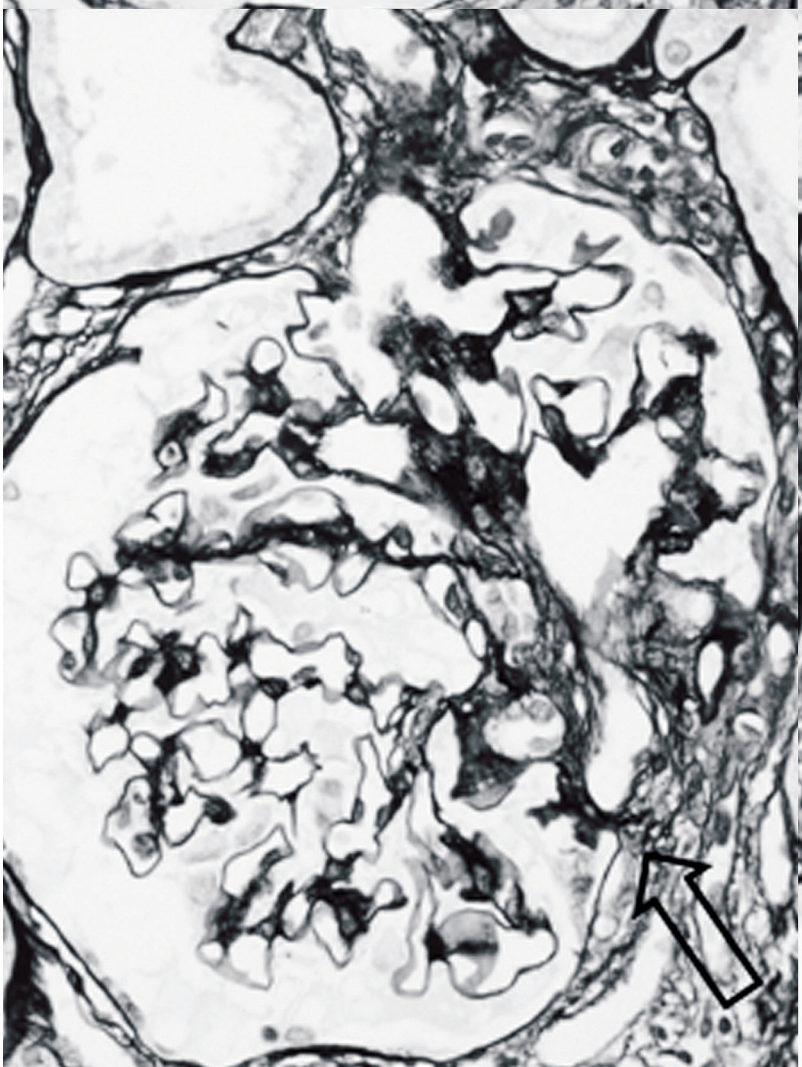

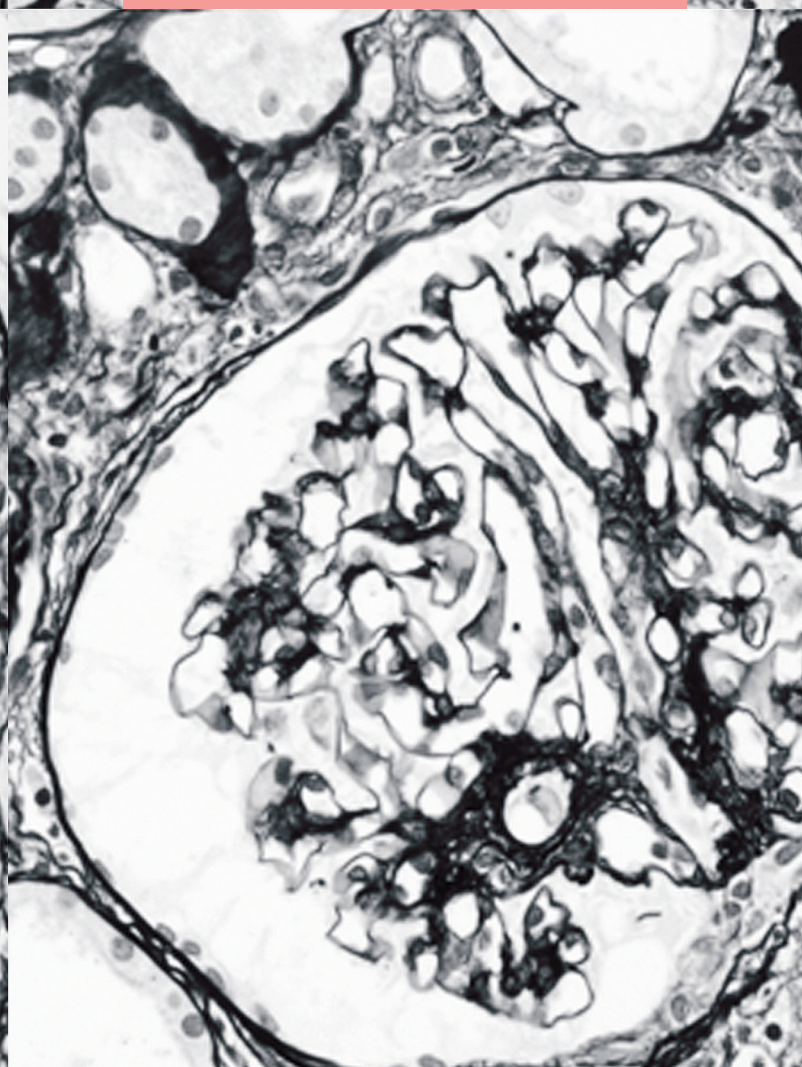

Journal of Pathology and Translational Medicine

Vol. 50, No. 3, pp 173-249, May 2016

Journal of Pathology and Translational Medicine

Volume 50 • Number 3 • May 2016 (bimonthly)
Published since 1967
Printed on 11 May 2016 Published on 15 May 2016

J Pathol Transl Med
pISSN: 2383-7837
eISSN: 2383-7845

Aims & Scope

The Journal of Pathology and Translational Medicine is an open venue for the rapid publication of major achievements in various fields of pathology, cytopathology, and biomedical and translational research. The Journal aims to share new insights into the molecular and cellular mechanisms of human diseases and to report major advances in both experimental and clinical medicine, with a particular emphasis on translational research. The investigations of human cells and tissues using high-dimensional biology techniques such as genomics and proteomics will be given a high priority. Articles on stem cell biology are also welcome. The categories of manuscript include original articles, review and perspective articles, case studies, brief case reports, and letters to the editor.

Subscription Information

To subscribe to this journal, please contact the Korean Society of Pathologists/the Korean Society for Cytopathology. Full text PDF files are also available at the official website (http://jpatholtm.org). *Journal of Pathology and Translational Medicine* is indexed by PubMed, PubMed Central, Scopus, KoreaMed, KoMCI, WRPIM and CrossRef. Circulation number per issue is 700.

Contact the Korean Society of Pathologists/the Korean Society for Cytopathology

Publishers: Min Cheol Lee, MD, So Young Jin, MD
Editors-in-Chief: Soon Won Hong, MD, Chong Jai Kim, MD
Published by the Korean Society of Pathologists/the Korean Society for Cytopathology

Editorial Office
Room 1209 Gwanghwamun Officia, 92 Saemunan-ro, Jongno-gu,
Seoul 03186, Korea/#406 Lilla Swami Bldg, 68 Dongsan-ro,
Seocho-gu, Seoul 06784, Korea
Tel: +82-2-795-3094/+82-2-593-6943
Fax: +82-2-790-6635/+82-2-593-6944
E-mail: office@jpatholtm.org

Printed by ML communications Co., Ltd.
Jungang Bldg. 18-8 Wonhyo-ro 89-gil, Yongsan-gu, Seoul 04314, Korea
Tel: +82-2-717-5511 Fax: +82-2-717-5515 E-mail: ml@smileml.com

Manuscript Editing by InfoLumi Co.
210-202, 421 Pangyo-ro, Bundang-gu, Seongnam 13522, Korea
Tel: +82-70-8839-8800 E-mail: infolumi.chang@gmail.com

Front cover image: Glomerulus showing extra-efferent vessel formation in focal segmental glomerulosclerosis-like IgA nephropathy (Fig. 1A). p213.

This journal was supported by the Korean Federation of Science and Technology Societies Grant funded by the Korean Government.

Journal of Pathology and Translational Medicine

J Pathol Transl Med
pISSN: 2383-7837
eISSN: 2383-7845

Volume 50, Number 3, May 2016

CONTENTS

REVIEW

ORIGINAL ARTICLES

CONTENTS CONTINUED

CASE REPORTS

Instructions for Authors for *Journal of Pathology and Translational Medicine* are available at http://jpatholtm.org/authors/authors.php

Journal of Pathology and Translational Medicine 2016; 50: 173-180
http://dx.doi.org/10.4132/jptm.2016.02.02

■ REVIEW ■

Pathologic Evaluation of Breast Cancer after Neoadjuvant Therapy

Cheol Keun Park · Woo-Hee Jung
Ja Seung Koo

Department of Pathology, Yonsei University College of Medicine, Seoul, Korea

Received: January 5, 2016
Revised: February 1, 2016
Accepted: February 2, 2016

Corresponding Author
Ja Seung Koo, MD
Department of Pathology, Severance Hospital, Yonsei University College of Medicine, 50-1 Yonsei-ro, Seodaemun-gu, Seoul 03722, Korea
Tel: +82-2-2228-1772
Fax: +82-2-362-0860
E-mail: kjs1976@yuhs.ac

Breast cancer, one of the most common cancers in women, has various treatment modalities. Neoadjuvant therapy (NAT) has been used in many clinical trials because it is easy to evaluate the treatment response to therapeutic agents in a short time period; consequently, NAT is currently a standard treatment modality for large-sized and locally advanced breast cancers, and its use in early-stage breast cancer is becoming more common. Thus, chances to encounter breast tissue from patients treated with NAT is increasing. However, systems for handling and evaluating such specimens have not been established. Several evaluation systems emphasize a multidisciplinary approach to increase the accuracy of breast cancer assessment. Thus, detailed and systematic evaluation of clinical, radiologic, and pathologic findings is important. In this review, we compare the major problems of each evaluation system and discuss important points for handling and evaluating NAT-treated breast specimens.

Key Words: Breast neoplasms; Neoadjuvant therapy; Pathologic response evaluation

Application of neoadjuvant therapy (NAT) has become a more common breast cancer treatment due to the diversity and rapid development of associated therapeutic agents. NAT is currently established as a standard therapeutic approach for patients with large (> 2 cm) and locally advanced breast cancer.[1] In addition, trials for NAT use in early-stage breast cancer are gradually increasing.[2] Although there is no gain in survival benefit from NAT for breast cancer, it does offer several significant advantages over other modalities: (1) Response efficiency to a new therapeutic agent can be assessed[3-5] because it is easy to detect a treatment response in a relatively short time period. In this respect, many clinical trials have been designed to evaluate NAT.[6] (2) Patients with large cancers who show a response to NAT can undergo breast-conservation surgery.[7,8] (3) The degree of response to NAT can play a role as a prognostic factor; one study reported that the rate of local recurrence depends on the extent of residual tumor after NAT.[9] Given the potential benefits, exact assessment of breast specimens after NAT is very important. However, standard guidelines for pathologic evaluation of breast specimens after NAT have not been established.[9-14] Herein, we offer a concise review of the various standard guidelines for pathologic assessment of breast cancer specimens after NAT.

EVALUATION OF BREAST CANCER SPECIMENS AFTER NEOADJUVANT THERAPY

Specimen handling

Identification of the tumor bed is important for the handling of breast specimens after NAT. Close examination of fresh specimens cut into 5-mm sections or smaller is required for identification of the tumor bed. However, some cases require extensive sampling because of uncertainty in the gross identification of tumor bed. There have been attempts to insert metallic clips while conducting breast core biopsy for easy recognition of the tumor bed.[15-18] However, this method cannot locate the tumor bed accurately because the inserted metallic clip shifts over time.[19] Some guidelines suggest that small specimens (< 5 cm at the widest diameter or < 30 g) should be thinly sectioned and submitted in their entirety so that the specimens can be reintegrated upon histologic evaluation. However, these methods have limitations in that samples for research use cannot be secured.[20] It is crucial to select representative sections when dealing with large specimens, such as those from a large lumpectomy or mastectomy. The important goal in specimen selection is to identify the area that correlates best with clinical and radiologic findings. This area, which is known as the pretreatment area, should com-

pISSN 2383-7837
eISSN 2383-7845

prise grossly identifiable tumor bed, a metallic clip, and peritumoral tissue.[20] After slicing surgical specimens into ≤5-mm sections, the cross-section that includes the largest pretreatment area should be selected for sampling. The extent of tissue sampling varies according to guidelines: one or two tissue blocks from every 1 cm of pretreatment tumor[13,20] or 10 blocks at least from an entire specimen.[4] Because histologic patterns of residual post-NAT breast cancer tumors are diverse, different sampling methods can yield different evaluation results (Fig. 1), potentially resulting in sampling error. Even so, submission of large surgical samples in their entirety is not recommended because it is inefficient and offers little information despite the intensive sampling effort required.[21] Thus, the extent of tissue sampling should be optimized and determined on a case-by-case basis considering clinical, macroscopic, and radiologic features. However, it is important, when creating sample specimens, to provide annotations and photographs of each tissue block to clarify the origin of tissue sections; this enables the pathologists conducting evaluations to identify correlations between macroscopic and histologic features.[20,21] Also, exact descriptions, including the size of any grossly visible tumor beds and distances from resection margins, should be recorded.

Microscopic pathologic report

Pathologic variables that describe surgical breast cancer specimens that were not exposed to NAT are also important for post-NAT specimen. However, several factors should be taken into account, due to the diversity of evaluation systems for post-NAT breast cancer, including differences in major variables of each evaluation system and histologic factors causing post-NAT changes (Table 1). A summary of the pathologic reports for breast cancer after NAT is provided in Table 2.

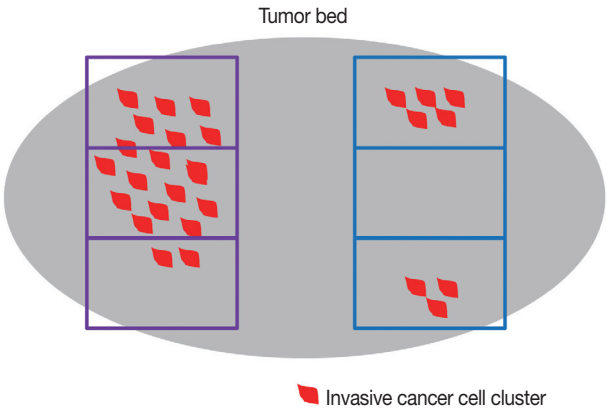

Fig. 1. Differences in tumor evaluation results according to tissue sampling method in breast cancer after neoadjuvant therapy. In this example, when sampling in the area indicated by the blue rectangle, aspects of the residual tumor (e.g., tumor size/extent) are observed and appear different from the sampling area indicated by the purple rectangle, where heterogeneity of the residual tumor and tumor bed is present.

Histologic tumor subtype and grade

In principle, the method to evaluate histologic subtype and tumor grade in breast cancer patients who received NAT is the same as that used for patients with non-neoadjuvant cancer. However, it is necessary to consider that NAT can affect histologic architecture, nuclear features, and tumor mitosis.[5,22-24] Thus, some cases require comparison with pretreatment biopsy findings.

Tumor size and extent

There are many potential variables that can be used for assessing tumor size/extent in breast cancer patients who received NAT. Variable relevance depends on which tumor-response evaluation system is being used, because each system offers a different definition of significant tumor size. For example, the largest contiguous focus of the invasive cancer is the most important factor in determining ypT stage in ypTNM system.[10] Contrarily, the two dimensions of the largest residual area of remaining invasive cancer are most important according to the Residual Cancer Burden (RCB) system.[14] For the RCB system, however, the residual invasive cancer does not need to be contiguous, leading to a discrepancy in perceived tumor size between the two systems.[14] The largest discrepancies in tumor size/extent due to the differences in measurement methods were observed when the tissue response pattern after NAT manifested as a scattered pattern (Fig. 2).

Tumor cellularity

Though NAT can affect several parameters of breast cancer, tumor cellularity is one of the most representative factors.[25] Tumor cellularity is not always recorded in pathologic reports because it is important in some tumor-response systems[11,13,14] but not in others.[10,12,26] There are several factors that should always be considered when evaluating tumor cellularity. The first factor is the comparison of cellularity in pre- and post-treatment specimens (Fig. 3). Differences between pre- and post-treatment cellularity are important for some tumor-response systems;[11] however, pretreatment cellularity is not considered in the RCB system.[14] The second factor is tumor heterogeneity. Because residual tumor cellularity can appear heterogeneous after NAT, extensive tissue sampling should be performed. However, the majority of systems do not specifically include the cellularity of

http://dx.doi.org/10.4132/jptm.2016.02.02

Table 1. Comparison of pathologic response evaluation system for breast cancer after neoadjuvant therapy

System	Included variable	Definition of pCR	Category status	Reference
AJCC (y)	Size of invasive carcinoma	No invasive carcinoma in breast and lymph node	Stage 0	Boughey *et al.*[8]
	Lymph nose status (the number of metastatic lymph node and size of metastatic deposit)		Stage 1	
			Stage 2	
			Stage 3	
B-18	Treatment effect in invasive carcinoma	No invasive carcinoma in breast and lymph node	No pathologic response	Diaz *et al.*[24]
	Lymph nose status (the number of metastatic lymph node and size of metastatic deposit)		Pathologic partial response	
			Pathologic complete response	
Miller-Payne	Presence of invasive carcinoma	No invasive carcinoma in breast	Grade 1: no change or some minor alteration in individual malignant cells, but no reduction in overall cellularity	Mamounas *et al.*[9]
	Tumor cellularity		Grade 2: a minor loss of tumor cells, but overall high cellularity; up to 30% reduction of cellularity	
			Grade 3: between an estimated 30% and 90% reduction in tumor cellularity	
			Grade 4: a marked disappearance of more than 90% of tumor cells such that only small clusters or widely dispersed individual cells remain	
			Grade 5: no invasive malignant cells identifiable in sections from the site of the tumor	
MNPI	Size of invasive carcinoma	No invasive carcinoma in breast and lymph node	MNPI=0.2×tumor size+lymph node stage+MSBR grade	Carey *et al.*[10]
	Tumor grade		Lymph node state: 1, node negative; 2, 1-3 positive; 3, ≥4 positive	
	Lymph nose status (the number of metastatic lymph node)			
Pinder	Tumor proportion (%) in remaining breast	No invasive carcinoma in breast and lymph node	Complete pathologic response	Ogston *et al.*[11]
	Lymph nose status (presence of evidence of response)		Partial response to therapy	
			<10% of tumor remaining	
			10%–50% of tumor remaining	
			>50% of tumor remaining	
			No evidence of response	
RCB	Size of tumor bed in two dimension	No invasive carcinoma in breast and lymph node	RCB 0: no residual disease	Abrial *et al.*[12]
	Tumor cellularity		RCB 1: minimal residual disease	
	Lymph node status (the number of metastatic lymph node and size of metastatic deposit)		RCB 2: moderate residual disease	
			RCB 3: extensive residual disease	

pCR, pathologic complete response; AJCC, American Joint Committee on Cancer; MNPI, Modified scores from Nottingham Prognostic Index; MSBR grade, Modified Scarff Bloom Richardson grade; RCB, residual cancer burden.

residual heterogeneous tumors, except for the RCB system, which recommends mentioning the average tumor cellularity.[14]

Lymphovascular invasion

Lymphovascular invasion (LVI) is documented in most pathologic reports because it is a significant prognostic factor in non-neoadjuvant breast cancer.[27,28] Though there are insufficient data on whether LVI is independently significant in neoadjuvant specimens, it should still be mentioned in pathologic reports.[20] Ductal carcinoma *in situ* (DCIS) and LVI are defined as resistant breast cancer components after NAT.[22] Therefore, in some situations, the only residual after NAT is tumor emboli in lymphovascular space, with no residual tumor in the breast parenchyma (Fig. 4).[29] According to these guidelines, researchers have recommended that such cases not be regarded as pathologic complete response (pCR).[20] Consequently, several LVI measurement methods have

Table 2. Example of pathologic report form in breast cancer after neoadjuvant therapy

Pathologic report form
Gross finding
Residual identified tumor: yes/no
Quadrant of tumor
Multifocality: yes/no
Size of residual tumor: xx mm
Identified clip of marker: yes/no
Microscopic finding
Histologic diagnosis: invasive carcinoma, NST
Histologic grade: I/II/III (tubule score–nuclear grade–mitosis score)
Size of residual tumor bed: x mm
Size of the largest residual invasive carcinoma: x mm
Residual tumor cellularity: %
Lymphovascular invasion: absent/present
DCIS component: yes/no
Total tumor size including DCIS: x mm
Extensive intraductal component: yes/no
Type: cribriform/micropapillary/solid/papillary
Nuclear grade: low/intermediate/high
Necrosis: absent/present (focal/commedo)
ER/PR/HER-2 status: optional
Resection margin
Invasive carcinoma: absent/present; distance to the closest margin
DCIS: absent/present; distance to the closest margin
Tumor bed: absent/present
Lymph node status
Number of sentinel lymph nodes
Number of total axillary lymph nodes
Number of lymph nodes with macrometastasis
Size of largest metastasis: mm
Number of lymph nodes with micrometastasis
Number of lymph nodes with isolated tumor cells
Number of lymph nodes with histologic evidence of treatment response but no tumor cells
Extracapsular extension: yes/no

NST, no specific type; DCIS, ductal carcinoma *in situ*; ER, estrogen receptor; PR, progesterone receptor; HER-2, human epidermal growth factor receptor-2.

been suggested, including measurement according to size[20] or using semi-quantitative methods (focal or extensive).[30]

Surgical margins

Evaluation of resection margins is identical to that for non-neoadjuvant breast cancer specimens. Careful examination is required for evaluation of resection margins in neoadjuvant specimens because grossly invisible residual tumors or multiple scattered microscopic tumor foci are common. Furthermore, when the resection margin involves the tumor bed, it should be documented in the pathological report.

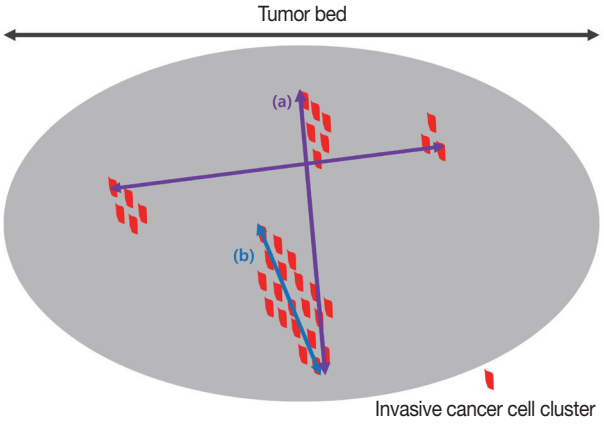

Fig. 2. Comparison of tumor size/extent measurements between the Residual Cancer Burden (RCB) and ypTNM systems. In the RCB system, the largest cross-section among areas with invasive tumors is measured in two dimensions (a). In the ypTNM system, the largest contiguous invasive carcinoma foci are measured (b).

Evaluation of the axillary lymph node after NAT

The evaluation method for axillary lymph nodes is the same as that for non-neoadjuvant cases. Generally, all lymph nodes are sectioned into 2-mm intervals and sampled in their entirety for microscopic evaluation. Sometimes lymph nodes with complete treatment response are observed under microscopic evaluation for characteristic features, such as fibrous scarring, lymphocytic depletion, or histiocytic aggregation, without any identifiable tumor cell clusters (Fig. 5). If lymph nodes with these features are identified during microscopic evaluation, the total number observed should be noted in the pathologic report.[31] When metastatic deposits are observed, the size of the largest metastatic tumor and presence/absence of extranodal extension should be recorded. It is difficult to measure the size of the largest metastatic tumor when the treatment response is accompanied by metastasis. In cases with multiple singly scattered tumor cells that involve the entire lymph node and when the treatment response is not accompanied by fibrosis, the size of the metastatic tumor is determined by measuring the size of the largest cell cluster. Some guidelines recommend measuring the sizes of the tumor cells and intervening stroma—not the largest cell cluster—when accompanied by a tumor response; consensus for these measurements has not been established among the various evaluation systems.[20] Thus, when metastatic deposits are observed during microscopic evaluation, conditions such as macrometastasis, micrometastasis, and isolated tumor cells can be altered by changes in the sizes of metastatic deposits according to applied systems. However, residual disease in the lymph nodes are not considered pCR in most systems.[10,20]

http://dx.doi.org/10.4132/jptm.2016.02.02

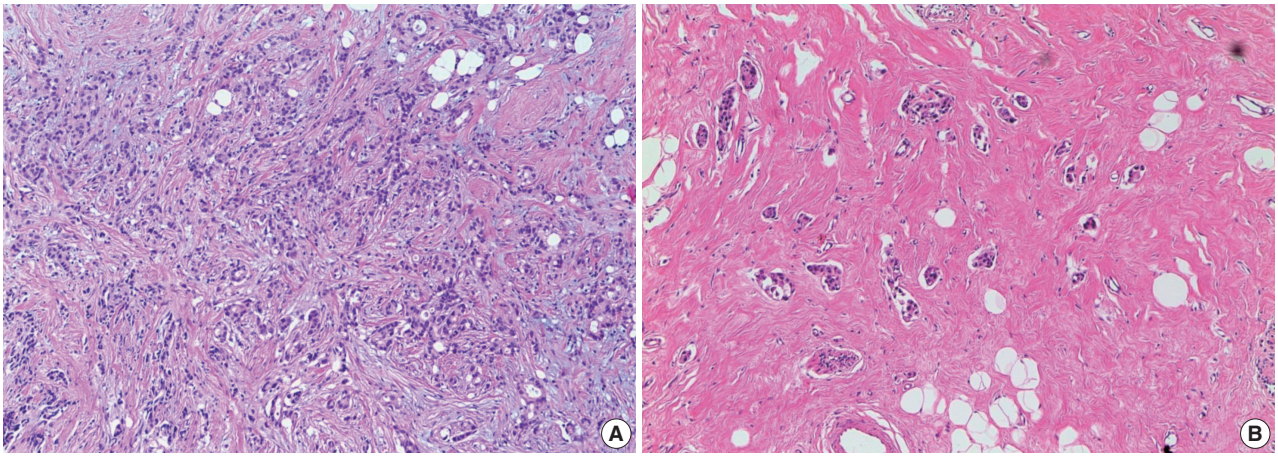

Fig. 3. Comparison of tumor cellularity between pre-neoadjuvant therapy (NAT) and post-NAT. In comparison with the tumor cellularity of a pre-NAT biopsy (A), the tumor cellularity observed in a post-NAT surgical specimen (B) is significantly low.

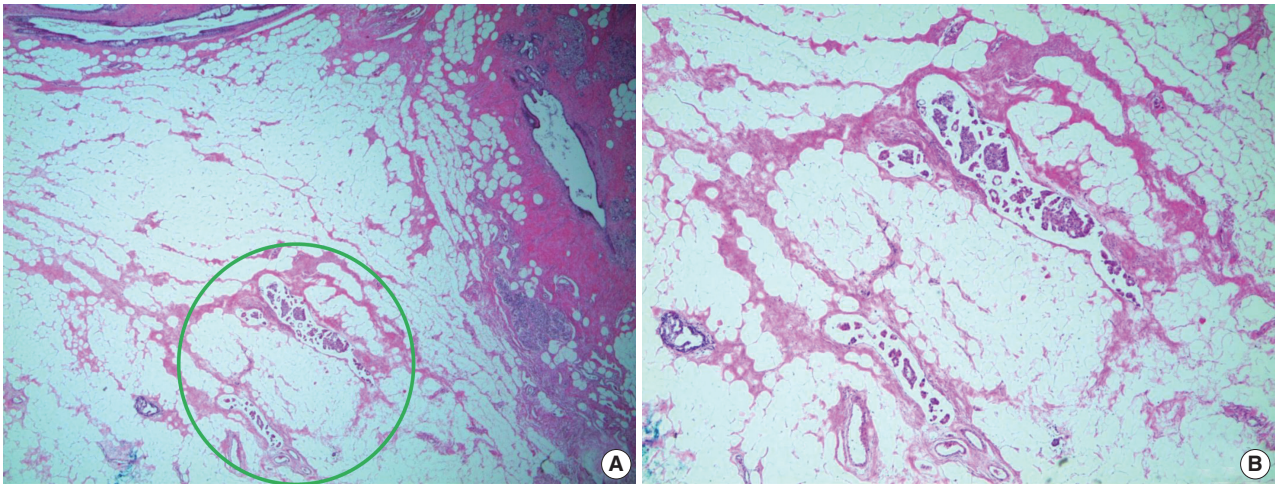

Fig. 4. Residual tumor emboli in lymphovascular space after neoadjuvant therapy (NAT) (A, B). There are only tumor emboli in the lymphovascular space after NAT.

Pathologic complete response

Though each system that evaluates treatment responses to NAT has a unique definition of pCR, all systems record whether the patient has invasive carcinoma and whether it is identified in the breast parenchyma.[9-14] Significant differences among these evaluation systems are based on the inclusion or exclusion of DCIS and axillary lymph node status. Thus, description of DCIS and axillary lymph node status should always be included in pathologic reports because the treatment response evaluation systems differ across institutions.

Re-evaluation of biomarkers in breast cancer after NAT

Estrogen receptor (ER), progesterone receptor (PR), and human epidermal growth factor receptor-2 (HER-2), which are representative biomarkers of breast cancer, should be used for evaluating invasive breast cancer; however, there is no consensus on whether ER, PR, and HER-2 status should be re-evaluated in breast cancer patients who received NAT. Different guidelines suggest different processes based on core biopsy results, because ER, PR, and HER-2 statuses after NAT are evaluated based on the biomarker status of pretreatment core biopsy. If ER, PR, and HER-2 statuses from pre-treatment core biopsy are all positive, there will be no changes in status for most patients; thus, re-evaluation is generally not recommended. However, re-evaluation is considered necessary in the following circumstances: (1) negative or equivocal results in core biopsy, (2) only DCIS or insufficient invasive carcinoma in core biopsy, (3) core biopsy performed at another institute, and (4) no treatment response.[20,21] Additionally, re-evaluation should be performed when the patient is enrolled in a clinical trial protocol or when ER, PR, or

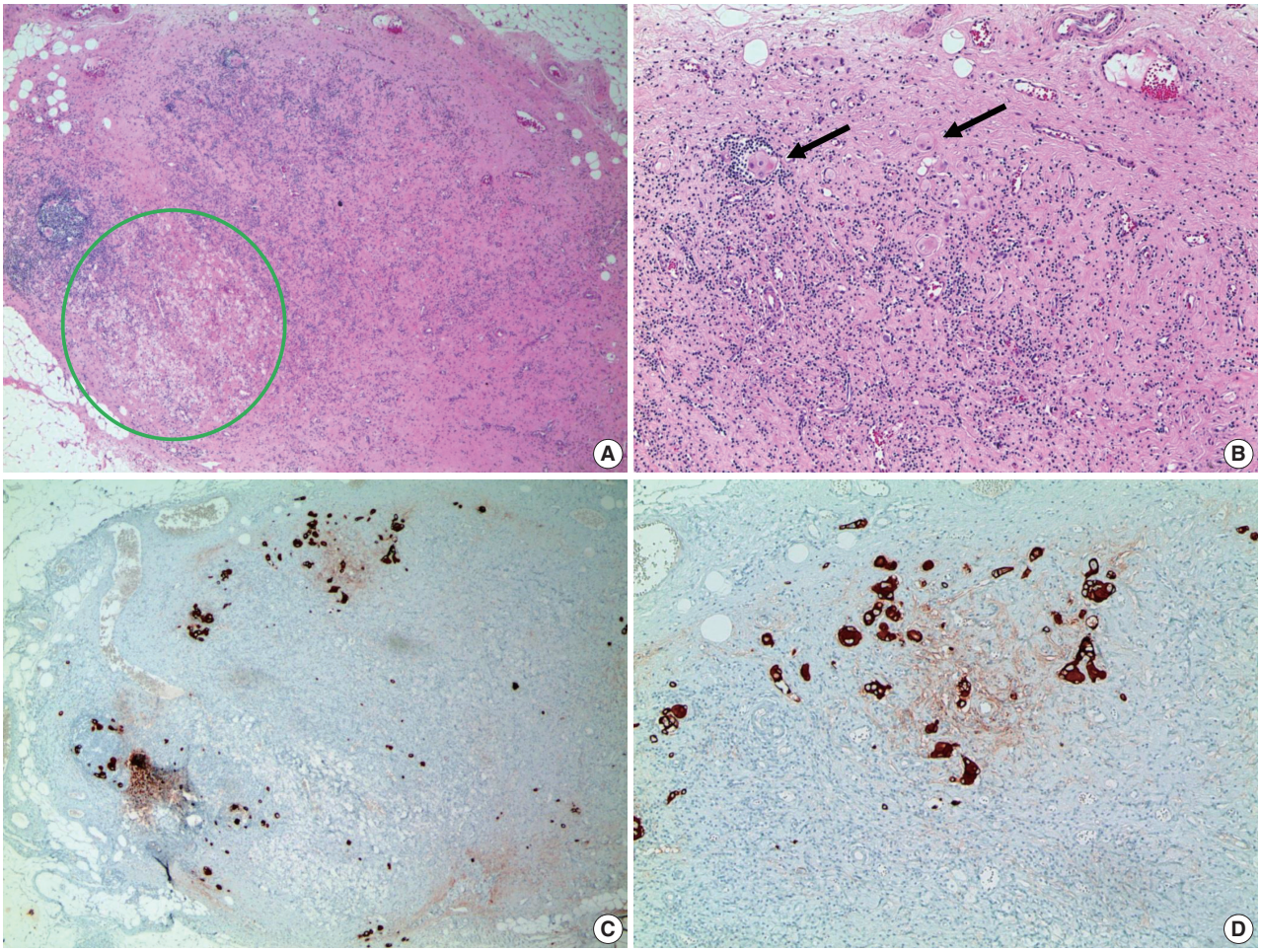

Fig. 5. Metastatic residual carcinoma in a lymph node with histologic features indicative of tumor regression: in low-power view, an axillary lymph node shows lymphocyte depletion, fibrosis, and aggregation of foamy histiocytes (green circle, A), which we suggest are histologic features indicative of tumor regression due to neoadjuvant therapy. In high-power view, metastatic tumor cell clusters are identified in a regressed lymph node (arrows, B). Immunohistochemistry for cytokeratin is helpful to identify metastatic tumor cell clusters in a regressed lymph node (C, D).

HER-2 status is unknown.

CONCLUSIONS

The number of existing post-NAT breast cancer specimens has recently increased because NAT is now established as an effective treatment approach for patients with large or locally advanced breast cancer and for cases of early-stage breast cancer. However, guidelines for pathologic evaluation of breast cancer after NAT have not been established; instead, there are several evaluation systems, each with different major main-effect variables. Moreover, from macroscopic examination to microscopic evaluation, there are several obstacles to pathologic evaluation of neoadjuvant breast cancer because there is a diverse range of histologic responses to NAT. Pathologic evaluation of residual disease is the most essential component of post-NAT breast cancer evaluation. Thus, the evaluation should be conducted based on close comparisons and correlations between clinical, radiologic, and pathologic findings.

Conflicts of Interest

No potential conflict of interest relevant to this article was reported.

Acknowledgments

This study was supported by a grant from the National R&D Program for Cancer Control, Ministry of Health & Welfare, Republic of Korea (1420080);the Basic Science Research Program through the National Research Foundation of Korea (NRF);

and by the Ministry of Science, ICT, and Future Planning (2015R1A1A1A05001209).

REFERENCES

1. Thompson AM, Moulder-Thompson SL. Neoadjuvant treatment of breast cancer. Ann Oncol 2012; 23 Suppl 10: x231-6.
2. Moreno-Aspitia A. Neoadjuvant therapy in early-stage breast cancer. Crit Rev Oncol Hematol 2012; 82: 187-99.
3. Pierga JY, Mouret E, Laurence V, *et al*. Prognostic factors for survival after neoadjuvant chemotherapy in operable breast cancer: the role of clinical response. Eur J Cancer 2003; 39: 1089-96.
4. Kuerer HM, Newman LA, Smith TL, *et al*. Clinical course of breast cancer patients with complete pathologic primary tumor and axillary lymph node response to doxorubicin-based neoadjuvant chemotherapy. J Clin Oncol 1999; 17: 460-9.
5. Fisher B, Bryant J, Wolmark N, *et al*. Effect of preoperative chemotherapy on the outcome of women with operable breast cancer. J Clin Oncol 1998; 16: 2672-85.
6. Esserman LJ, Woodcock J. Accelerating identification and regulatory approval of investigational cancer drugs. JAMA 2011; 306: 2608-9.
7. Bonadonna G, Veronesi U, Brambilla C, *et al*. Primary chemotherapy to avoid mastectomy in tumors with diameters of three centimeters or more. J Natl Cancer Inst 1990; 82: 1539-45.
8. Boughey JC, Peintinger F, Meric-Bernstam F, *et al*. Impact of preoperative versus postoperative chemotherapy on the extent and number of surgical procedures in patients treated in randomized clinical trials for breast cancer. Ann Surg 2006; 244: 464-70.
9. Mamounas EP, Anderson SJ, Dignam JJ, *et al*. Predictors of locoregional recurrence after neoadjuvant chemotherapy: results from combined analysis of National Surgical Adjuvant Breast and Bowel Project B-18 and B-27. J Clin Oncol 2012; 30: 3960-6.
10. Carey LA, Metzger R, Dees EC, *et al*. American Joint Committee on Cancer tumor-node-metastasis stage after neoadjuvant chemotherapy and breast cancer outcome. J Natl Cancer Inst 2005; 97: 1137-42.
11. Ogston KN, Miller ID, Payne S, *et al*. A new histological grading system to assess response of breast cancers to primary chemotherapy: prognostic significance and survival. Breast 2003; 12: 320-7.
12. Abrial SC, Penault-Llorca F, Delva R, *et al*. High prognostic significance of residual disease after neoadjuvant chemotherapy: a retrospective study in 710 patients with operable breast cancer. Breast Cancer Res Treat 2005; 94: 255-63.
13. Pinder SE, Provenzano E, Earl H, Ellis IO. Laboratory handling and histology reporting of breast specimens from patients who have received neoadjuvant chemotherapy. Histopathology 2007; 50: 409-17.
14. Symmans WF, Peintinger F, Hatzis C, *et al*. Measurement of residual breast cancer burden to predict survival after neoadjuvant chemotherapy. J Clin Oncol 2007; 25: 4414-22.
15. Dash N, Chafin SH, Johnson RR, Contractor FM. Usefulness of tissue marker clips in patients undergoing neoadjuvant chemotherapy for breast cancer. AJR Am J Roentgenol 1999; 173: 911-7.
16. Oh JL, Nguyen G, Whitman GJ, *et al*. Placement of radiopaque clips for tumor localization in patients undergoing neoadjuvant chemotherapy and breast conservation therapy. Cancer 2007; 110: 2420-7.
17. Schulz-Wendtland R, Heywang-Köbrunner SH, Aichinger U, Krämer S, Wenkel E, Bautz W. Do tissue marker clips after sonographically or stereotactically guided breast biopsy improve follow-up of small breast lesions and localisation of breast cancer after chemotherapy? Rofo 2002; 174: 620-4.
18. Youn I, Choi SH, Kook SH, *et al*. Ultrasonography-guided surgical clip placement for tumor localization in patients undergoing neoadjuvant chemotherapy for breast cancer. J Breast Cancer 2015; 18: 44-9.
19. Margolin FR, Kaufman L, Denny SR, Jacobs RP, Schrumpf JD. Metallic marker placement after stereotactic core biopsy of breast calcifications: comparison of two clips and deployment techniques. AJR Am J Roentgenol 2003; 181: 1685-90.
20. Provenzano E, Bossuyt V, Viale G, *et al*. Standardization of pathologic evaluation and reporting of postneoadjuvant specimens in clinical trials of breast cancer: recommendations from an international working group. Mod Pathol 2015; 28: 1185-201.
21. Bossuyt V, Provenzano E, Symmans WF, *et al*. Recommendations for standardized pathological characterization of residual disease for neoadjuvant clinical trials of breast cancer by the BIG-NABCG collaboration. Ann Oncol 2015; 26: 1280-91.
22. Sharkey FE, Addington SL, Fowler LJ, Page CP, Cruz AB. Effects of preoperative chemotherapy on the morphology of resectable breast carcinoma. Mod Pathol 1996; 9: 893-900.
23. Honkoop AH, Pinedo HM, De Jong JS, *et al*. Effects of chemotherapy on pathologic and biologic characteristics of locally advanced breast cancer. Am J Clin Pathol 1997; 107: 211-8.
24. Diaz J, Stead L, Shapiro N, *et al*. Mitotic counts in breast cancer after neoadjuvant systemic chemotherapy and development of metastatic disease. Breast Cancer Res Treat 2013; 138: 91-7.
25. Rajan R, Poniecka A, Smith TL, *et al*. Change in tumor cellularity of breast carcinoma after neoadjuvant chemotherapy as a variable in the pathologic assessment of response. Cancer 2004; 100: 1365-73.
26. Fisher ER, Wang J, Bryant J, Fisher B, Mamounas E, Wolmark N. Pathobiology of preoperative chemotherapy: findings from the National Surgical Adjuvant Breast and Bowel (NSABP) protocol B-18. Cancer 2002; 95: 681-95.
27. Leitner SP, Swern AS, Weinberger D, Duncan LJ, Hutter RV. Predictors of recurrence for patients with small (one centimeter or less)

localized breast cancer (T1a,b N0 M0). Cancer 1995; 76: 2266-74.
28. Lee AK, Loda M, Mackarem G, *et al*. Lymph node negative invasive breast carcinoma 1 centimeter or less in size (T1a,bNOMO): clinicopathologic features and outcome. Cancer 1997; 79: 761-71.
29. Rabban JT, Glidden D, Kwan ML, Chen YY. Pure and predominantly pure intralymphatic breast carcinoma after neoadjuvant chemotherapy: an unusual and adverse pattern of residual disease. Am J Surg Pathol 2009; 33: 256-63.
30. Colleoni M, Rotmensz N, Maisonneuve P, *et al*. Prognostic role of the extent of peritumoral vascular invasion in operable breast cancer. Ann Oncol 2007; 18: 1632-40.
31. Sahoo S, Lester SC. Pathology of breast carcinomas after neoadjuvant chemotherapy: an overview with recommendations on specimen processing and reporting. Arch Pathol Lab Med 2009; 133: 633-42.

 http://dx.doi.org/10.4132/jptm.2016.02.02

Journal of Pathology and Translational Medicine 2016; 50: 181-189
http://dx.doi.org/10.4132/jptm.2016.03.18

■ ORIGINAL ARTICLE ■

Nuclear Expression of Hepatitis B Virus X Protein Is Associated with Recurrence of Early-Stage Hepatocellular Carcinomas: Role of Viral Protein in Tumor Recurrence

Jing Jin · Hae Yoen Jung · Kyu Ho Lee
Nam-Joon Yi[1] · Kyung-Suk Suh[1]
Ja-June Jang · Kyoung-Bun Lee

Departments of Pathology and [1]Surgery, Seoul National University College of Medicine, Seoul, Korea

Received: September 30, 2015
Revised: March 12, 2016
Accepted: March 18, 2016

Corresponding Author
Kyoung-Bun Lee, MD, PhD
Department of Pathology, Seoul National University Hospital, 101 Daehak-ro, Jongno-gu, Seoul 03080, Korea
Tel: +82-2-2072-2968
Fax: +82-2-743-5530
E-mail: kblee@snuh.org

Background: Hepatitis B virus (HBV) plays well-known roles in tumorigenesis of hepatocellular carcinoma (HCC) in infected patients. However, HBV-associated protein status in tumor tissues and the relevance to tumor behavior has not been reported. Our study aimed to examine the expression of HBV-associated proteins in HCC and adjacent nontumorous tissue and their clinicopathologic implication in HCC patients. **Methods:** HBV surface antigen (HBsAg), HBV core antigen (HBcAg), and HBV X protein (HBx) were assessed in 328 HBV-associated HCCs and in 155 matched nontumorous tissues by immunohistochemistry staining. **Results:** The positive rates of HBsAg and cytoplasmic HBx staining in tumor tissue were lower than those in nontumorous tissue (7.3% vs. 57.4%, $p < .001$; 43.4% vs. 81.3%, $p < .001$). Conversely, nuclear HBx was detected more frequently in tumors than in nontumorous tissue (52.1% vs. 30.3%, $p < .001$). HCCs expressing HBsAg, HBcAg, or cytoplasmic HBx had smaller size; lower Edmondson-Steiner (ES) nuclear grade, pT stage, and serum alpha-fetoprotein, and less angioinvasion than HCCs not expressing HBV-associated proteins. Exceptionally, nuclear HBx-positive HCCs showed higher ES nuclear grade and more frequent large-vessel invasion than did nuclear HBx-negative HCCs. In survival analysis, only nuclear HBx-positive HCCs had shorter disease-free survival than nuclear HBx-negative HCCs in pT1 and ES nuclear grade 1–2 HCC subgroup (median, 126 months vs. 35 months; $p = .015$). **Conclusions:** Our data confirmed that expression of normal HBV-associated proteins generally decreases in tumor cells in comparison to nontumorous hepatocytes, with the exception of nuclear HBx, which suggests that nuclear HBx plays a role in recurrence of well-differentiated and early-stage HCCs.

Key Words: Hepatitis B X protein; Hepatitis B surface antigens; Hepatitis B core antigens; Carcinoma, hepatocellular

Hepatocellular carcinoma (HCC) is the third most fatal cancer worldwide and poses a major burden to the healthcare system.[1] More than 50% of HCC cases overall and 70%–80% of HCC cases in hepatitic B virus (HBV)–endemic regions are attributable to chronic HBV infection.[2] The mechanism of viral hepatitis-mediated induction of HCC involves the direct mutagenic effect of the virus on the host genome and the indirect effect of the inflammation-necrosis regeneration cycle in the setting of chronic hepatitis.[3]

HBV is a member of the Hepadnaviridae family and has four important viral proteins: hepatitis B virus surface antigen (HBsAg), hepatitis B virus core antigen (HBcAg), hepatitis B virus X protein (HBx), and viral DNA polymerase. HBsAg and HBcAg are structural proteins that are the main components of the viral capsule and core. These proteins induce an immune response in infected hosts and can be used for the assessment of viral replication activity. Thus, they serve as clinical markers for diagnosis and follow-up of viral hepatitis patients via serum tests.[4] HBx is a key regulatory nonstructural protein of the virus that is at the intersection of HBV infection, replication, pathogenesis, and carcinogenesis.[5]

Integration of viral genomes in the host genome is considered a possible mechanism of hepatocarcinogenesis, and this notion is supported by the observation that a large portion of HCC have integrated HBV sequence encoding HBx and a truncated pre-S2/S protein.[6] HBx protein regulates the cell cycle and DNA repair genes of host cells and induces cellular transformation via transactivation (protein interactions) in the nucleus and cytoplasm.[5]

Clinically, a high viral load of HBV is associated with HCC

pISSN 2383-7837
eISSN 2383-7845

recurrence, and early antiviral treatment can increase disease-free survival (DFS) and overall survival of HCC patients.[7,8] A specific mutated form of HBV known as genotype C was reported to be associated with HCC occurrence in cirrhotic patients.[9] HBsAg positivity in non-neoplastic liver tissue was reported as a risk factor for HCC recurrence.[10]

HBsAg expression is generally lower in tumor cells compared with adjacent non-neoplastic hepatocytes, and the HBx protein expression in non-neoplastic hepatic parenchyma is associated with the development of HCC in patients with chronic viral hepatitis.[11,12] Previous studies of the expression of HBV genes and HBx protein in HCC and adjacent non-neoplastic hepatic parenchyma generally focused on the mechanisms underlying the HBV-related hepatocarcinogenesis.

The aim of this study was to assess the expression of the HBsAg, HBcAg, and HBx proteins in HCC and nontumorous liver tissue and to examine the histologic features of HCCs, possible correlations with hepatitis serum markers, and their influence on cancer prognosis.

MATERIALS AND METHODS

Patients and clinicopathologic parameters

We enrolled 328 HBV hepatitis patients who had been diagnosed with HCC based on a resected specimen and whose medical records and formalin-fixed paraffin blocks of tumor tissue were available from the archives of the Department of Pathology at Seoul National University Hospital (SNUH) from 1998 to 2004. We excluded co-infected hepatitis C virus hepatitis patients and patients who had neither serologic nor clinical evidence of HBV infection. The matched non-neoplastic hepatic parenchyma was available for 155 of the 328 patients. Clinical information, such as age, sex, surgical procedure, underlying etiology of liver disease, preoperative serum α-fetoprotein (AFP, μg/mL), preoperative treatment, and postoperative tumor recurrence, was collected from the medical records. Serological results of HBsAg, anti-HBs (HBsAb), IgG anti-HBc (HBcAb), hepatitis B virus e antigen (HBeAg), and anti-HBe (HBeAb) were based on the most recent preoperative tests from medical records. Depending on the state of the serum viral marker, liver function test, and clinical symptom of hepatic failure or portal hypertension (e.g., hypoalbuminemia, prolonged prothrombin time, ascites, hyperbilirubinemia, or hepatic encephalopathy), "asymptomatic carriers" had positive serum viral markers, but a normal liver function test and no clinical symptom of hepatic failure, while "noncirrhotic" patients had positive serum viral marker with abnormal liver function test, but no symptom of hepatic failure. Patients with symptom of hepatic failure were assigned to the cirrhotic patient group. Disease recurrence was defined as newly appearing lesions diagnosed by radiologic examinations such as ultrasonography and X-ray computed tomography, or based on serum tumor markers such as AFP, after an operation. Pathologic information, such as tumor size, number of tumors, gross type (vaguely nodular, expanding nodular, nodular with perinodal extension, and multinodular confluent), angioinvasion, large vessel invasion, Edmondson-Steiner (ES) nuclear grade, histologic pattern of the tumor, cellular type of tumor cells (hepatic vs. non-hepatic including giant, pleomorphic, spindle, and clear cell types), and extent of tumor invasion, was collected from pathology reports and review of the slides. Criteria for pathologic T stage (pT) followed the liver tumor staging of the American Joint Committee on Cancer, seventh edition.[13] Clinicopathologic parameters were assessed according to the general rules for examining primary liver cancer.[14]

Of the 328 patients, 283 were male and 45 were female (M:F ratio of 6.3:1), with a median age of 55 years (range, 25 to 80 years). The mean size of a tumor was 5.44 cm (range, 0.8 to 24.0 cm). Most patients (92.1%, 302/328) had undergone partial hepatectomy, such as right or left lobectomy, caudate lobectomy, or segmentectomy, whereas the remaining patients (7.9%, 26/328) had undergone total hepatectomy for transplantation. Follow-up periods ranged from 0 to 161 months (median, 51 months). This study was approved by the Institutional Review Board of Seoul National University Hospital (H-1011-046-339).

Tissue microarray construction

Hematoxylin and eosin slides were reviewed, and one representative formalin-fixed paraffin-embedded (FFPE) archival block was selected for each case. Each core tissue biopsy (2 mm in diameter) was taken from individual FFPE blocks (donor blocks) and arranged in recipient paraffin blocks (tissue array blocks) using a trephine. Immunohistochemical studies were performed on 13 array blocks containing 328 HCC samples and on six array blocks containing 155 samples of HCC-adjacent non-neoplastic tissue as a healthy control (Superbiochips Laboratories, Seoul, Korea). Each tissue microarray had four cores of normal liver, normal bile duct, and normal gastrointestinal tract mucosa as a negative control.

Immunohistochemistry and interpretation

Sections (4 μm) were stained for HBcAg (1:800, hepatitis B core antigen rabbit polyclonal antibody, Cat. No. B0586, DAKO,

http://dx.doi.org/10.4132/jptm.2016.03.18

Copenhagen, Denmark), HBsAg (1:200, HBsAg mouse monoclonal antibody, clone number S1-210, Cell Marque, Rocklin, CA, USA), and HBx (1:100, HBx mouse monoclonal antibody, clone number 3F6-G10, Thermo, Rockford, IL, USA) after antigen retrieval using a microwave and pH 6.0 citrate buffer. The slides were stained according to methods specified in the Ultravision LP kit (Lab Vision, Fremont, CA, USA) or the Envision kit (Dako, Glostrup, Denmark) using the Bond polymer Refine Detection kit (Leica, Wetzlar, Germany). Unequivocal cytoplasmic staining for HBsAg in more than 5% of tumor cells was considered positive, and unequivocal nuclear and cytoplasmic staining for HBcAg in more than 5% of tumor cells was considered positive as described in a previous study.[4] For HBx, both cytoplasmic and nuclear staining were observed in tumorous and nontumorous liver tissue; thus, we separately assessed the cytoplasmic and nuclear expression of HBx. The intensity of cytoplasmic staining was graded as weak, moderate, or strong by two pathologist (H.Y.Jung and K.-B.Lee), and a grade higher than moderate was considered as positive criteria. Nuclear staining was assessed by image analysis of digitally scanned slides (Nuclear V9 algorithm, ScanScope, Aperio Technologies, Vista, CA, USA). The intensity of nuclear staining was graded as 1+ (intensity range, 230 to 210), 2+ (intensity range, 210 to 188), or 3+ (intensity range, 188 to 162), and more than 5% of tumor cells with more than 2+ intensity were considered as positive criteria.

Statistical analysis

Comparative analysis of HBsAg, HBcAg, and HBx expression with clinicopathologic parameters was assessed using the chisqaure test. Survival analysis was performed using the Kaplan-Meier method. The results were considered statistically significant when p-values were < .05. All calculations were performed using the PASW statistics ver. 18.0 (SPSS Inc., Chicago, IL, USA).

RESULTS

Positive rates of HBsAg, HBcAg, and HBx expression in HCC

The representative immunohistochemical stainings and expression rates of HBsAg, HBcAg, and HBx in the nucleus and cytoplasm are summarized in Table 1 and Fig. 1, respectively. Among the 328 patients with HBV, the positive rate for HBsAg was significantly lower in HCC than in nontumorous tissue (7.3% vs 57.4%, respectively; p < .001), and the positive rate for nuclear HBx was higher in HCC than in nontumorous tissue (52.1% [171/328] vs 30.3% [47/155], respectively; p < .001). Cytoplasmic HBx expression was less frequent in HCC samples than in nontumorous tissue (43.3% [142/328] vs 81.3% [126/155], respectively; p < .001).

Clinicopathologic characteristics of HBsAg-, HBcAg-, and HBx-expressing HCC

The clinicopathologic features and expression of HBsAg, HBcAg, and HBx are summarized in Table 2. HBsAg-expressing HCCs had lower ES nuclear grade and lower pT stage than HCCs without HBsAg expression (p < .001 and p = .013, respectively). HBcAg was more frequently expressed in well-differentiated HCCs (lower ES grade) and in HCCs without preoperative treatment, such as transarterial chemoembolization, radiofrequency ablation, or percutaneous ethanol injection, as well as in patients who had lower serum AFP (p = .018, p = .037, and p = .015, respectively). Cytoplasmic expression of HBx was associated with similar features: lower ES nuclear grade, smaller tumor size, less frequent angioinvasion, lower pT stage, and a lower serum AFP level compared to HCCs not expressing cytoplasmic HBx (p < .05) (Table 2). Compared to HBsAg and HBcAg, nuclear HBx was more frequently expressed in HCCs with higher ES grade and with large-vessel invasion (p = .008, and p = .017, respectively).

Table 1. The percentage of patients positive for HBV proteins in the hepatocellular carcinoma and non-tumorous liver

		Tumor (n = 328)	Non-tumor (n = 155)	p-value
HBsAg	Negative	304 (92.7)	66 (42.6)	< .001*
	Positive	24 (7.3)	89 (57.4)	
HBcAg	Negative	292 (89.0)	141 (91.0)	.632
	Positive	36 (11.0)	14 (9.0)	
HBx_nu	Negative	157 (47.9)	108 (69.7)	< .001*
	Positive	171 (52.1)	47 (30.3)	
HBx_cyto	Negative	186 (56.7)	29 (18.7)	< .001*
	Positive	142 (43.3)	126 (81.3)	

Values are presented as number (%).
HBV, hepatitis B virus; HBsAg, HBV surface antigen; HBcAg, HBV core antigen; HBX, HBV X protein; nu, nuclear staining; cyto, cytoplasmic staining.
*p < .05.

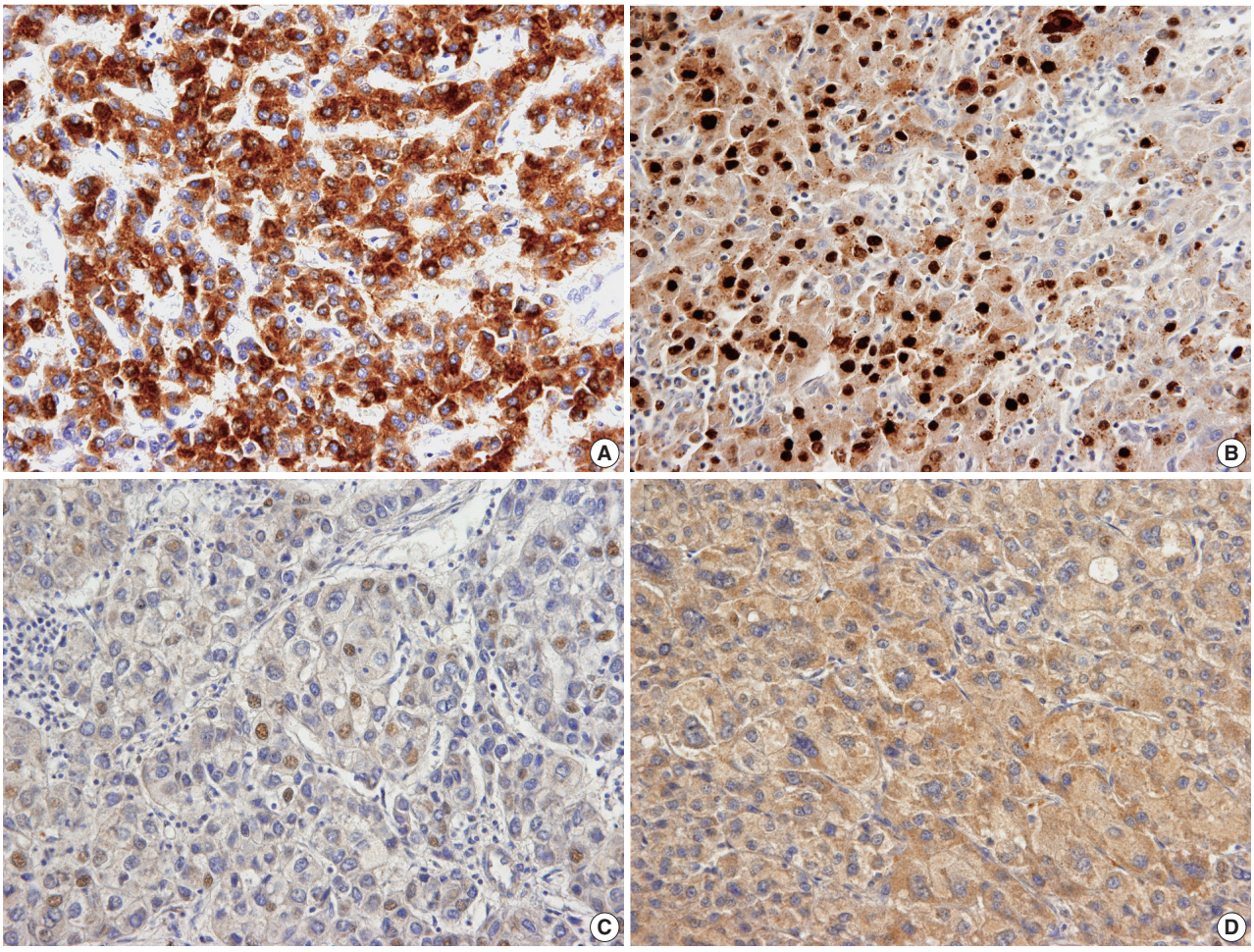

Fig. 1. Representative pictures of hepatitis B virus (HBV) surface antigen (HBsAg), HBV core antigen (HBcAg), and HBV X protein (HBx) proteins in hepatocellular carcinoma. Positive HBsAg (A), positive HBcAg (B), positive HBx in nuclei (C), and positive HBx (D) in the cytoplasm.

Although nuclear HBx was more frequently expressed in HCCs with high ES nuclear grade, the histologic pattern of HCCs with nuclear HBx expression was mostly trabecular and retained the hepatic cell type (p = .002 and p = .086, respectively) (Table 2). Age and sex were not different between HBV protein positive groups and negative groups (data not shown).

Correlation between serum hepatitis B markers and expression of HBV proteins in HCC

We set out to test whether the serum level of hepatitis B markers or the expression profile of nontumorous liver tissue showed any correlation with the expression of HBV proteins in HCCs. All patients with HBsAg-positive HCCs were HBsAg positive in serum. Patients with positive serum HBeAb results showed lower positive rates of HBsAg in HCCs than did patients with negative serum HBeAb (10.8% [7/65] vs 1.8% [2/108], p = .027). Expression of HBcAg and expression of nuclear HBx in HCCs were not significantly concordant with the serum status of HBsAg, HBsAb, HBcAb, HBeAg, and HBeAb. As for the clinical stage of hepatitis, nuclear HBx was more frequently expressed in HCCs of noncirrhotic chronic hepatitis patients compared to asymptomatic carriers or cirrhotic patients (noncirrhotic vs asymptomatic vs cirrhosis; 75% [15/20] vs 35% [13/37] vs 43.9% [54/123], p = .023).

Progression of HBsAg-, HBcAg-, and HBx-expressing HCC

To test whether the HBsAg, HBcAg, or HBx status of tumors influences cancer progression, we analyzed DFS time after operation in the 328 patients with HBV-associated HCC using Kaplan-Meier analysis. We could not determine any correlation between DFS time and the expression status of HBsAg, HBcAg, and HBx in tumors and nontumorous tissue or the serum levels of hepatitis markers (data not shown). The size and multiplicity of the tumor, angioinvasion, ES nuclear grade, and the extent of

http://dx.doi.org/10.4132/jptm.2016.03.18

Table 2. Clinicopathologic characteristics of hepatocellular carcinomas expressing HBV proteins

Variable		HBsAg		HBcAg		HBx_nu		HBx_cyto	
	No. (n=328)	Negative (n=304)	Positive (n=24)	Negative (n=292)	Positive (n=36)	Negative (n=157)	Positive (n=171)	Negative (n=186)	Positive (n=142)
Size (cm)									
≤3	97	91 (29.9)	6 (25.0)	85 (29.1)	12 (33.3)	43 (27.4)	54 (31.6)	44 (23.7)	53 (37.3)
>3	231	213 (70.1)	18 (75.0)	207 (70.9)	24 (66.7)	114 (72.6)	117 (68.4)	142 (76.3)	89 (62.7)
p-value		.401		.364		.239		.005*	
Angioinvasion									
Absent	167	151 (49.7)	16 (66.7)	148 (50.7)	19 (52.8)	82 (52.2)	85 (49.7)	80 (43.0)	87 (61.3)
Present	161	153 (50.3)	8 (33.3)	144 (49.3)	17 (47.2)	75 (47.8)	86 (50.3)	106 (57.0)	55 (38.7)
p-value		.109		.813		.648		.001*	
Large vessel invasion									
Absent	312	288 (94.7)	24 (100.0)	277 (94.9)	35 (97.2)	154 (98.1)	158 (92.4)	173 (93.0)	139 (97.9)
Present	16	16 (5.3)	0 (0.0)	15 (5.1)	1 (2.8)	3 (1.9)	13 (7.6)	13 (7.0)	3 (2.1)
p-value		.618		1.000		.017*		.042*	
ES nuclear grade									
1	30	21 (6.9)	9 (37.5)	22 (7.5)	8 (22.2)	21 (13.4)	9 (5.3)	10 (5.4)	20 (14.1)
2	170	159 (52.3)	11 (45.8)	151 (51.7)	19 (52.8)	83 (52.9)	87 (50.9)	96 (51.6)	74 (52.1)
3	120	116 (38.2)	4 (16.7)	111 (38.0)	9 (25.0)	47 (29.9)	73 (42.7)	74 (39.8)	46 (32.4)
4	8	8 (2.6)	0 (0.0)	8 (2.7)	0 (0.0)	6 (3.8)	2 (1.2)	6 (3.2)	2 (1.4)
p-value		<.001		.018		.008*		.008*	
Histologic pattern									
Trabecular	294	272 (89.5)	22 (91.7)	260 (89.0)	34 (94.4)	132 (84.1)	162 (94.7)	168 (90.3)	126 (88.7)
Nontrabecular	34	32 (10.5)	2 (8.3)	32 (11.0)	2 (5.6)	25 (15.9)	9 (5.3)	18 (9.7)	16 (11.3)
p-value		.734		.316		.002*		.640	
Cellular type									
Hepatic	312	289 (95.1)	23 (95.8)	280 (95.9)	32 (88.9)	146 (93.0)	166 (97.1)	174 (93.5)	138 (97.2)
Nonhepatic	16	15 (4.9)	1 (4.2)	12 (4.1)	4 (11.1)	11 (7.0)	5 (2.9)	12 (6.5)	4 (2.8)
p-value		.867		.085		.086		.130	
pT (AJCC 7th ed)									
1	132	117 (38.5)	15 (62.5)	120 (41.1)	12 (33.3)	62 (39.5)	70 (40.9)	66 (35.5)	66 (46.5)
2	137	129 (42.4)	8 (33.3)	117 (40.1)	20 (55.6)	68 (43.3)	69 (40.4)	79 (42.5)	58 (40.8)
3	42	41 (13.5)	1 (4.2)	39 (13.4)	3 (8.3)	20 (12.7)	22 (12.9)	30 (16.1)	12 (8.5)
4	17	17 (5.6)	0 (0.0)	16 (5.5)	1 (2.8)	7 (4.5)	10 (5.8)	11 (5.9)	6 (4.2)
p-value		.013*		.334		.914		.019*	
Preoperative treatment									
Not done	203	189 (62.2)	14 (58.3)	175 (59.9)	28 (77.8)	93 (59.2)	110 (64.3)	106 (57.0)	97 (68.3)
Done	125	115 (37.8)	10 (41.7)	117 (40.1)	8 (22.2)	64 (40.8)	61 (35.7)	80 (43.0)	45 (31.7)
p-value		.709		.037*		.343		.036*	
Serum AFP (μg/mL)									
≤20.0	187	170 (55.9)	17 (70.8)	160 (54.8)	27 (75.0)	83 (52.9)	104 (60.8)	92 (49.5)	95 (66.9)
>20.0	141	134 (44.1)	7 (29.2)	132 (45.2)	9 (25.0)	74 (47.1)	67 (39.2)	94 (50.5)	47 (33.1)
p-value		.113		.015*		.090		.001*	

Values are presented as number (%).
HBV, hepatitis B virus; HBsAg, HBV surface antigen; HBcAg, HBV core antigen; HBX, HBV X protein; nu, nuclear staining; cyto, cytoplasmic staining; ES, Edmondson-Steiner; AJCC, American Joint Committee on Cancer; AFP, α-fetoprotein.
*p<.05.

tumor invasion were statistically significant prognostic factors for tumor recurrence in the entire sample of 328 patients (data not shown). The low frequency of positive HBsAg in HCCs and well-differentiated histology of HBsAg-expressing HCCs may be a confounder of the above-mentioned negative results in the entire group, so we stratified the study group and analyzed progression-free survival in 99 patients with early-stage (pT1) and well-differentiated HCC (ES nuclear grade 1 and 2); these patients were a relatively low-risk group for HCC recurrence. In 48.5% (48/99) of the patients, the tumor recurred and median DFS time was 84 months, ranging from 2 to 153 months. As shown in Table 3, nuclear HBx in tumors was a statistically sig-

Table 3. Disease-free survival analysis of 99 pT1 and well-differentiated HBV-related HCCs in relation to the expression of HBV proteins

		Recurrence rate	Median DFS (mo)	p-value
Tumor (n=99)				
HBsAg	(–) vs (+)	38/84 (45.2%) vs 10/15 (66.7%)	126 vs 35	.095
HBcAg	(–) vs (+)	44/88 (50.0%) vs 4/11 (36.4%)	84 vs NA	.619
HBx_nu	(–) vs (+)	20/51 (39.2%) vs 28/48 (58.3%)	126 vs 35	.015*
HBx_cyto	(–) vs (+)	22/46 (47.8%) vs 26/53 (49.1%)	126 vs 61	.541
Nontumorous tissue (n=45)				
HBsAg	(–) vs (+)	8/18 (44.4%) vs 16/27 (59.3%)	135 vs 21	.379
HBcAg	(–) vs (+)	22/41 (53.7%) vs 2/4 (50.0%)	135 vs 7	.805
HBx_nu	(–) vs (+)	17/31 (54.8%) vs 7/14 (50.0%)	135 vs 33	.870
HBx_cyto	(–) vs (+)	5/10 (50.0%) vs 19/35 (54.3%)	33 vs 135	.837
Serum				
HBsAg (n=98)	(–) vs (+)	3/11 (27.3%) vs 44/87 (50.6%)	126 vs 84	.296
HBsAb (n=94)	(–) vs (+)	32/74 (43.2%) vs 11/20 (55.0%)	126 vs 35	.163
HBcAb (n=37)	(–) vs (+)	2/4 (50.0%) vs 13/33 (39.4%)	7 vs 84	.473
HBeAg (n=55)	(–) vs (+)	19/41 (46.3%) vs 6/14 (42.9%)	84 vs 153	.505
HBeAb (n=51)	(–) vs (+)	12/21 (57.1%) vs 12/30 (40.0%)	33 vs 84	.406

HBV, hepatitis B virus; HCC, hepatocellular carcinoma; DFS, disease-free survival; HBsAg, HBV surface antigen; HBcAg, HBV core antigen; NA, not applicable; HBx, HBV X protein; nu, nuclear staining; cyto, cytoplasmic staining; HBsAb, anti-HBs; HBcAb, IgG anti-HBc; HBeAg, hepatitis B virus e antigen; HBeAb, anti-HBe.
*$p < .05$.

nificant prognostic factor ($p = .015$), whereas the presence of HBsAg in a tumor showed a tendency for poor prognosis of early-stage HCCs, but did not reach statistical significance ($p = .095$). Cytoplasmic expression of HBx in tumor and nontumorous tissue was not associated with tumor recurrence. In nontumorous liver tissue, HBsAg-, HBcAg-, and HBx-positive patients had a relatively lower median DFS, but this effect was statistically insignificant (log-rank $p > .05$) (Table 3). The presence of HBsAg in the tumor, serum, and nontumorous tissue was correlated with shorter DFS and early recurrence compared to HBsAg-negative patients, as shown in Fig. 2, but this effect was not statistically significant (Table 3). Survival analysis for the high-risk group (advanced stages, pT2–4) or higher nuclear grade (ES nuclear grade 3 and 4) showed no significant difference in DFS according to the status of HBV-associated proteins in serum, tumor, and nontumor tissues (data not shown).

DISCUSSION

In this study, we found that the expression of HBsAg, representing normal viral replication in infected cells, is less frequent in tumors than nontumorous hepatocytes, and HBx, which is one of the key proteins in hepatocarcinogenesis, could be preferentially expressed in different subcellular compartments. The nuclear expression of HBx occurs more frequently in tumors than in nontumorous hepatocytes, whereas the cytoplasmic expression of HBx is less frequent in tumors, according to our results. HCCs with pronounced expression of HBsAg have well-differentiated histology, but HCCs with nuclear expression of HBx showed increased nuclear atypia and aggressive behavior. When the test group is restricted to well-differentiated and to early-stage tumors to minimize the influence of tumor-related prognostic factors, then HCCs expressing nuclear HBx proteins show a higher risk of early recurrence after operation.

Persistence of HBx is important for the pathogenesis of early HCC development, and HBx expression in the liver during chronic HBV infection may be an important prognostic marker for the development of HCC.[5,12] Even seronegative HBV patients have HBx gene and protein expression in HCC, which are consistent with the hepatocarcinogenic properties of HBx.[15] The subcellular location of HBx, as assessed by immunohistochemistry in previous studies, is generally in the cytoplasm of hepatocytes or tumor cells and is consistent with the biological functions of HBx, i.e., protein-protein interactions in cytoplasmic signaling pathways.[5] The biological role of HBx in the nucleus may involve direct interaction with DNA, RNA, or transcription factors, but the existing data are scarce. Recently, it was shown in an *in vitro* study using a human cell line that when HBx is targeted to the nucleus by a nuclear localization signal, it can restore HBx-deficient HBV replication, whereas HBx containing a nuclear export signal cannot, suggesting that nuclear localization of HBx is required for viral replication.[16] In addition, chip-based chromatin immunoprecipitation with expression microarray profiling for HCCs identified 184 gene targets that might

http://dx.doi.org/10.4132/jptm.2016.03.18

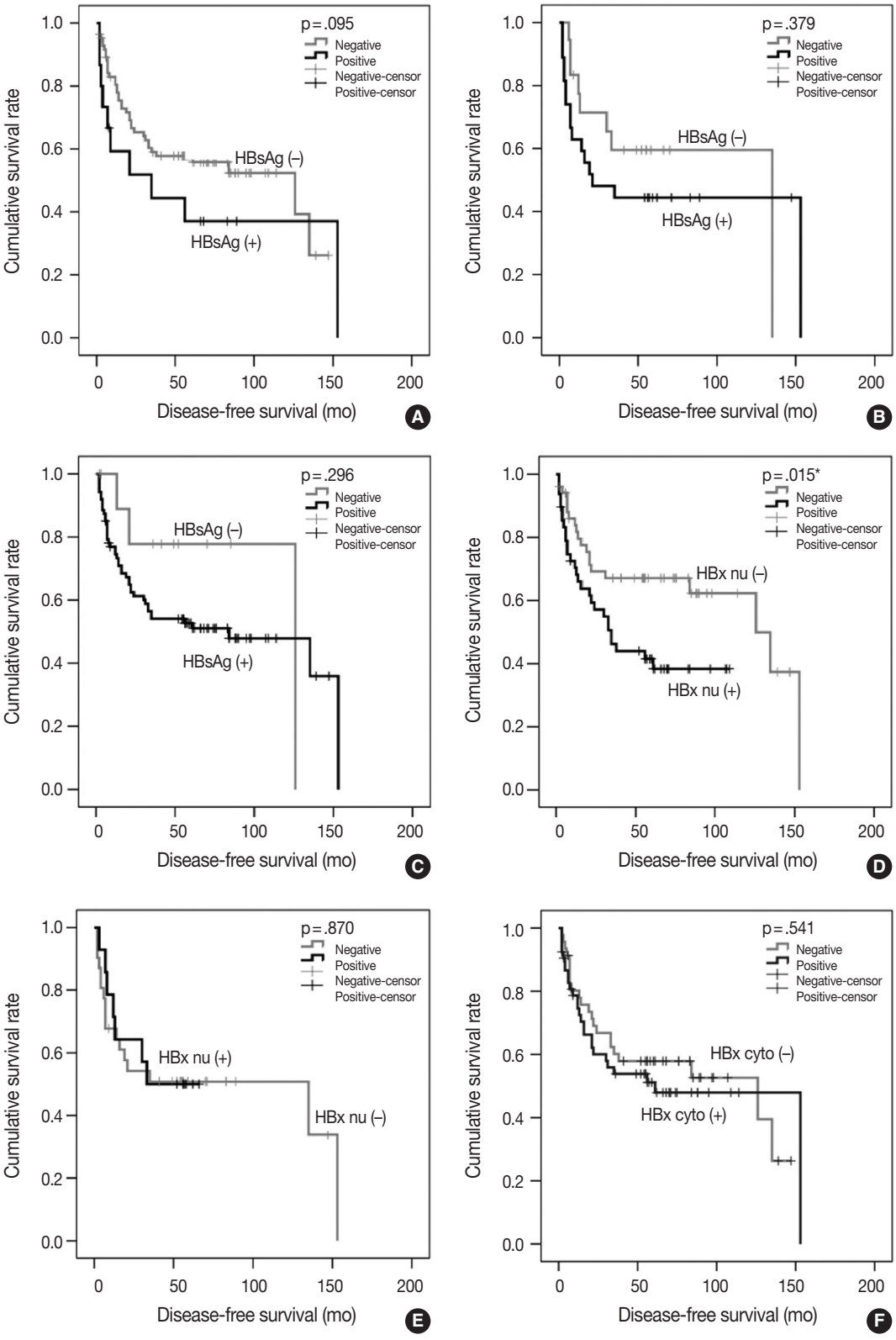

Fig. 2. Cumulative disease-free survival curves of 99 patients with pT1 and well-differentiated hepatocellular carcinoma in relation to the presence of hepatitis B virus (HBV) surface antigen (HBsAg) and HBV X protein (HBx) in a tumor, nontumorous tissue, and serum. HBsAg in tumors (A), HBsAg in nontumorous tissue (B), HBsAg in serum (C), nuclear HBx (HBx nu) in tumors (D), HBX nu in nontumorous tissues (E), and cytoplasmic HBx (HBx cyto) (F) in tumors. *$p < .05$.

be directly deregulated by HBx via targeting from indirect protein-DNA binding as well as transcriptional factors directly interacting with HBx.[17]

Our results show that nuclear, not cytoplasmic, HBx expression correlates with aggressiveness of HCC tumors, such as nuclear grade or large vessel invasion, and with early recurrence after an operation. These data suggest that the interaction of HBx with nuclear proteins might be more important for tumor progression than for cytoplasmic interactions of HBx. Although the HBx protein may be involved in metastasis and tumor invasiveness by regulating proteins that control the extracellular matrix, angiogenesis, or epithelial mesenchymal transition, the reason for the paucity of clinical evidence regarding the HBx protein and HCC recurrence or prognosis could be the difficulties with interpretation of HBx immunohistochemistry.[18-21] In the majority of the studies on HBx, cytoplasmic staining was considered positive expression, and nuclear staining was not investigated.[15,18,19,22] Because we minimized the influence of well-known prognostic factors, such as vascular invasion, size, multiplicity, extent of tumor invasion, and differentiation, by selecting HCCs of pT1 stage and ES nuclear grade 1 and 2, we expected that HBx in nontumorous tissue would be a prognostic factor, but the results showed that it was not. We tried to find a link between the pattern of recurrence and the HBx expression, but the recurrence pattern (presented as a single intrahepatic mass versus multiple or disseminated intrahepatic or extrahepatic masses) was not different depending on the HBx expression in tumor and non-tumor tissues. However, nuclear HBx (–) HCCs both in tumor and nontumor were more frequently presented as a single intrahepatic mass at recurrence time after resection (rate of a single intrahepatic mass, HBx_nu[+] in tumor and non-tumor vs HBx_nu[+] in tumor or non-tumor 59.3% [16/27] vs 37.0% [27/73], p = .388), but this result was not statistically significant. Further research is needed to understand how nuclear expression of HBx promotes tumor recurrence before pathologic features of tumor aggressiveness have appeared.

The mechanism of HCC recurrence in HBV patients is regrowth of microscopically or macroscopically leftover tumor cells or *de novo* occurrence of HCC. The viral influence on HCC recurrence can be explained by the *de novo* tumor recurrence. Su *et al*.[23] reported that a higher serum HBV DNA load was an important risk factor associated with recurrence in patients with HBV-associated HCC without antiviral therapy after resection, but this observation was not applicable in advanced stage HCC. Tsai *et al*.[10] reported that a ground-glass hepatocyte pattern or HBsAg expression in nontumorous liver tissues was a prognostic marker for the recurrence of HBV-related HCC after hepatic resection; these data also support the viral influence on HCC recurrence. Our finding that HBsAg-expressing HCCs recur earlier than do HBsAg-negative HCCs in patients with early-stage and well-differentiated HCC is in line with the previous reports except for the source of HBsAg production, although this finding was not statistically significant.

Last, our results were limited due to the one core-construct of the tissue microarrays that were used. However, staining on full sections for preliminary study showed that staining pattern was relatively patched, but generally weak to moderate areas were alternatively mixed with strongly stained areas, not totally negative areas, and the size of the study groups (n = 483) might be large enough to compensate this problem.

In summary, we report that nuclear expression of HBx in HBV-associated HCCs increases in tumors compared to nontumorous tissue, and HBsAg-expressing HCCs have a tendency to recur early, even if they are well-differentiated histologically and the surgical procedure is performed at an early stage. Tissue expression of HBsAg was correlated with serum HBsAg. Nuclear expression of HBx in tumor tissue assessed by immunohistochemistry can be a useful prognostic marker for prediction of tumor recurrence in early-stage HCC patients and may ultimately lead to novel therapeutic strategies for managing HBV-associated HCC and for researching HBV-associated hepatocarcinogenesis.

Conflicts of Interest

No potential conflict of interest relevant to this article was reported.

Acknowledgments

This research was supported by a grant of the Korea Health Technology R&D Project through the Korea Health Industry Development Institute (KHIDI), funded by the Ministry of Health & Welfare, Republic of Korea (grant number: HI14C3298).

REFERENCES

1. Ferlay J, Shin HR, Bray F, Forman D, Mathers C, Parkin DM. Estimates of worldwide burden of cancer in 2008: GLOBOCAN 2008. Int J Cancer 2010; 127: 2893-917.
2. Nordenstedt H, White DL, El-Serag HB. The changing pattern of epidemiology in hepatocellular carcinoma. Dig Liver Dis 2010; 42 Suppl 3: S206-14.

3. Brechot C, Jaffredo F, Lagorce D, *et al*. Impact of HBV, HCV and GBV-C/HGV on hepatocellular carcinomas in Europe: results of a European concerted action. J Hepatol 1998; 29: 173-83.
4. Theise ND, Bodenheimer HC Jr, Ferrell LD. Acute and chronic viral hepatitis. In: Burt AD, Portmann BC, Ferrell LD, eds. MacSween's pathology of the liver. 6th ed. Edinburgh: Churchill Livingstone Elsevier, 2012; 361-401.
5. Ng SA, Lee C. Hepatitis B virus X gene and hepatocarcinogenesis. J Gastroenterol 2011; 46: 974-90.
6. Goodman ZD, Terraciano LM, Wee A. Tumours and tumour-like lesions of the liver. In: Burt A, Portmann B, Ferrell L, eds. MacSween's pathology of the liver. 6th ed. Edinburgh: Churchill Livingstone Elsevier, 2012; 761-851.
7. Xia F, Lai EC, Lau WY, *et al*. High serum hyaluronic acid and HBV viral load are main prognostic factors of local recurrence after complete radiofrequency ablation of hepatitis B-related small hepatocellular carcinoma. Ann Surg Oncol 2012; 19: 1284-91.
8. Huang G, Yang Y, Shen F, *et al*. Early viral suppression predicts good postoperative survivals in patients with hepatocellular carcinoma with a high baseline HBV-DNA load. Ann Surg Oncol 2013; 20: 1482-90.
9. Yin J, Xie J, Liu S, *et al*. Association between the various mutations in viral core promoter region to different stages of hepatitis B, ranging of asymptomatic carrier state to hepatocellular carcinoma. Am J Gastroenterol 2011; 106: 81-92.
10. Tsai HW, Lin YJ, Lin PW, *et al*. A clustered ground-glass hepatocyte pattern represents a new prognostic marker for the recurrence of hepatocellular carcinoma after surgery. Cancer 2011; 117: 2951-60.
11. Kremsdorf D, Soussan P, Paterlini-Brechot P, Brechot C. Hepatitis B virus-related hepatocellular carcinoma: paradigms for viral-related human carcinogenesis. Oncogene 2006; 25: 3823-33.
12. Zhu M, London WT, Duan LX, Feitelson MA. The value of hepatitis B x antigen as a prognostic marker in the development of hepatocellular carcinoma. Int J Cancer 1993; 55: 571-6.
13. Edge SB, Compton CC. The American Joint Committee on Cancer: the 7th edition of the AJCC cancer staging manual and the future of TNM. Ann Surg Oncol 2010; 17: 1471-4.
14. The general rules for the clinical and pathological study of primary liver cancer. Liver Cancer Study Group of Japan. Jpn J Surg 1989; 19: 98-129.
15. Shiota G, Oyama K, Udagawa A, *et al*. Occult hepatitis B virus infection in HBs antigen-negative hepatocellular carcinoma in a Japanese population: involvement of HBx and p53. J Med Virol 2000; 62: 151-8.
16. Keasler VV, Hodgson AJ, Madden CR, Slagle BL. Hepatitis B virus HBx protein localized to the nucleus restores HBx-deficient virus replication in HepG2 cells and *in vivo* in hydrodynamically-injected mice. Virology 2009; 390: 122-9.
17. Sung WK, Lu Y, Lee CW, Zhang D, Ronaghi M, Lee CG. Deregulated direct targets of the hepatitis B virus (HBV) protein, HBx, identified through chromatin immunoprecipitation and expression microarray profiling. J Biol Chem 2009; 284: 21941-54.
18. Ou DP, Tao YM, Tang FQ, Yang LY. The hepatitis B virus X protein promotes hepatocellular carcinoma metastasis by upregulation of matrix metalloproteinases. Int J Cancer 2007; 120: 1208-14.
19. Xie H, Song J, Liu K, *et al*. The expression of hypoxia-inducible factor-1alpha in hepatitis B virus-related hepatocellular carcinoma: correlation with patients' prognosis and hepatitis B virus X protein. Dig Dis Sci 2008; 53: 3225-33.
20. Xia L, Huang W, Tian D, *et al*. Upregulated FoxM1 expression induced by hepatitis B virus X protein promotes tumor metastasis and indicates poor prognosis in hepatitis B virus-related hepatocellular carcinoma. J Hepatol 2012; 57: 600-12.
21. Liu H, Xu L, He H, *et al*. Hepatitis B virus X protein promotes hepatoma cell invasion and metastasis by stabilizing Snail protein. Cancer Sci 2012; 103: 2072-81.
22. Zhang X, Dong N, Zhang H, You J, Wang H, Ye L. Effects of hepatitis B virus X protein on human telomerase reverse transcriptase expression and activity in hepatoma cells. J Lab Clin Med 2005; 145: 98-104.
23. Su CW, Chiou YW, Tsai YH, *et al*. The influence of hepatitis B viral load and pre-S deletion mutations on post-operative recurrence of hepatocellular carcinoma and the tertiary preventive effects by anti-viral therapy. PLoS One 2013; 8: e66457.

Journal of Pathology and Translational Medicine 2016; 50: 190-196
http://dx.doi.org/10.4132/jptm.2016.03.01

■ ORIGINAL ARTICLE ■

Interobserver Agreement on Pathologic Features of Liver Biopsy Tissue in Patients with Nonalcoholic Fatty Liver Disease

Eun Sun Jung[1,2] · Kyoungbun Lee[1,3] Eunsil Yu[1,4] · Yun Kyung Kang[1,5] Mee-Yon Cho[1,6] · Joon Mee Kim[1,7] Woo Sung Moon[1,8] · Jin Sook Jeong[1,9] Cheol Keun Park[1,10] · Jae-Bok Park[1,11] Dae Young Kang[1,12] · Jin Hee Sohn[1,13] So-Young Jin[1,14]

[1]Gastrointestinal Pathology Study Group of Korean Society of Pathologist; [2]Department of Pathology, Seoul St. Mary's Hospital, College of Medicine, The Catholic University of Korea, Seoul; [3]Department of Pathology, Seoul National University College of Medicine, Seoul; [4]Department of Pathology, Asan Medical Center, University of Ulsan College of Medicine, Seoul; [5]Department of Pathology, Inje University Seoul Paik Hospital, Seoul; [6]Department of Pathology, Yonsei University Wonju College of Medicine, Wonju; [7]Department of Pathology, Inha University Hospital, Incheon; [8]Department of Pathology, Chonbuk National University Medical School, Jeonju; [9]Department of Pathology, Dong-A University College of Medicine, Busan; [10]Department of Pathology, Samsung Medical Center, Sungkyunkwan University School of Medicine, Seoul; [11]Department of Pathology, Daegu Catholic University College of Medicine, Daegu; [12]Department of Pathology, Chungnam National University Hospital, Chungnam National University School of Medicine, Daejeon; [13]Department of Pathology, Kangbuk Samsung Hospital, Sungkyunkwan University School of Medicine, Seoul; [14]Department of Pathology, Soon Chun Hyang University Seoul Hospital, Seoul, Korea

Received: January 11, 2016
Revised: February 25, 2016
Accepted: March 1, 2016

Corresponding Author
So-Young Jin, MD
Department of Pathology, Soon Chun Hyang University Seoul Hospital, 59 Daesagwan-ro, Yongsan-gu, Seoul 04401, Korea
Tel: +82-2-709-9424
Fax: +82-2-709-9441
E-mail: jin0924@schmc.ac.kr

Background: The histomorphologic criteria for the pathological features of liver tissue from patients with non-alcoholic fatty liver disease (NAFLD) remain subjective, causing confusion among pathologists and clinicians. In this report, we studied interobserver agreement of NAFLD pathologic features and analyzed causes of disagreement. **Methods:** Thirty-one cases of clinicopathologically diagnosed NAFLD from 10 hospitals were selected. One hematoxylin and eosin and one Masson's trichrome-stained virtual slide from each case were blindly reviewed with regard to 12 histological parameters by 13 pathologists in a gastrointestinal study group of the Korean Society of Pathologists. After the first review, we analyzed the causes of disagreement and defined detailed morphological criteria. The glass slides from each case were reviewed a second time after a consensus meeting. The degree of interobserver agreement was determined by multi-rater kappa statistics. **Results:** Kappa values of the first review ranged from 0.0091–0.7618. Acidophilic bodies (k = 0.7618) and portal inflammation (k = 0.5914) showed high levels of agreement, whereas microgranuloma (k = 0.0984) and microvesicular fatty change (k = 0.0091) showed low levels of agreement. After the second review, the kappa values of the four major pathological features increased from 0.3830 to 0.5638 for steatosis grade, from 0.1398 to 0.2815 for lobular inflammation, from 0.1923 to 0.3362 for ballooning degeneration, and from 0.3303 to 0.4664 for fibrosis. **Conclusions:** More detailed histomorphological criteria must be defined for correct diagnosis and high interobserver agreement of NAFLD.

Key Words: Non-alcoholic fatty liver disease; Pathologic features; Interobserver agreement

pISSN 2383-7837
eISSN 2383-7845

Nonalcoholic fatty liver disease (NAFLD) is a clinicopathological spectrum characterized by hepatic steatosis without history of significant alcohol use or other known liver disease. The commonly associated factors include obesity, insulin resistance syndrome, and hyperlipidemia. Other associations include jejuno-ileal bypass/gastroplasty surgery for morbid obesity, parenteral nutrition, forms of malnutrition, bacterial contamination of the small bowel, certain inherited metabolic disorders, and a wide range of drugs and environmental toxins.[1] The natural history and histological spectrum of NAFLD range from stable simple steatosis to progressive or advanced disease, such as steatohepatitis, cirrhosis, and even hepatocellular carcinoma.[2-13] A clinicopathological correlation is needed to diagnose NAFLD, as clinical assessment, laboratory tests, and imaging techniques alone provide limited pertinent information. Liver biopsy is the only reliable diagnostic tool to evaluate a patient with suspected NAFLD. Degree of steatosis, liver injury, and fibrosis associated with NAFLD can be identified and differentiated from simple steatosis and nonalcoholic steatohepatitis (NASH), which is the progressive form of NAFLD.[14,15] A NAFLD histopathological grading system was proposed by Brunt *et al*. in 1999.[16] They proposed to classify each of steatosis, inflammation, and ballooning degeneration into three grades and fibrosis into four stages. Since then, Kleiner *et al*.[17] of the NASH Clinical Research Network have proposed a more relevant classification. Other than steatosis, inflammation, and ballooning degeneration, they proposed the classification of fibrosis around the central area into three more detailed grades. Also, they scored each finding and suggested that a score greater than five indicates NASH. However, until now, classifications for NAFLD or NASH have differed depending on the researcher, and no NAFLD histopathological grading system has been standardized, causing confusion for clinicians and pathologists. Furthermore, the histomorphological criteria for NAFLD pathologic features in liver tissue remain subjective. Thus, in this study, we determined the interobserver agreement of NAFLD pathologic features between pathologists and analyzed the causes of the disagreement in order to define the histopathological features in more detail as the basis for a grading system.

MATERIALS AND METHODS

Thirty-one patients with clinically and pathologically diagnosed NAFLD from 10 hospitals (Daegu Catholic University Medical Center, Dong-A University Hospital, Samsung Medical Center, Seoul National University Hospital, Inje University Seoul Paik Hospital, Seoul St. Mary's Hospital, Soon Chun Hyang University Seoul Hospital, Wonju Severance Christian Hospital, Inha University Hospital, Chungnam National University Hospital) were selected. Selection criteria were clinical NAFLD (nonalcoholic, serologically negative for viral and autoimmune markers, abnormal levels of liver enzymes such as aspartate aminotransferase and alanine aminotransferase) and age ≥19 years. Cirrhosis cases were included, and cases of drug and toxic injury conditions were excluded. Fifty-one liver biopsies from 10 hospitals were collected. Among them, 31 biopsies (≥1.5 cm in length and ≥16 G needle size) were selected. One hematoxylin and eosin (H&E)- and one Masson's trichrome–stained slide were selected from each of the 31 cases. The biopsy specimens were anonymized and randomized by a researcher not involved in the study. All selected slides were scanned by a virtual slide scanning system (3DHistotech Ltd., Budapest, Hungary) at Asan Medical Center in Seoul.

The following 12 NAFLD pathologic features were selected: steatosis grade, steatosis location, microvesicular steatosis, fibrosis stage, lobular inflammation, microgranuloma, large lipogranuloma, portal inflammation, ballooning degeneration, acidophilic bodies, Mallory's hyaline, and glycogenated nuclei. Each parameter was reviewed and scored using the detailed scoring criteria shown in Table 1.

One H&E- and one Masson's trichrome–stained virtual slide from each case were reviewed for the 12 parameters. Reviews were performed blindly by 13 pathologists from a gastrointestinal study group of the Korean Society of Pathologists. The degree of interobserver agreement for the first review was analyzed by multi-rater Kappa statistics.

The results were shared with all 13 pathologists, and a consensus meeting was held after the first review to analyze the reasons for disagreement and to define the morphologic criteria in more detail.

After the consensus meeting, a second review of the 12 pathological parameters was performed using glass slides from each of the 31 cases. The degree of interobserver agreement after the second review was analyzed by multi-rater Kappa statistics and compared with the results of the first review.

The Institutional Review Board of Seoul St. Mary's Hospital approved this study (KIRB-00562_5-001).

RESULTS

Kappa values of interobserver agreement for the first review ranged from 0.0091 to 0.7618 (Table 2). The order of agreement,

Table 1. Pathological parameters and detailed scoring criteria of non-alcoholic fatty liver disease

	Pathologic parameter	Criteria for scoring
1	Steatosis grade	1: <5%, 2: 5–33%, 3: 34–66%, 4: >66%
2	Steatosis location	1: zone 1, 2: zone 3, 3: azonal, 4: panacinar
3	Microvesicular steatosis	0: absent, 1: present
4	Fibrosis	0: none
		1A: mild, zone 3, perisinusoidal
		1B: moderate, zone 3, perisinusoidal
		1C: portal/periportal
		2: perisinusoidal and portal/periportal
		3: bridging fibrosis
		4: cirrhosis
5	Lobular inflammation	0: no foci
		1: <2 foci per 200× field
		2: 2–4 foci per 200× field
		3: >4 foci per 200× field
6	Microgranuloma	0: absent, 1: present
7	Large lipogranuloma	0: absent, 1: present
8	Portal inflammation	0: none to minimal, 1: greater than minimal
9	Ballooning	0: absent, 1: few, 2: many/prominent
10	Acidophilic bodies	0: none to rare, 1: many
11	Mallory's hyaline	0: none to rare, 1: many
12	Glycogenated nuclei	0: none to rare, 1: many

according to the kappa value, was acidophilic bodies (k = 0.7618), portal inflammation (k = 0.5914), large lipogranuloma (k = 0.4822), Mallory's hyaline (k = 0.4603), steatosis grade (k = 0.3830), steatosis location (k = 0.3388), fibrosis (k = 0.3303), glycogenated nuclei (0.3218), ballooning degeneration (k = 0.1923), lobular inflammation (0.1398), microgranuloma (0.0984), and microvesicular fatty change (0.0091). The kappa values of the four major pathologic features (steatosis grade, portal inflammation, ballooning degeneration, and fibrosis) were measured as 0.3829, 0.5913, 0.1923, and 0.3303, respectively. In particular, ballooning degeneration (k = 0.1923), which is an important feature for diagnosis of NASH, showed a low level of agreement.

Kappa values of interobserver agreement for the second review ranged from 0.1199 to 0.7386 (Table 2). The order of kappa values for interobserver agreement after the second review were portal inflammation (k = 0.7386), acidophilic bodies (k = 0.6493), steatosis grade (k = 0.5638), Mallory's hyaline (k = 0.5236), large lipogranuloma (k = 0.5004), fibrosis (k = 0.4664), steatosis location (k = 0.4502), glycogenated nuclei (k = 0.3846), ballooning degeneration (k = 0.3362), microvesicular fatty change (k = 0.2916), lobular inflammation (k = 0.2815), and microgranuloma (k = 0.1199). The kappa values of interobserver agreement increased for all parameters except acidophilic bodies. Microvesicular steatosis demonstrated the largest improvement (k = 0.0091 to 0.2916), and microgranuloma the smallest (k = 0.0984 to 0.1199). All kappa values of the four major pathological features increased as follows: steatosis grade from k = 0.3830 to 0.5638, portal inflammation from k = 0.5914 to 0.7386, ballooning degeneration from k = 0.1923 to 0.3362, and fibrosis from k = 0.3303 to 0.4664.

Table 2. Comparison of kappa values after the first and second reviews of non-alcoholic fatty liver disease pathological features

	Pathologic parameters	First review	Second review
1	Steatosis grade	0.3830	0.5638
2	Steatosis location	0.3388	0.4502
3	Microvesicular steatosis	0.0091	0.2916
4	Fibrosis	0.3303	0.4664
5	Lobular inflammation	0.1398	0.2815
6	Microgranuloma	0.0984	0.1199
7	Large lipogranuloma	0.4822	0.5004
8	Portal inflammation	0.5914	0.7386
9	Ballooning	0.1923	0.3362
10	Acidophilic bodies	0.7618	0.6493
11	Mallory's hyaline	0.4603	0.5236
12	Glycogenated nuclei	0.3218	0.3846

DISCUSSION

Since the first description of NASH by Ludwig *et al*. in 1980,[18] several NAFLD scoring schemes have been proposed.[16,17,19,20] Among them, the NAFLD activity score (NAS) proposed by Kleiner *et al*.[17] is the most well-known and popular system. Their

http://dx.doi.org/10.4132/jptm.2016.03.01

proposed NAS system is based on agreement data and a multiple regression analysis of the[14] histological features of steatosis grade, steatosis location, microvesicular steatosis, fibrosis, lobular inflammation, microgranuloma, large lipogranuloma, portal inflammation, ballooning degeneration, acidophilic bodies, pigmented macrophages, megamitochondria, Mallory's hyaline, and glycogenated nuclei. The NAS is defined as the unweighted sum of the scores for steatosis (0–3), lobular inflammation (0–3), and ballooning (0–2) and ranges from 0 to 8. Fibrosis was not included as an NAS component. Kleiner *et al*.[17] reported that the interobserver agreement values for the four major features were 0.79 for steatosis grade, 0.45 for lobular inflammation, 0.56 for ballooning degeneration, and 0.84 for fibrosis. The agreement for other histologic features ranged from k = 0.15 to 0.58. However, the histomorphological features of some parameters remain ambiguous, contributing to low interobserver agreement. We studied interobserver agreement among 13 pathologists for each of the 12 well-known parameters and analyzed the reasons for disagreement. At the first circulation of slides, we reviewed each case without consensus to identify current discrepancies in diagnostic criteria. The kappa values in this review ranged widely from 0.0091 to 0.7618. Kappa values of the four major pathological features at the first review were 0.3830 for steatosis grade, 0.1398 for lobular inflammation, 0.1923 for ballooning degeneration, and 0.3303 for fibrosis, lower than those of Kleiner *et al*.[17]

After the first review, we discussed several points of debate surrounding the definition of each parameter. As a result, we identified several details regarding steatosis grade, lobular inflammation, ballooning degeneration, fibrosis, Mallory's body, and microvesicular fatty change and recommend the following:

(1) Steatosis grade: steatosis grade should be determined by fat volume rather than the number of fatty hepatocytes at 100× optical magnification (Fig. 1).

(2) Lobular inflammation: lobular inflammation should be graded under 200× magnification throughout the entire biopsy field, and the mean, not the maximum number in the most active field, should be determined. Spotty necrosis of hepatocytes, lymphocyte aggregations, and acidophilic bodes should be included, whereas lipogranuloma resulting from fat phagocytosis should be excluded as in the histomorphologic criteria for chronic hepatitis grading (Fig. 2).

(3) Ballooning degeneration: the histomorphological criteria of ballooning degeneration are enlarged round cells with loss of

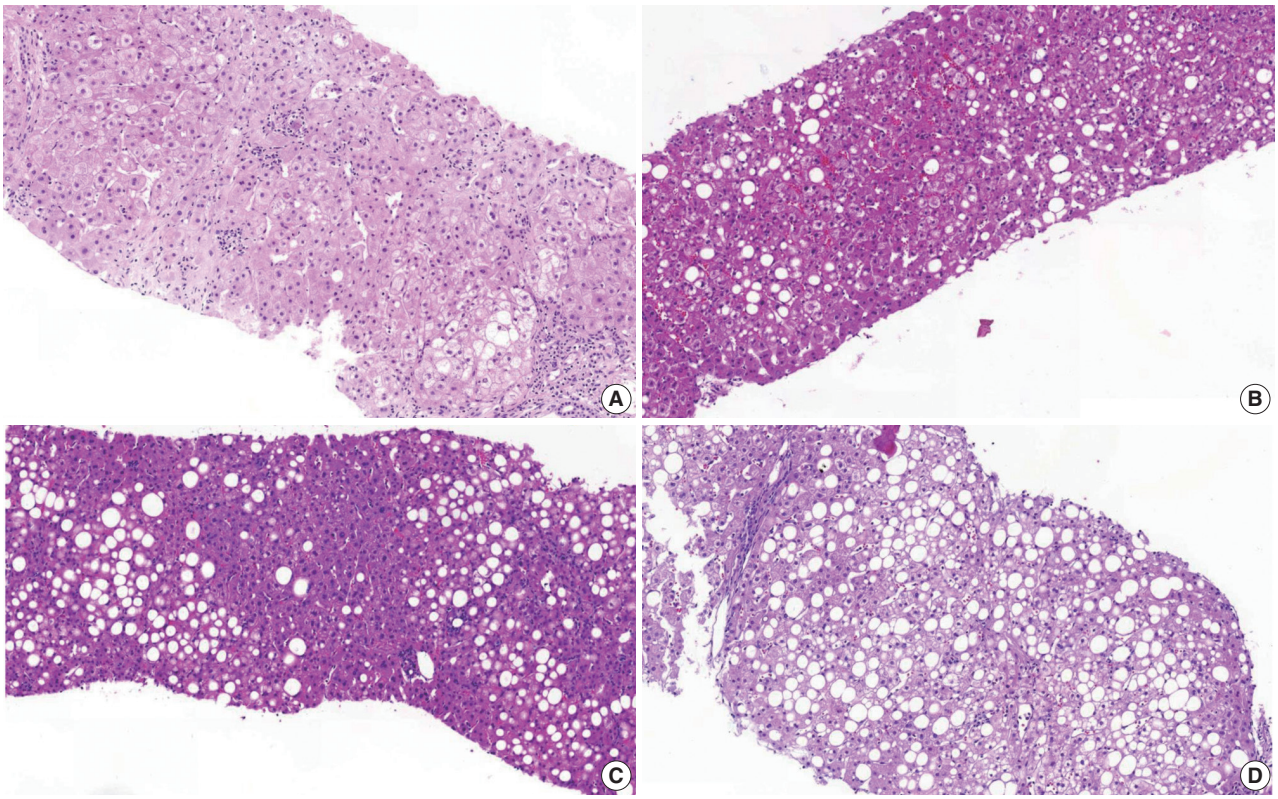

Fig. 1. Grading of steatosis. It is determined by fat volume rather than number of fatty hepatocytes. (A) <5%. (B) 5%–33%. (C) 34%–66%. (D) > 66%.

polygonal features and cytoplasm showing heterogeneous granular features (Fig. 3). Hydropic swelling and microvesicular fatty changes should be carefully distinguished from ballooning degeneration. In cases of hydropic swelling, the hepatocyte has large, swollen, and homogenously granular cytoplasm with well-preserved polygonal features. In particular, microvesicular fatty changes can also be enlarged and can be confused with ballooning degeneration. Microvesicular fatty changes show centrally located nuclei indented by a small fat droplet with a lipoblast-like feature (Fig. 4). When only one or two ballooned cells can be seen throughout the entire field, the term "few" can be applied.

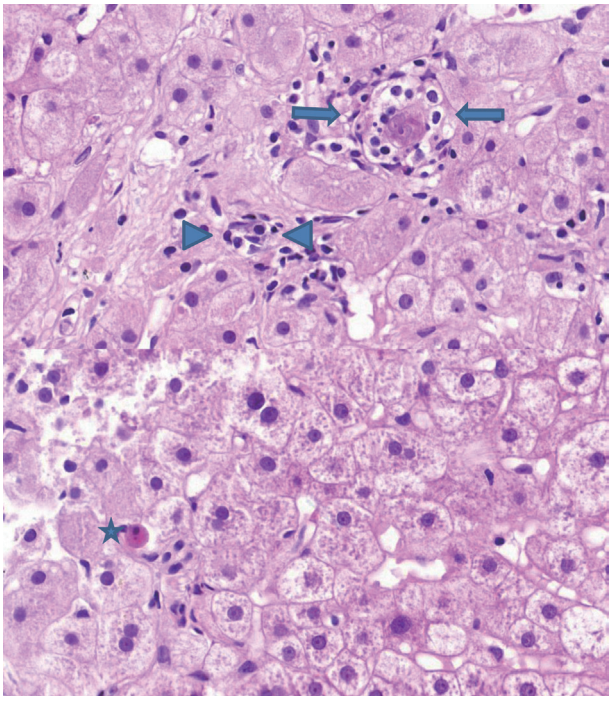

Fig. 2. Lobular inflammation. A focus spotty necrosis of hepatocytes (arrows), lymphocyte aggregation (arrowheads), and acidophilic bodies (asterisk) can be seen.

(4) Fibrosis: mild fibrosis should be carefully distinguished from the normal framework around the central area. Only obvious fibrosis with pericellular collagen deposition should be considered as existence of fibrosis (Fig. 5).

(5) Mallory's body: Mallory's body should be defined as a definite eosinophilic lump in the cytoplasm (Fig. 3B).

(6) Microvesicular fatty changes: these are defined as lipoblast-like features showing centrally located nucleus and numerous intracytoplasmic micro-fat vacuoles inducing nuclear indentation. Microvesicular fatty changes should be carefully differentiated from cells having small- or medium-sized fat vacuoles without cytoplasmic enlargement and nuclear indentation, as mentioned by Yeh and Brunt (Fig. 6).[21]

All kappa values increased in the second review based on the above criteria. In particular, kappa values for the four major parameters increased from 0.3830 to 0.5638 for steatosis grade, from 0.1398 to 0.2815 for lobular inflammation, from 0.1923 to 0.3362 for ballooning degeneration, and from 0.3303 to 0.4664 for fibrosis.

This increased agreement likely resulted from the consensus

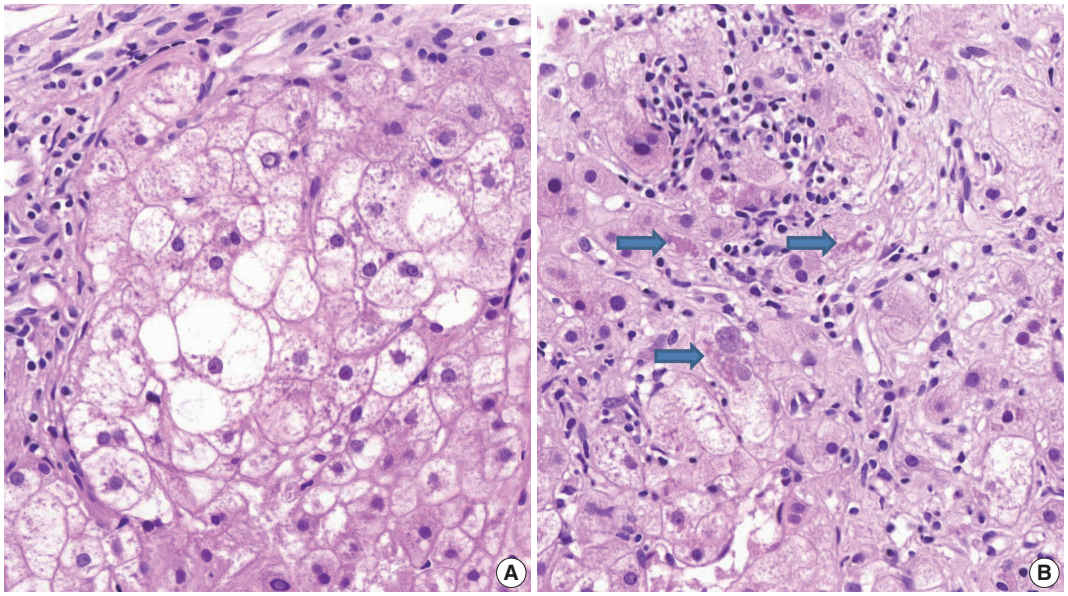

Fig. 3. Ballooning degeneration. (A) Group of enlarged round cells with loss of polygonal features and heterogeneous granular cytoplasm are noted. (B) Ballooning degeneration with cytoplasmic Mallory's bodies (arrows) are found.

http://dx.doi.org/10.4132/jptm.2016.03.01

meeting and the determination of more detailed histomorphologic criteria. However, the method used in the second review is more familiar to most pathologists and may have also contributed to increased agreement. Despite the differences in review method (virtual vs glass), there is no doubt that the exact histomorphologic criteria of NAFLD remain ambiguous and con-

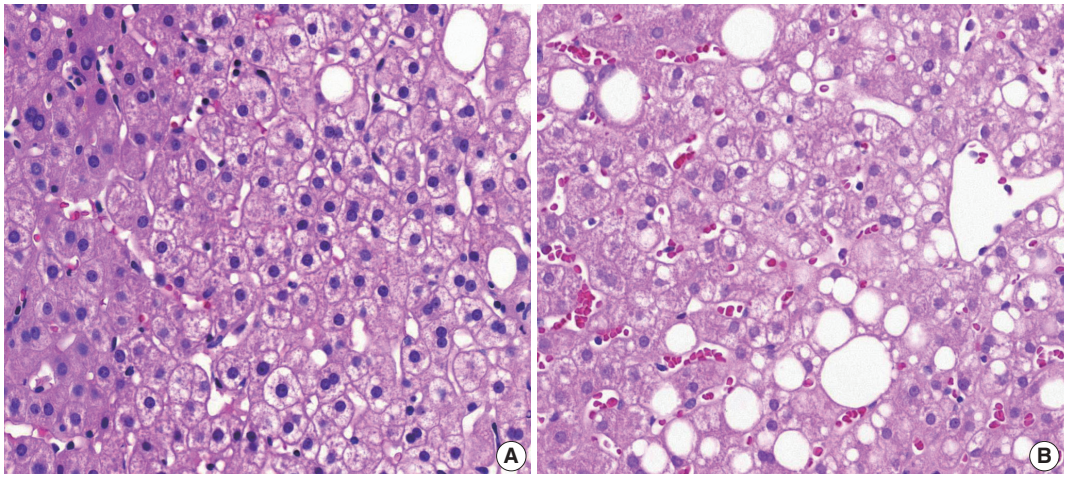

Fig. 4. Mimickers of ballooning degeneration. (A, B) Hydropic swelling and microvesicular fatty changes mimicking ballooning degeneration.

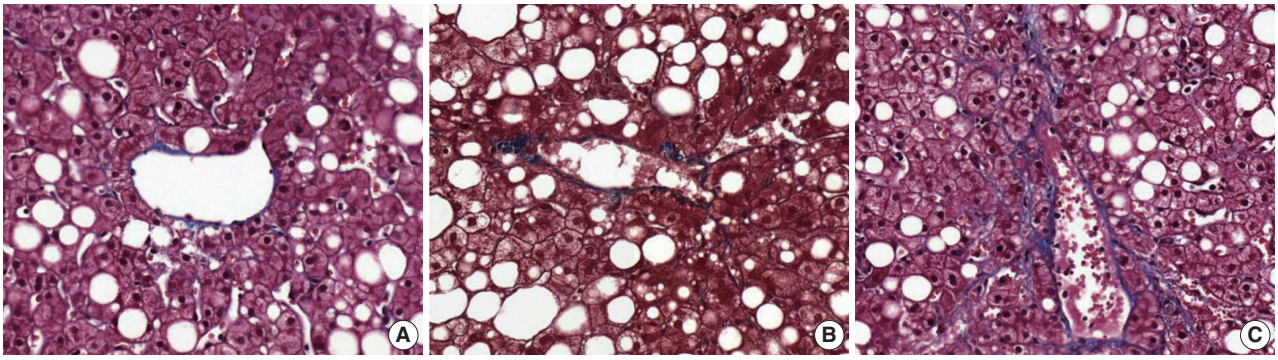

Fig. 5. Fibrosis around the central area (A), normal framework (B), normal range framework without pericelluar collagen deposition (C), and mild perisinusoidal fibrosis with definite pericellular collagen deposition.

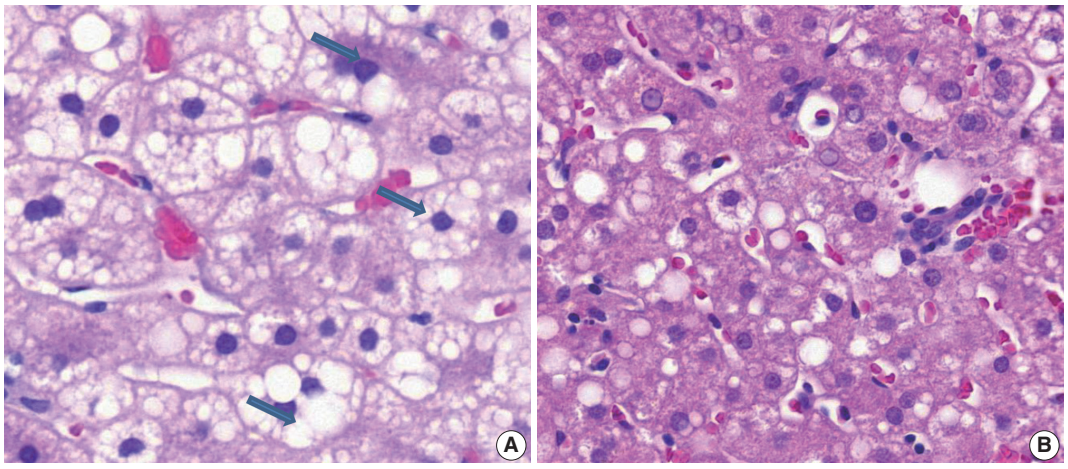

Fig. 6. Microvesicular steatosis. (A) Microvesicular fatty changes including lipoblast-like features showing numerous intracytoplasmic micro-fat vacuoles with nuclear indentation (arrows). (B) Excluding small- or medium-sized fat vacuoles without cytoplasmic enlargement and nuclear indentation should not be confused with microvesicular steatosis.

tribute to low interobserver agreement between pathologists.

Therefore, our more detailed suggestions for NAFLD histomorphologic criteria—including steatosis grade, lobular inflammation, ballooning degeneration, and fibrosis, as mentioned above—will increase the accuracy of diagnosis and grading of NAFLD and improve interobserver agreement. Through this work and recommendations, we expect that a more exact basis for research of NAFLD and development of a new grading and scoring system will follow.

Conflicts of Interest

No potential conflict of interest relevant to this article was reported.

Acknowledgments

This study was supported by the Academic Research Fund 2012 from the Korean Society of Pathologists. We appreciate all members of the Gastrointestinal Pathology Study Group of the Korean Society of Pathologists, particularly Kyung Bun Lee for statistical analysis and Eunsil Yu for scanning the virtual slides.

REFERENCES

1. Brunt EM, Tiniakos DG. Pathology of steatohepatitis. Best Pract Res Clin Gastroenterol 2002; 16: 691-707.
2. Lee RG. Nonalcoholic steatohepatitis: a study of 49 patients. Hum Pathol 1989; 20: 594-8.
3. Powell EE, Cooksley WG, Hanson R, Searle J, Halliday JW, Powell LW. The natural history of nonalcoholic steatohepatitis: a follow-up study of forty-two patients for up to 21 years. Hepatology 1990; 11: 74-80.
4. Teli MR, James OF, Burt AD, Bennett MK, Day CP. The natural history of nonalcoholic fatty liver: a follow-up study. Hepatology 1995; 22: 1714-9.
5. Ong JP, Younossi ZM. Epidemiology and natural history of NAFLD and NASH. Clin Liver Dis 2007; 11: 1-16.
6. Dunn W, Xu R, Wingard DL, *et al*. Suspected nonalcoholic fatty liver disease and mortality risk in a population-based cohort study. Am J Gastroenterol 2008; 103: 2263-71.
7. Ong JP, Pitts A, Younossi ZM. Increased overall mortality and liver-related mortality in non-alcoholic fatty liver disease. J Hepatol 2008; 49: 608-12.
8. Carter-Kent C, Yerian LM, Brunt EM, *et al*. Nonalcoholic steatohepatitis in children: a multicenter clinicopathological study. Hepatology 2009; 50: 1113-20.
9. Musso G, Gambino R, Cassader M, Pagano G. A meta-analysis of randomized trials for the treatment of nonalcoholic fatty liver disease. Hepatology 2010; 52: 79-104.
10. Starley BQ, Calcagno CJ, Harrison SA. Nonalcoholic fatty liver disease and hepatocellular carcinoma: a weighty connection. Hepatology 2010; 51: 1820-32.
11. Abrams GA, Kunde SS, Lazenby AJ, Clements RH. Portal fibrosis and hepatic steatosis in morbidly obese subjects: a spectrum of nonalcoholic fatty liver disease. Hepatology 2004; 40: 475-83.
12. Adams LA, Sanderson S, Lindor KD, Angulo P. The histological course of nonalcoholic fatty liver disease: a longitudinal study of 103 patients with sequential liver biopsies. J Hepatol 2005; 42: 132-8.
13. Xanthakos S, Miles L, Bucuvalas J, Daniels S, Garcia V, Inge T. Histologic spectrum of nonalcoholic fatty liver disease in morbidly obese adolescents. Clin Gastroenterol Hepatol 2006; 4: 226-32.
14. Brunt EM. Pathology of nonalcoholic fatty liver disease. Nat Rev Gastroenterol Hepatol 2010; 7: 195-203.
15. Kleiner DE, Brunt EM. Nonalcoholic fatty liver disease: pathologic patterns and biopsy evaluation in clinical research. Semin Liver Dis 2012; 32: 3-13.
16. Brunt EM, Janney CG, Di Bisceglie AM, Neuschwander-Tetri BA, Bacon BR. Nonalcoholic steatohepatitis: a proposal for grading and staging the histological lesions. Am J Gastroenterol 1999; 94: 2467-74.
17. Kleiner DE, Brunt EM, Van Natta M, *et al*. Design and validation of a histological scoring system for nonalcoholic fatty liver disease. Hepatology 2005; 41: 1313-21.
18. Ludwig J, Viggiano TR, McGill DB, Oh BJ. Nonalcoholic steatohepatitis: Mayo Clinic experiences with a hitherto unnamed disease. Mayo Clin Proc 1980; 55: 434-8.
19. Matteoni CA, Younossi ZM, Gramlich T, Boparai N, Liu YC, McCullough AJ. Nonalcoholic fatty liver disease: a spectrum of clinical and pathological severity. Gastroenterology 1999; 116: 1413-9.
20. Promrat K, Lutchman G, Uwaifo GI, *et al*. A pilot study of pioglitazone treatment for nonalcoholic steatohepatitis. Hepatology 2004; 39: 188-96.
21. Yeh MM, Brunt EM. Pathology of nonalcoholic fatty liver disease. Am J Clin Pathol 2007; 128: 837-47.

Journal of Pathology and Translational Medicine 2016; 50: 197-203
http://dx.doi.org/10.4132/jptm.2016.03.09

■ ORIGINAL ARTICLE ■

Non-small Cell Lung Cancer with Concomitant *EGFR*, *KRAS*, and *ALK* Mutation: Clinicopathologic Features of 12 Cases

Taebum Lee · Boram Lee
Yoon-La Choi · Joungho Han
Myung-Ju Ahn[1] · Sang-Won Um[2]

Department of Pathology, [1]Division of Hematology-Oncology, Department of Medicine, [2]Division of Pulmonary and Critical Care Medicine, Department of Medicine, Samsung Medical Center, Sungkyunkwan University School of Medicine, Seoul, Korea

Received: January 4, 2016
Revised: March 7, 2016
Accepted: March 9, 2016

Corresponding Author
Joungho Han, MD
Department of Pathology, Samsung Medical Center, Sungkyunkwan University School of Medicine, 81 Irwon-ro, Gangnam-gu, Seoul 06351, Korea
Tel: +82-2-3410-2800
Fax: +82-2-3410-0025
E-mail: hanjho@skku.edu

Background: Although epidermal growth factor receptor (*EGFR*), v-Ki-ras2 Kirsten rat sarcoma viral oncogene (*KRAS*), and anaplastic lymphoma kinase (*ALK*) mutations in non-small cell lung cancer (NSCLC) were thought to be mutually exclusive, some tumors harbor concomitant mutations. Discovering a driver mutation on the basis of morphologic features and therapeutic responses with mutation analysis can be used to understand pathogenesis and predict resistance in targeted therapy. **Methods:** In 6,637 patients with NSCLC, 12 patients who had concomitant mutations were selected and clinicopathologic features were reviewed. Clinical characteristics included sex, age, smoking history, previous treatment, and targeted therapy with response and disease-free survival. Histologic features included dominant patterns, nuclear and cytoplasmic features. **Results:** All patients were diagnosed with adenocarcinoma and had an *EGFR* mutation. Six patients had concomitant *KRAS* mutations and the other six had *ALK* mutations. Five of six *EGFR-KRAS* mutation patients showed papillary and acinar histologic patterns with hobnail cells. Three of six received EGFR tyrosine kinase inhibitor (TKI) and showed partial response for 7–29 months. All six *EGFR-ALK* mutation patients showed solid or cribriform patterns and three had signet ring cells. Five of six *EGFR-ALK* mutation patients received EGFR TKI and/or ALK inhibitor and four showed partial response or stable disease, except for one patient who had acquired an *EGFR* mutation. **Conclusions:** *EGFR* and *ALK* mutations play an important role as driver mutations in double mutated NSCLC, and morphologic analysis can be used to predict treatment response.

Key Words: Carcinoma, non-small-cell lung; Receptor, epidermal growth factor; KRAS; Anaplastic lymphoma kinase; Targeted therapy

Genetic alterations in non-small cell lung cancer (NSCLC) have been identified in recent years.[1-4] Epidermal growth factor receptor (*EGFR*), v-Ki-ras2 Kirsten rat sarcoma viral oncogene (*KRAS*), and anaplastic lymphoma kinase (*ALK*) are the most commonly mutated oncogenes that involve the pathogenesis of lung cancer as "genetic drivers." Advanced NSCLC has a dismal prognosis with a short median overall survival,[5] but several selective EGFR tyrosine kinase inhibitors (TKIs) and an ALK inhibitor show effectiveness as personalized target therapy in patients who harbor those specific genetic mutations.[3,6] According to guidelines from the College of American Pathologists, the International Association for the Study of Lung Cancer (IASLC) and the Association for Molecular Pathology, mutation analysis is recommended and recent studies have demonstrated the cost-effectiveness of genetic screening, especially in Asians, who have a higher prevalence of *EGFR* mutations.[7,8]

Chromosomal alterations, closely related to unique histologic phenotypes through protein expression, determine differentiation, patterns, and cell types. The identification of typical morphological features of certain mutations allows retrospective speculation on underlying genetic alterations. Although *EGFR*, *KRAS*, and *ALK* mutations have generally been considered mutually exclusive in NSCLCs,[9] some cases harbor double mutations in a single tumor.[10-13] Identifying driver oncogenes in double-mutated tumors through morphologic differences and comparing the responsiveness of targeted therapies can help explain the pathogenesis of lung cancer and predict resistance to targeted therapy. Hence, we explored histologic features and genetic drivers of tumors with concomitant mutations and discovered the dominant mutation in carcinogenesis for each.

MATERIALS AND METHODS

A retrospective review was performed of biopsied and/or sur-

pISSN 2383-7837
eISSN 2383-7845

gically resected cases diagnosed as NSCLC and tested for *EGFR*, *KRAS*, and *ALK* mutations in the Department of Pathology and Translational Genomics at Samsung Medical Center, Seoul, Korea from 2006 to 2014. Of 6,637 NSCLC patients, 6,595 *EGFR*, 5,177 *KRAS*, and 4,869 *ALK* mutation tests were performed. Among them, 2,387 patients (36.2%) had *EGFR*, 398 (7.7%) had *KRAS*, and 281 (5.8%) had *ALK* mutations. Based on these tests, we selected 12 patients with concomitant mutations in the same tumor.

Clinical data, including gender, age, smoking history, and previous concurrent chemoradiation therapy history were extracted from electronic medical records. All hematoxylin and eosin stained slides of selected cases were reviewed by two pathologists (T.L. and B.L.). Histologic classification was made according to the IASLC/American Thoracic Society (ATS)/European Respiratory Society (ERS) International Multidisciplinary Classification of Lung Adenocarcinoma, and typical pathologic features were re-evaluated, including cell type, nuclear and cytoplasmic characteristics.

We used two methods to evaluate *EGFR* mutations in the 18th, 19th, 20th, and 21st exon: Sanger sequencing and real time polymerase chain reaction after peptide nucleic acid (PNA)–clamping using the PNA clamping EGFR Mutation Detection Kit (Panagene, Inc., Daejeon, Korea). *KRAS* mutations were evaluated with Sanger sequencing in the 12th and 13th exon. Extracted genomic DNA isolated from formalin-fixed paraffin-embedded (FFPE) tissue was used for *EGFR* and *KRAS* analyses. *ALK* mutation tests were performed using immunohistochemical (IHC) (1:40, NCL-ALK, clone 5A4, Novocastra, Newcastle upon Tyne, UK) and fluorescence *in situ* hybridization (FISH) analysis (LSI ALK dual color break-apart probe, Dako, Glostrup, Denmark) with FFPE tissue. Diffuse strong positivity in the cytoplasm was regarded as positive in ALK IHC. In the FISH analysis, 50 non-overlapping nuclei were counted and 15% of break-apart probes were used as a cutoff value for positivity. Diffuse strong positive ALK IHC results were interpreted as a surrogate marker of *ALK* rearrangement.[14]

RESULTS

Clinical characteristics

Clinical data and pathologic features of the 12 patients with concomitant mutations are summarized in Table 1. The age at diagnosis of patients ranged from 48 to 78 years old (median, 62 years old) and 75% of patients were female. All three male patients had a history of smoking (15–57 pack-years) in contrast to none of female patients. Five surgically resectable patients underwent lobectomy and seven clinical stage IV patients had a needle aspiration or biopsy from the lung, bronchus, lymph node, or adrenal gland.

Patient No. 5 received EGFR TKI targeted therapy for bone metastasis at 15 months after lobectomy. Patient No. 6 refused treatment with chemo- or targeted therapy and patient No. 7 had a history of lobectomy at an outside hospital without any other treatment 9 years prior to the lymph node biopsy. Patient No. 10 received neoadjuvant concurrent chemoradiation therapy prior to surgery. Patient No. 12 previously underwent lobectomy and was treated with gefitinib for 1 month and crizotinib for 4 months in China. She had no *EGFR* or *KRAS* mutation at the time of diagnosis at China. Aside from this patient, all other patients had no history of prior targeted therapy before mutation testing.

Mutational and histologic characteristics

All 12 patients were diagnosed with adenocarcinoma and had an *EGFR* mutation. *EGFR* mutations of three patients were only detected with the PNA clamping method, while nine were confirmed by Sanger sequencing. Five (41.7%) had the missense L858R mutation in exon 21, four (33.3%) had the missense G719X mutation in exon 18, and three (25%) had a deletion in exon 19. Patient No. 8 had the L858R and G719X mutations at the same time and patient No. 12 had a missense R803W mutation at exon 20 that was not identified before targeted therapy at the outside hospital. No patient had a T790M point mutation, which is associated with resistance. Six patients had additional *KRAS* mutations and the other six had an *ALK* mutation (referred to as '*EGFR-KRAS*' and '*EGFR-ALK*' hereafter). Three among the six patients who showed positivity at ALK IHC were confirmed with FISH analysis.

EGFR-KRAS and *EGFR-ALK* tumors showed distinct morphologic characteristics. Six *EGFR-KRAS* patients had papillary, acinar, solid, and micropapillary patterns (Fig. 1). Among them, five patients had typical hobnail cell features with apical snouts; the remaining patient (patient No. 2) underwent needle aspiration and did not show any typical cell features. One patient (patient No. 4) had a focal columnar cell component and intra- and extracytoplasmic mucin, which are similar morphologic features of NSCLC with a *KRAS* mutation. The other five patients did not show any mucin. Two of the six patients had intranuclear inclusions.

In contrast, six *EGFR-ALK* patients showed solid, cribriform and micropapillary patterns. Three of six patients had signet ring

 http://dx.doi.org/10.4132/jptm.2016.03.09

Table 1. Clinicopathologic features of 12 patients with double mutated pulmonary adenocarcinoma

Patient No.	Sex/ Age (yr)	Smoking	Specimen	Stage	*EGFR* mutation	Additional mutation	Dominant pattern	Typical cell feature	Mucin	Intranuclear inclusion	Surgery	Targeted therapy	Response	Status	PFS (mo)
1	M/74	57PY	Lung/R	pT1bN1	E21 L858R	*KRAS* I21S	Papillary and micropapillary	Hobnail cells	No	No	+	-	-	DOD[a]	-
2	F/62	Never	Lung/A	M1(IV)	E21 L858R	*KRAS* G12D	[b]	No	No	Present		Gefitinib	PR → PD	DOD	7
3	F/63	Never	Lung/R	pT1bN0	E21 L858R	*KRAS* G13A	Papillary and acinar	Hobnail cells	No	No	+	-	-	NED	-
4	F/48	Never	Lung/R	pT1bN2	E19 deletion	*KRAS* G12V	Acinar and solid	Hobnail and columnar cells	Intra- and extracytoplasmic	No	+	Erlotinib	PR → PD	DOD	20
5	M/55	20PY	Lung/R	pT2N2	E19 deletion	*KRAS* G13C	Solid and acinar	Hobnail cells	No	Present	+	Gefitinib	PR	AWD	29
6	F/78	Never	Lung/B	M1(IV)	E18 G719X	*KRAS* G12D	Papillary and acinar	Hobnail cells	No	No	-	(refused)	-	AWD[a]	-
7	F/62	Never	LN/B	M1(IV)	E21 L858R[c]	*ALK*	Solid and cribriform	Signet ring cells	Intracytoplasmic	No	+[d]	Gefitinib	PR	AWD[a]	18[e]
8	F/62	Never	Lung/B	M1(IV)	E21 L858R E18 G719X	*ALK*	Solid and cribriform	No	No	No	-	Gefitinib and Crizotinib	SD and PR	AWD	24
9	M/56	15PY	Lung/B	M1(IV)	E18 G719X[c]	*ALK*	Solid	No	No	No		Crizotinib	SD	DOD	4
10	F/68	Never	Lung/R	ypT2N2	E18 G719X[c]	*ALK*	Solid, micropapillary and cribriform	Signet ring cells	Intra- and extracytoplasmic	Present	+	-	-	NED	-
11	F/58	Never	Lung/B	M1(IV)	E19 deletion	*ALK*	Solid	Signet ring cells	Intracytoplasmic	No	-	Crizotinib	-	AWD[a]	[e]
12	F/66	Never	Adrenal/B	M1(IV)	E20 R803W	*ALK*	Solid	No	No	No	+[d]	Erlotinib	PD	AWD[a]	0.7

EGFR, epidermal growth factor receptor; PFS, progression-free survival; M, male; PY, pack-year; R, resection; E, exon; KRAS, v-Ki-ras2 Kirsten rat sarcoma viral oncogene; DOD, died of disease; F, female; A, aspiration; PR, partial response; PD, progressive disease; NED, no evidence of disease; AWD, alive with disease; B, biopsy; LN, lymph node; ALK, anaplastic lymphoma kinase; SD, stable disease.
[a]Lost to follow-up; [b]Cannot identify dominant architectural patterns in an aspiration slide; [c]Mutation detected only in PNA clamping method; [d]Have a history of lobectomy at outside hospital, prior to biopsy of metastatic lesion; [e]Cannot evaluate due to lost to follow-up.

cells and intracytoplasmic mucin with or without extracytoplasmic mucin production, which are typical features of *ALK*-positive NSCLC. The others did not show any typical cell features or mucins. One patient had intranuclear inclusions.

Treatment responses and follow-up status

Seven patients had surgical resection and two were alive without targeted therapy and any evidence of relapse or progression, including one patient who received neoadjuvant concurrent chemoradiation therapy. One patient who had surgery and de-

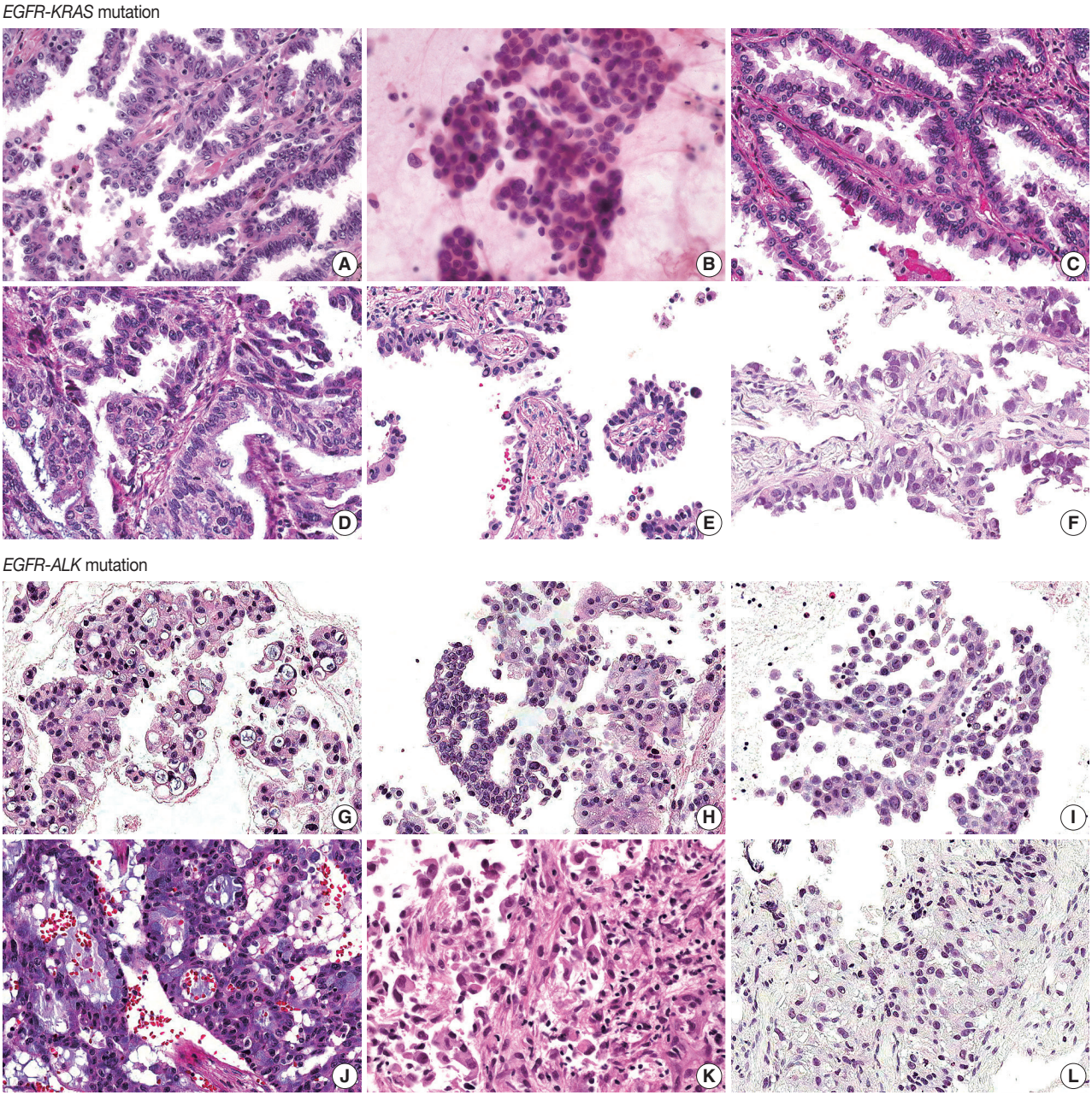

Fig. 1. Histologic features of 12 pulmonary adenocarcinomas with concomitant mutations. (A–F) In the six *EGFR-KRAS* patients, patients No. 1 (A), No. 3 (C), No. 5 (E), and No. 6 (F) have papillary, micropapillary and acinar patterns with hobnail cells. (D) Patient No. 4 has an acinar pattern and hobnail cells for the most part but shows focal columnar cells with intra- and extracellular mucin. (B) Patient No. 2 does not show any typical cell features. (G–L) In the six *EGFR-ALK* patients, all patients show solid, cribriform or micropapillary patterns rather than the papillary or acinar patterns that are easily identified as *EGFR-KRAS* tumors. Patients No. 7 (G), No. 10 (J), and No. 11 (K) have signet ring cells with intra- or extracytoplasmic mucin. But in the other three patients, No. 8 (H), No. 9 (I), and No. 12 (L), typical cell features are not identified, as neither signet ring cells nor hobnail cells. *EGFR*, epidermal growth factor receptor; *KRAS*, v-Ki-ras2 Kirsten rat sarcoma viral oncogene; *ALK*, anaplastic lymphoma kinase.

http://dx.doi.org/10.4132/jptm.2016.03.09

cided not to receive targeted therapy due to old age and underlying diabetes mellitus died of disease after 53 months from surgery (patient No. 1).

EGFR TKI included gefitinib (250 mg, orally, every day) and erlotinib (150 mg, orally, every day) and the ALK inhibitor was crizotinib (250 mg, orally, every day or twice daily). Three among six *EGFR-KRAS* patients received targeted therapy with EGFR TKI. All three patients showed partial responses, but two also showed disease progression after 7 and 20 months. In the *EGFR-ALK* patients, two were treated with EGFR TKI, two with ALK inhibitor and one received both EGFR TKI and ALK inhibitor therapy. Most patients treated with ALK inhibitor or EGFR TKI showed partial response or stable disease, but patient No. 12 with EGFR TKI showed progressive disease.

DISCUSSION

Concomitant genetic alteration of NSCLC is unusual because *EGFR*, *KRAS*, and *ALK* mutations are widely known as mutually exclusive. Most are associated with acquired mutation after targeted therapy and are related to drug resistance. In previous studies, two different hypotheses were proposed to explain dual mutation in NSCLC.[12] Underlying intratumoral heterogeneity of *EGFR* mutations,[15] different tumor cells may have different oncogenic driver mutations. Some authors have also suggested coexistence of mutations in the same tumor cells using IHC expression and mutation-specific antibodies.[12,16]

EGFR, as a growth factor membrane-bound receptor tyrosine kinase, controls cell proliferation and survival. Approximately 36% of patients with NSCLC in East Asia have *EGFR* mutations and 90% of mutations are exon 21 L858R or exon 19 deletion.[17] These mutations increase tyrosine kinase activity, resulting in hyperactivation of the RAS-RAF-MEK-ERK pathway, which regulates cell proliferation, and the phosphoinositide 3-kinase–AKT–mammalian target of rapamycin pathway, which is associated with cell survival. RAS proteins are central mediators in EGFR tyrosine kinase signaling and also associated with cell proliferation and differentiation. In particular, *KRAS* mutations are common in lung cancer but less common in East Asia than in Western countries.[18] ALK is a receptor tyrosine kinase. *ALK* fusion with various N-terminal fusion partners stimulates kinase activity, and signaling of these mutations are involved in cell growth, proliferation and apoptosis. Among NSCLCs, 3%–7% harbor *ALK* fusion[3,4] and the majority of these fusions are associated with the echinoderm microtubule-associated protein-like 4 (*EML4*) gene. *EML4-ALK* fusions are associated with EGFR TKI resistance.[19]

Typical histologic features of lung cancer with *EGFR*, *KRAS*, and *ALK* mutations have been described.[20-24] All of these mutations are frequent in adenocarcinoma and *EGFR* mutations are more common in tumors with papillary, micropapillary, acinar, and lepidic patterns than in others. Hobnail cell type and intranuclear inclusion are typical nuclear features of *EGFR* mutation-harboring tumors. A solid pattern and mucinous type are more frequent in *KRAS* mutation tumors. Extracellular mucin production, cribriform patterns, and signet ring cell features are more common in *ALK* mutation tumors.

In this study, we analyzed six *EGFR-KRAS* (1.5%) and six *EGFR-ALK* patients (2.1%) among *KRAS* and *ALK* mutation-positive NSCLC patients. The majority of *EGFR-KRAS* tumors showed typical histologic features of *EGFR* mutation, except one case which had focal morphologic features similar to *KRAS* mutation. In a previous study, NSCLC harboring a *KRAS* mutation showed resistance to EGFR TKI and adjuvant chemotherapy.[2] In our study, however, three patients showed partial response to gefitinib and erlotinib for 7–29 months. Intratumoral heterogeneity of the mutation may explain this discordance between coexistent *KRAS* mutation and response to EGFR TKI therapy. Patient No. 2 had short progression-free survival (PFS) and disease progressed rapidly, while the other two patients had 20–29 months of PFS. Based on the evidence of morphologic phenotypes and responsiveness to targeted therapy, we expected these two patients to have coexistent mutations in the same tumor cells, and hypothesized that the *EGFR* mutation was the dominant driver oncogene in lung cancer, even if the tumor cells harbored an additional *KRAS* mutation.

In *EGFR-ALK* patients, some previous studies have shown acquired *EGFR* mutations as a mechanism of resistance to ALK inhibitor therapy.[25,26] In our case, patient No. 12 had no *EGFR* or *KRAS* mutation and was treated with crizotinib in an outside hospital. After 4 months of ALK-targeted therapy, she acquired an additional *EGFR* mutation and showed poor response to erlotinib, which is consistent with previous studies. In the other four patients, however, diverse responses were identified with no resistance to gefitinib or crizotinib. Conflicting results of responsiveness to EGFR TKI and ALK inhibitor in *EGFR-ALK* patients in NSCLC have been reported in a few limited studies.[10,27] Recently, Yang *et al*.[16] investigated relationships between receptor phosphorylation and response to targeted therapy, and suggested that relative phospho-EGFR and ALK levels can be used to predict response.

Although the G719X mutation accounts for about 7% of

EGFR mutated NSCLC in East Asia,[17] three of five *EGFR-ALK* patients had the *EGFR* exon 18 G719X missense mutation in our study. In addition, three of five *EGFR-ALK* patients showed typical histologic features of ALK-expressing adenocarcinoma. From these findings, we suspect that the *ALK* mutation determines morphological phenotypes and acts as a driver oncogene, and the *EGFR* mutation may also play an important role in oncogenesis. Accordingly, based on evaluation of the signaling pathway, including phosphorylation of receptor kinase, the modification or combination of EGFR TKI and ALK inhibitor offer promising treatments.

The small number of cases limited our analysis. Baldi *et al*.[12] revealed the possibility of more frequent concomitant mutations than expected and Won *et al*.[13] reported an increased proportion of NSCLC harboring concomitant *EGFR* and *ALK* mutations from 4.4% to 15.4% using more sensitive methods such as targeted next-generation sequencing (NGS) and mutant-enriched NGS. Greater numbers of previously undisclosed concomitantly mutated tumors can be identified using more sensitive and advanced techniques. Some authors also suggest that tumor burden of each mutation affects responses to targeted therapy. There may be a limitation to evaluating mutations from biopsy specimens, but the majority of patients who need to receive targeted therapy might be clinically unresectable and may only be diagnosed with biopsy. Thus, the expectation of tumor burden in a limited biopsy specimen is unfavorable.

To the best of our knowledge, this is the first study to describe double mutated NSCLC with histologic findings. Morphologic findings might help predict underlying driver mutations and further studies are warranted.

In conclusion, we investigated genetic driver mutations in 12 double mutated NSCLCs with analysis of clinical and pathologic features. The majority of *EGFR-KRAS* tumors showed typical histologic patterns and cell features of *EGFR*-mutated tumors and partially responded to EGFR TKI. In *EGFR-ALK* tumors, however, some showed *ALK*-mutated features and partially responded to ALK inhibitor or EGFR TKI. EGFR and ALK play an important role in the oncogenesis of NSCLC and tumor morphology can provide important clues to predict treatment response. We suggest that patients with histologic features of *EGFR* mutations can be treated with EGFR TKI, even with coexistence of a *KRAS* mutation. We also suggest that *EGFR-ALK* patients should have underlying mutational pathways evaluated and be treated with a selection and/or combination of ALK inhibitor and EGFR TKI. Further studies are needed to support these interesting findings.

Conflicts of Interest

No potential conflict of interest relevant to this article was reported.

Acknowledgments

This research was supported by a grant from the Korean Society of Pathologists (KSP).

REFERENCES

1. Lynch TJ, Bell DW, Sordella R, *et al*. Activating mutations in the epidermal growth factor receptor underlying responsiveness of non-small-cell lung cancer to gefitinib. N Engl J Med 2004; 350: 2129-39.
2. Riely GJ, Marks J, Pao W. *KRAS* mutations in non-small cell lung cancer. Proc Am Thorac Soc 2009; 6: 201-5.
3. Kwak EL, Bang YJ, Camidge DR, *et al*. Anaplastic lymphoma kinase inhibition in non-small-cell lung cancer. N Engl J Med 2010; 363: 1693-703.
4. Soda M, Choi YL, Enomoto M, *et al*. Identification of the transforming *EML4-ALK* fusion gene in non-small-cell lung cancer. Nature 2007; 448: 561-6.
5. Siegel RL, Miller KD, Jemal A. Cancer statistics, 2015. CA Cancer J Clin 2015; 65: 5-29.
6. Paez JG, Jänne PA, Lee JC, *et al*. *EGFR* mutations in lung cancer: correlation with clinical response to gefitinib therapy. Science 2004; 304: 1497-500.
7. Lindeman NI, Cagle PT, Beasley MB, *et al*. Molecular testing guideline for selection of lung cancer patients for EGFR and ALK tyrosine kinase inhibitors: guideline from the College of American Pathologists, International Association for the Study of Lung Cancer, and Association for Molecular Pathology. J Thorac Oncol 2013; 8: 823-59.
8. Narita Y, Matsushima Y, Shiroiwa T, *et al*. Cost-effectiveness analysis of *EGFR* mutation testing and gefitinib as first-line therapy for non-small cell lung cancer. Lung Cancer 2015; 90: 71-7.
9. Gainor JF, Varghese AM, Ou SH, *et al*. *ALK* rearrangements are mutually exclusive with mutations in *EGFR* or *KRAS*: an analysis of 1,683 patients with non-small cell lung cancer. Clin Cancer Res 2013; 19: 4273-81.
10. Tiseo M, Gelsomino F, Boggiani D, *et al*. *EGFR* and *EML4-ALK* gene mutations in NSCLC: a case report of erlotinib-resistant patient with both concomitant mutations. Lung Cancer 2011; 71: 241-3.
11. Lee JK, Kim TM, Koh Y, *et al*. Differential sensitivities to tyrosine kinase inhibitors in NSCLC harboring *EGFR* mutation and *ALK*

translocation. Lung Cancer 2012; 77: 460-3.
12. Baldi L, Mengoli MC, Bisagni A, Banzi MC, Boni C, Rossi G. Concomitant *EGFR* mutation and *ALK* rearrangement in lung adenocarcinoma is more frequent than expected: report of a case and review of the literature with demonstration of genes alteration into the same tumor cells. Lung Cancer 2014; 86: 291-5.
13. Won JK, Keam B, Koh J, *et al*. Concomitant *ALK* translocation and *EGFR* mutation in lung cancer: a comparison of direct sequencing and sensitive assays and the impact on responsiveness to tyrosine kinase inhibitor. Ann Oncol 2015; 26: 348-54.
14. Paik JH, Choe G, Kim H, *et al*. Screening of anaplastic lymphoma kinase rearrangement by immunohistochemistry in non-small cell lung cancer: correlation with fluorescence *in situ* hybridization. J Thorac Oncol 2011; 6: 466-72.
15. Bai H, Wang Z, Wang Y, *et al*. Detection and clinical significance of intratumoral *EGFR* mutational heterogeneity in Chinese patients with advanced non-small cell lung cancer. PLoS One 2013; 8: e54170.
16. Yang JJ, Zhang XC, Su J, *et al*. Lung cancers with concomitant *EGFR* mutations and *ALK* rearrangements: diverse responses to EGFR-TKI and crizotinib in relation to diverse receptors phosphorylation. Clin Cancer Res 2014; 20: 1383-92.
17. Choi YL, Sun JM, Cho J, *et al*. *EGFR* mutation testing in patients with advanced non-small cell lung cancer: a comprehensive evaluation of real-world practice in an East Asian tertiary hospital. PLoS One 2013; 8: e56011.
18. Sun Y, Ren Y, Fang Z, *et al*. Lung adenocarcinoma from East Asian never-smokers is a disease largely defined by targetable oncogenic mutant kinases. J Clin Oncol 2010; 28: 4616-20.
19. Shaw AT, Yeap BY, Mino-Kenudson M, *et al*. Clinical features and outcome of patients with non-small-cell lung cancer who harbor *EML4-ALK*. J Clin Oncol 2009; 27: 4247-53.
20. Ninomiya H, Hiramatsu M, Inamura K, *et al*. Correlation between morphology and *EGFR* mutations in lung adenocarcinomas significance of the micropapillary pattern and the hobnail cell type. Lung Cancer 2009; 63: 235-40.
21. Rekhtman N, Ang DC, Riely GJ, Ladanyi M, Moreira AL. *KRAS* mutations are associated with solid growth pattern and tumor-infiltrating leukocytes in lung adenocarcinoma. Mod Pathol 2013; 26: 1307-19.
22. Nishino M, Klepeis VE, Yeap BY, *et al*. Histologic and cytomorphologic features of *ALK*-rearranged lung adenocarcinomas. Mod Pathol 2012; 25: 1462-72.
23. Ha SY, Choi SJ, Cho JH, *et al*. Lung cancer in never-smoker Asian females is driven by oncogenic mutations, most often involving EGFR. Oncotarget 2015; 6: 5465-74.
24. Choi IH, Kim DW, Ha SY, Choi YL, Lee HJ, Han J. Analysis of histologic features suspecting anaplastic lymphoma kinase (ALK)-expressing pulmonary adenocarcinoma. J Pathol Transl Med 2015; 49: 310-7.
25. Sasaki T, Koivunen J, Ogino A, *et al*. A novel *ALK* secondary mutation and EGFR signaling cause resistance to *ALK* kinase inhibitors. Cancer Res 2011; 71: 6051-60.
26. Kim S, Kim TM, Kim DW, *et al*. Heterogeneity of genetic changes associated with acquired crizotinib resistance in *ALK*-rearranged lung cancer. J Thorac Oncol 2013; 8: 415-22.
27. Kuo YW, Wu SG, Ho CC, Shih JY. Good response to gefitinib in lung adenocarcinoma harboring coexisting *EML4-ALK* fusion gene and *EGFR* mutation. J Thorac Oncol 2010; 5: 2039-40.

Journal of Pathology and Translational Medicine 2016; 50: 204-210
http://dx.doi.org/10.4132/jptm.2016.03.04

■ ORIGINAL ARTICLE ■

Analysis of Surgical Pathology Data in the HIRA Database: Emphasis on Current Status and Endoscopic Submucosal Dissection Specimens

Sun-ju Byeon · Woo Ho Kim

Department of Pathology, Seoul National University Hospital, Seoul, Korea

Received: January 6, 2016
Revised: February 15, 2016
Accepted: March 4, 2016

Corresponding Author
Woo Ho Kim, MD, PhD
Department of Pathology, Seoul National University Hospital, 103 Daehak-ro, Jongno-gu, Seoul 03080, Korea
Tel: +82-2-740-8269
Fax: +82-2-765-5600
E-mail: woohokim@snu.ac.kr

Background: In Korea, medical institutions make claims for insurance reimbursement to the Health Insurance Review and Assessment Service (HIRA). Thus, HIRA databases reflect the general medical services that are provided in Korea. We conducted two pathology-related studies using a HIRA national patient sample (NPS) data (selection probability, 0.03). First, we evaluated the current status of general pathologic examination in Korea. Second, we evaluated pathologic issues associated with endoscopic submucosal dissection (ESD). **Methods:** The sample data used in this study was HIRA-NPS-2013-0094. **Results:** In the NPS dataset, 163,372 pathologic examinations were performed in 103,528 patients during the year 2013. Considering sampling weight (33.3), it is estimated that 5,440,288 (163,372 × 33.3) pathologic examinations were performed. Internal medicine and general surgery were the most common departments requesting pathologic examinations. The region performing pathologic examinations were different according to type of medical institution. In total, 490 patients underwent ESD, and 43.4% (213/490) underwent ESD due to gastric carcinoma. The results of the ESD led to a change in disease code for 10.5% (29/277) of non-gastric carcinoma patients. In addition, 21 patients (4.3%) underwent surgery following the ESD. The average period between ESD and surgery was 44 days. **Conclusions:** HIRA sample data provide the nation-wide landscape of specific procedure. However, in order to reduce the statistical error, further studies using entire HIRA data are needed.

Key Words: Statistics; Sample size; Pathology; Surgery

In Korea, all medical institutions claim insurance reimbursements for services to the Health Insurance Review and Assessment Service (HIRA). Thus, HIRA databases reflect the general medical services provided in Korea. Since the entire HIRA database is too big to analyze, HIRA provides a specific set of data according to researcher's requests. HIRA also provides some relatively small sized data sets (statistically extracted, anonymized, and annualized) for research and public purposes.[1] These sample data included national patient sample (NPS), a national inpatient sample, an adult patient sample (65 years or older), and a pediatric patient sample. To the best of our knowledge, this is the first pathology-related analysis using HIRA data.

We conducted two pathology-related studies using HIRA-NPS data. First, we analyzed the rate of surgical pathologic examinations in Korea. After Kamegoro Inamoto introduced pathology to Korea in 1914, pathologic examinations have played a major role in medical services for the improvement of overall care.[2] However, research on the frequency of pathologic examinations in this nation as a whole have not been performed due to a restriction on the sharing of personal medical records.

Next, we analyzed the pathologic results of endoscopic submucosal dissection (ESD) specimens. ESD is considered as an initial treatment modality for early and localized gastric carcinoma or benign epithelial neoplasm.[3] We evaluated several ESD-related parameters. After ESD and pathologic examination, surgical treatment is called for in those cases that show tumor cells in the resection margins, endolymphatic tumor emboli, or submucosal invasion.[4] Several papers have been published on this subject, but most of them are from a single institute and so do not incorporate the data of those patients who later went on to undergo additional surgery in different hospitals.[5,6] One of the advantageous features of the HIRA database is that patients can be tracked through several medical institutions, thereby enabling the study of a more complete data set including those that received secondary treatment in one hospital after ESD in another hospital.

MATERIALS AND METHODS

The sample data used in this study was HIRA-NPS-2013-0094.

pISSN 2383-7837
eISSN 2383-7845

This sample was composed of 26 text files, and the total file size was 16.6 gigabytes (GB). The HIRA data tables were composed of five main tables (general specification, healthcare services, diagnosis information, prescriptions, and general information about the medical institutions). Each table was conjoined with proper claim numbers or medical institution numbers. The disease codes were based on the Korean Standard Classification of Disease (KCD). Specifications of the computer that was used to analyze the data were as follows: central processing unit (CPU), i3-2120 3.30 GHz (Intel, Santa Clara, CA, USA); 32 GB main memory; operating system (OS), Ubuntu 14.04.3 long-term support (LTS); and R 3.2.2 analysis software. The pathologic examination codes used in this study are summarized in Table 1. The sample data contained 22,344,536 claims in 1,361,717 patients (selection probability, 0.03; sampling weight, 33.3).

Table 1. Pathologic examination claim codes using in this study

Histologic examination	Code
Biopsy: 1–3 pieces/4–6 pieces/7–9 pieces/10–12 pieces/more than 13 pieces	C5911/C5912/C5913/C5914/C5915
Resected specimen requiring gross sectioning (non-malignant): paraffin blocks ≤6/paraffin blocks ≥7	C5916/C5917
Resected specimen for malignant tumor requiring gross sectioning	
With lymph node dissection: paraffin blocks ≤20/paraffin blocks ≥21	C5918/C5919
Without lymph node dissection: paraffin blocks ≤15/paraffin blocks ≥16	C5500/C5504
Histologic mapping of tumor: with lymph node dissection/without lymph node dissection	C5505/C5508
Emergency histopathologic examination during surgery (frozen section): 1–2 specimens/3–6 specimens/more than 7 specimens	C5511/C5512/C5513
Tissue immunofluorescent microscopic examination: IgG/IgA/IgM/IgE/C3/C4/HbsAg/fibrinogen/others	C5541/C5542/C5543/C5544/C5545/C5549/C5546/C5547/C5548
Tissue electron microscopy	C5550
Enzyme histochemistry: ATPase-pH 9.4/ATPase-pH 4.9/NADH/acetylcholinesterase/chloroacetate esterase/others	C5561/C5562/C5563/C5564/C5565/C5566
Immunohisto(cyto)chemistry	C5575/C5575006
Cervicovaginal smear/Liquid-based cervicovaginal cytology	C5920/CX541
Body fluid: general/cytospin/cell block after cytopathologic examination/liquid-based body fluid cytopathology	C5930/C5931/C5940/CZ521
Aspiration/Aspiration and cell block	C5941/C5942
Liquid-based aspiration cytopathology/Liquid-based aspiration cytopathology and Cell block	C5943/C5944
Flurescence *in situ* hybridization: *HER2* gene	C5967/C5967006
Silver *in situ* hybridization: *HER2* gene	CZ968/CZ968006

HBsAg, hepatitis B surface antigen.

Table 2. Pathologic examinations claims and requesting medical institutions according to administrative districts (sort based on the total number of claims)

Administrative district	Tertiary hospital	General hospital	Other institutions	Total	Total estimates
Seoul	25,547	16,164	12,000	53,711	1,788,576
Gyeonggi-do	1,632	16,203	10,905	28,740	957,042
Busan	3,276	4,877	5,135	13,288	442,490
Daegu	1,164	5,933	5,185	12,282	408,991
Incheon	2,545	2,377	2,465	7,387	245,987
Gyeongsangnam-do	760	3,561	3,053	7,374	245,554
Gwangju	1,211	2,438	1,910	5,559	185,115
Daejeon	970	2,300	1,781	5,051	168,198
Jeollabuk-do	857	1,935	2,162	4,954	164,968
Gyeongsangbuk-do	-	2,252	2,638	4,890	162,837
Jeollanam-do	-	2,655	1,621	4,276	142,391
Chungcheongnam-do	-	2,024	1,861	3,885	129,371
Gangwon-do	850	1,791	1,046	3,687	122,777
Chungcheongbuk-do	573	1,178	1,611	3,362	111,955
Ulsan	-	1,561	1,799	3,360	111,888
Jeju	-	1,135	380	1,515	50,450
Sejong-si	-	-	51	51	1,698
Total	39,385	68,384	55,603	163,372	5,440,288

http://jpatholtm.org/

Table 3. Pathologic examinations requests statuses according to medical departments (sort based on the total number of claims)

Department code	Biopsy	Resection, non-malignant	Resection, malignant (LN/non-LN)	Histologic mapping (LN/non-LN)	Frozen sections	IF	EM	Enzyme	IHC	Uterine cervical examinations (smear/liquid)	Body fluid (conventional/liquid)	Aspiration (conventional/liquid)	HER2 (FISH/SISH)	Total	Total estimates
Internal medicine	40,683	12,463	120 (62/58)	636 (2/634)	85	1,329	184	12	5,248	189 (89/100)	8,219 (5,531/2,688)	5,053 (4,752/301)	11 (6/5)	74,232	2,471,926
General surgery	8,066	9,614	2,893 (2,466/427)	335 (292/43)	1,870	178	31	0	7,495	49 (18/31)	722 (519/203)	3,533 (3,457/76)	22 (3/19)	34,808	1,159,106
Obstetrics and gynecology	5,042	6,090	263 (172/91)	27 (10/17)	236	0	1	0	754	6,413 (1,090/5,323)	351 (198/153)	205 (196/9)	0 (0/0)	19,382	645,421
Urology	1,586	1,245	337 (86/251)	112 (52/60)	148	8	4	0	1,176	108 (26/82)	5,056 (3,030/2,026)	171 (167/4)	0 (0/0)	9,951	331,368
Otorhinolaryngology	721	2,283	333 (229/104)	1 (1/0)	299	0	4	0	686	1 (0/1)	61 (39/22)	709 (667/42)	0 (0/0)	5,098	169,763
Dermatology	2,156	1,270	21 (1/20)	2 (0/2)	28	203	0	2	436	3 (1/2)	20 (20/0)	21 (20/1)	0 (0/0)	4,162	138,595
Orthopedic surgery	750	2,672	44 (5/39)	1 (0/1)	77	5	1	0	193	24 (11/13)	261 (226/35)	63 (61/2)	0 (0/0)	4,091	136,230
Neurosurgery	330	1,062	75 (1/74)	0 (0/0)	183	0	16	0	645	9 (3/6)	207 (124/83)	27 (25/2)	0 (0/0)	2,554	85,048
Thoracic surgery	161	589	251 (199/52)	14 (13/1)	277	0	1	0	502	1 (1/0)	324 (233/91)	35 (26/9)	0 (0/0)	2,155	71,762
Family medicine	905	307	0 (0/0)	0 (0/0)	0	0	0	0	23	16 (5/11)	106 (91/15)	110 (109/1)	0 (0/0)	1,467	48,851
Radiology	541	49	0 (0/0)	0 (0/0)	0	0	0	0	207	5 (3/2)	17 (15/2)	306 (260/46)	0 (0/0)	1,125	37,463
Plastic surgery	50	680	46 (6/40)	9 (7/2)	84	0	0	0	117	0 (0/0)	3 (2/1)	3 (2/1)	0 (0/0)	992	33,034
Pediatrics	227	56	0 (0/0)	0 (0/0)	2	132	24	5	193	0 (0/0)	245 (132/113)	4 (4/0)	0 (0/0)	888	29,570
Neurology	171	58	1 (0/1)	0 (0/0)	5	11	7	18	40	11 (7/4)	337 (225/112)	23 (23/0)	0 (0/0)	682	22,711
Dental department	123	333	8 (4/4)	0 (0/0)	15	17	0	0	27	0 (0/0)	17 (15/2)	2 (2/0)	0 (0/0)	542	18,049
Emergency medicine	74	42	1 (0/1)	0 (0/0)	1	13	3	0	20	9 (1/8)	203 (160/43)	5 (4/1)	0 (0/0)	371	12,354
Ophthalmology	140	123	5 (1/4)	0 (0/0)	10	0	0	0	51	0 (0/0)	10 (6/4)	8 (8/0)	0 (0/0)	347	11,555
Rehabilitation medicine	51	17	0 (0/0)	0 (0/0)	1	12	2	3	5	7 (2/5)	46 (38/8)	2 (2/0)	0 (0/0)	146	4,862
Laboratory medicine	5	-	0 (0/0)	0 (0/0)	0	0	0	0	71	1 (0/1)	0 (0/0)	0 (0/0)	0 (0/0)	77	2,564
Psychiatry	43	13	0 (0/0)	0 (0/0)	0	0	0	0	1	3 (2/1)	15 (10/5)	2 (2/0)	0 (0/0)	77	2,564
Pathology	2	-	0 (0/0)	0 (0/0)	0	0	0	0	0	0 (0/0)	5 (5/0)	45 (45/0)	0 (0/0)	52	1,732
General (NOS)	12	16	0 (0/0)	0 (0/0)	0	0	0	0	0	1 (0/1)	6 (6/0)	10 (10/0)	0 (0/0)	45	1,499
Radiation oncology	16	-	0 (0/0)	0 (0/0)	0	0	0	0	0	20 (0/20)	1 (0/1)	6 (6/0)	0 (0/0)	43	1,432
Preventive medicine	4	25	0 (0/0)	0 (0/0)	0	0	0	0	0	0 (0/0)	0 (0/0)	0 (0/0)	0 (0/0)	29	966
Nuclear medicine	-	-	0 (0/0)	0 (0/0)	0	0	0	0	0	0 (0/0)	0 (0/0)	26 (24/2)	0 (0/0)	26	866
Anesthesiology	6	8	1 (1/0)	0 (0/0)	1	0	0	0	1	0 (0/0)	1 (1/0)	0 (0/0)	0 (0/0)	18	599
Occupational and environmental medicine	9	-	0 (0/0)	0 (0/0)	0	0	0	0	1	0 (0/0)	1 (1/0)	0 (0/0)	0 (0/0)	11	366
Tuberculosis	1	-	0 (0/0)	0 (0/0)	0	0	0	0	0	0 (0/0)	0 (0/0)	0 (0/0)	0 (0/0)	1	33
Total	61,875	39,015	4,399 (3,233/1,166)	1,137 (377/760)	3,322	1,908	278	40	17,892	6,870 (1,259/5,611)	16,234 (10,627/5,607)	10,369 (9,872/497)	33 (9/24)	163,372	5,440,288

LN, with lymph node dissection; non-LN, without lymph node dissection; IF, immunofluorescent; EM, electron microscopy; IHC, immunohisto(cyto)chemistry; FISH, flurescence *in situ* hybridization; SISH, silver *in situ* hybridization; NOS, not otherwise specified.

http://dx.doi.org/10.4132/jptm.2016.03.04

RESULTS

Pathologic examination statistics in Korea

In the year 2013, 163,372 pathologic examinations were performed in 103,528 patients (45,897 men and 57,631 women). The mean and median ages of the patients were 51.8 and 53 years, respectively. The skewness and kurtosis of patient age were –0.251 and 2.775, respectively. The pathologic examination data and medical institutions according to administrative district are summarized in Table 2. The total numbers of medical institutions according to administrative district are summarized in Appendix 1. In total, 43.5% of the tertiary hospitals (10/23), 15.6% of the general hospitals (48/307), and 23.8% of the other institutions (12,090/50,868) were located in Seoul. In addition, 32.9% of the surgical pathologic examinations (53,711/163,372) were requested in medical institutions located in Seoul.

Almost all medical and dental departments requested pathologic examinations (Table 3). Internal medicine (74,232, 45.4%), general surgery (34,808, 21.3%), obstetrics and gynecology (19,382, 11.9%), and urology (9,951, 6.1%) were the most common medical departments (84.7%) requesting pathology examinations. A small subset (38/17,892, 0.2%) of immunohistochemical (IHC) stains were not interpreted by qualified doctors (not claimed as "C5575006") (data not shown). Claims for acetylcholinesterase (C5564) and chloroacetate esterase (C5565) examinations were not found in our data.

Among pathologic examination-associated claims, 162,002 examinations (99.2%) had proper claim codes (examination codes 09 and sub-code 01 (performed in their own institutions) or 02 (performed in outside institutions). Among pathologic examinations, 65.8% were performed in tertiary or general hospitals (39,385 and 67,225 cases, respectively) (Table 4). Almost all examinations claimed by tertiary hospitals were performed in their institute (39,349/39,385, 99.9%), and 85% of examinations claimed by general hospitals were performed (57,163/67,225) in their institute. The other medical institutions claimed considerable pathologic examinations performed by outside services (52,214/55,392, 94.3%).

According to the claims, 76,016 pathologic examinations (44.7%) were performed due to malignancy (disease code "C") or non-malignant tumorous conditions (disease code "D00-D48") (Table 5). IHC stains were more frequently performed in tumorous conditions (15,336/17,892, 85.7%). Pathologic examination of biopsy specimens was performed more frequently in non-tumorous conditions (42,661/61,875, 68.9%).

ESD-related statistics

In total, 509 ESDs were performed in 490 patients (341 males

Table 4. Pathologic examination performing places according to medical institutions

Institution	Tertiary hospital	General hospital	Other medical institutions	Total
In own hospital	39,349 (99.9)	57,163 (85.0)	3,178 (5.7)	99,690 (61.5)
Outside services	36 (0.1)	10,062 (15.0)	52,214 (94.3)	62,312 (38.5)
Total	39,385 (100)	67,225 (100)	55,392 (100)	162,002 (100)

Values are presented as number (%).

Table 5. Disease codes of patients at time of pathologic examinations requests

	Tumorous condition	Non-tumorous condition	Total
Biopsy	19,214	42,661	61,875
Resection, non-malignant	14,900	24,115	39,015
Resection, malignant (LN/non-LN)	4,333 (3,203/1,130)	66 (30/36)	4,399 (3,233/1,166)
Histologic mapping (LN/non-LN)	1,045 (377/668)	92 (0/92)	1,137 (377/760)
Frozen sections	3,041	281	3,322
IF	213	1,695	1,908
EM	51	227	278
Enzyme	0	40	40
IHC	15,336	2,556	17,892
Uterine cervical examinations (smear/liquid)	3,199 (554/2,645)	3,671 (705/2,966)	6,870 (1,259/5,611)
Body fluid (conventional/liquid)	7,137 (4,118/3,019)	9,097 (6,509/2,588)	16,234 (10,627/5,607)
Aspiration (conventional/liquid)	4,514 (4,234/280)	5,855 (5,638/217)	10,369 (9,872/497)
HER2 (FISH/SISH)	33 (9/24)	0 (0/0)	33 (9/24)
Total	73,016	90,356	163,372

LN, with lymph node dissection; non-LN, without lymph node dissection; IF, immunofluorescent; EM, electron microscopy; IHC, immunohisto(cyto)chemistry; FISH, flurescence *in situ* hybridization; SISH, silver *in situ* hybridization.

and 149 females) in 109 medical institutions. The median age of the patients was 66 years (age, 29 to 89 years; 1st quantile, 58 years; 3rd quantile, 71.75 years). The majority of patients (n=472) underwent one ESD; 17 patients underwent two ESDs (10 patients underwent simultaneous ESD, while seven patients underwent ESDs at different times), and one patient underwent three ESDs (two ESDs at the same time).

The disease codes noted when patients underwent ESD were as follows: C16 (malignant neoplasm of stomach), 213 patients (43.5%); non-C16, 277 patients (56.5%); D00.2 (carcinoma *in situ* of stomach), 17 patients; D13.1 (benign neoplasm of stomach), 226 patients; D13.9 (benign neoplasm of ill-defined site within the digestive system), one patient; and other, 33 patients. Disease codes changed after the ESD in 10.5% of the non-C16 patients (29/277): D00.2 to C16, seven patients; D13.1 to D00.2, three patients; D13.1 to C16, 18 patients; and D13.9 to C16, one patient (Table 6).

Twenty-one patients (21/490, 4.3%) underwent gastrectomy following ESD, and all of these patients underwent ESD for only once. Fifteen patients received surgery at the same medical institution where ESD was performed, and six patients received surgery at different medical institutions. The mean time between ESD and surgery was 44 days. Two patients changed diagnosis (benign to malignant) after ESD. One patient underwent ESD and surgery during the same hospitalization period.

For further analysis, 472 patients who underwent ESD for only once were selected (Table 7) (C16, 202 patients; D00.2, 17 patients; D13.1, 220 patients; D13.9, one patient; other, 32 patients). In total, 70.0% of these pathologic examinations (329/472) were requested for histologic mapping (C5508). IHC studies were performed in 22.5% of ESDs (106/472). Approximately one-third of the gastric cancer specimens (66/202, 32.7%) and 15.0% of the gastric benign neoplasm specimens (33/220) were subject to IHC studies.

Table 6. Changes of disease codes after endoscopic submucosal dissections

Disease code at ESD	Disease code after ESD		
	Unchanged	Changed to C16	Changed to D00.2
D00.2	10	7	-
D13.1	205	18	3
D13.9	0	1	0
Others	33	0	0
Total	248	26	3

ESD, endoscopic submucosal dissections.

DISCUSSION

In this study, we examined nation-wide statistics regarding surgical pathologic examination. Considering sampling weight, we estimate that 5,440,288 (163,372×33.3) pathologic examinations were performed in Korea in 2013. We also surveyed pathologic examinations according to administrative district, requesting department, type of medical institutions, and patient conditions. These data will be useful for future planning and allocation of resources in the field of pathology and for the Korean Society of Pathologists.

There have been several reports regarding diagnostic discrepancies between endoscopic forceps biopsy and ESD, as well as between ESD and surgery. Recently, two large, single-center, retrospective studies revealed that 22.8% (465/2,041) and 31.7%

Table 7. Pathologic examination codes and number of immunohistochemical stains according to diseases codes at endoscopic submucosal dissections

	C16	D00.2	D13.1	D13.9	Others	Total
Pathologic examination codes						
C5500	6	0	5	0	0	11
C5508	158	3	139	1	28	329
C5916	16	3	51	0	2	72
C5917	22	11	25	0	2	60
Total	202	17	220	1	32	472
No. of immunohistochemical stains						
0	136	14	187	1	28	366
1	42	1	25	0	1	69
2	12	0	5	0	2	19
3	2	1	3	0	1	7
4	2	1	0	0	0	3
5	3	0	0	0	0	3
6	5	0	0	0	0	5
Total	202	17	220	1	32	472

http://dx.doi.org/10.4132/jptm.2016.03.04

(587/1,850) of cases changed diagnosis after endoscopic resection in Asan Medical Center (Seoul, Korea) and Samsung Medical Center (Seoul, Korea), respectively.[5,6] Our HIRA-NPS data revealed that only 10.9% of nation-wide cases experienced a change of diagnosis after ESD. HIRA-NPS data does not include detailed pathologic diagnosis information such as tumor size, tumor differentiations, dysplastic degrees, etc., so further analysis for clarifying such differences was limited. Shin *et al*.[7] reported that complete resection rates were not different according to absolute or expanded ESD indications, though their data were not HIRA data. Although HIRA-NPS data was not available for a sufficient number of ESD patients (509 ESDs in 490 patients) to allow for an accurate assessment, and only limited clinicopathological information was available, the problems associated with the relatively few number of patients can be overcome through further research using the raw HIRA data.

Histologic mapping of ESD specimens is recommended by The Gastrointestinal Pathology Study Group of the Korean Society of Pathologists.[8] However, 30.2% (143/472) of ESD specimens were not claimed as "C5508" (histologic mapping without lymph node dissection). Because precise histologic diagnosis of the ESD specimen is essential to treat patients, we suggest that nationwide surveys be conducted in order to assure quality of pathologic examination of ESD specimens. IHC staining was performed in 22.5% (106/472) of ESD cases. Unlike tissue immunofluorescent microscopic examinations or enzyme histochemistries, HIRA data does not list the specific antibodies used for IHC stains. Thus, further analysis of IHC studies using HIRA data was limited.

The main limitations of our analysis are statistical issues based on probability sampling. Our estimates were calculated from statistically extracted data from one year. Further analysis using HIRA raw data will be needed to decrease the statistical errors and bias and to evaluate changes over time. During our analysis, we experienced many challenges; therefore, we provide advice and guidance for other researchers who would like to analyze the HIRA database.

(1) It is essential to understand the framework of the HIRA database.[9] The HIRA data is intended for insurance claims and not for research. Detailed clinicopathological data are not provided. (2) Sample data are not appropriate for analyses requiring long-term follow-up. (3) Some claim codes have sub-codes (in most cases, additional charges by experts). (4) Disease codes and claims are not always accurate. (5) The analysis system should have at least 32 GB of main memory. (6) It is helpful to create relatively small data tables to decrease operation time. In the usual setting, R should use only one CPU core during calculation.

Conflicts of Interest

No potential conflict of interest relevant to this article was reported.

REFERENCES

1. Kim L, Kim JA, Kim S. A guide for the utilization of Health Insurance Review and Assessment Service National Patient Samples. Epidemiol Health 2014; 36: e2014008.
2. Chi JG. The establishment of hospital pathology in Korea. Korean J Pathol 1994; 28: 109-17.
3. Lee CK, Chung IK, Cho JY, *et al*. A survey on the indication for endoscopic submucosal dissection in early gastric cancer. Korean J Gastrointest Endosc 2009; 39: 78-84.
4. Song KY, Hyung WJ, Kim HH, *et al*. Is gastrectomy mandatory for all residual or recurrent gastric cancer following endoscopic resection? A large-scale Korean multi-center study. J Surg Oncol 2008; 98: 6-10.
5. Lee JH, Min YW, Lee JH, *et al*. Diagnostic group classifications of gastric neoplasms by endoscopic resection criteria before and after treatment: real-world experience. Surg Endosc 2015 Dec 22 [Epub]. http://dx.doi.org/10.1007/s00464-015-4710-z.
6. Lim H, Jung HY, Park YS, *et al*. Discrepancy between endoscopic forceps biopsy and endoscopic resection in gastric epithelial neoplasia. Surg Endosc 2014; 28: 1256-62.
7. Shin KY, Jeon SW, Cho KB, *et al*. Clinical outcomes of the endoscopic submucosal dissection of early gastric cancer are comparable between absolute and new expanded criteria. Gut Liver 2015; 9: 181-7.
8. Kim WH, Park CK, Kim YB, *et al*. A standardized pathology report for gastric cancer. Korean J Pathol 2005; 39: 106-13.
9. Kim L, Sakong J, Kim Y, *et al*. Developing the inpatient sample for the national health insurance claims data. Health Policy Manag 2013; 23: 152-61.

Appendix 1. Numbers of medical institutions according to administrative districts

Administrative district	Tertiary hospital	General hospital	Other institutions (clinic)
Seoul	10	48	12,090 (6,952)
Busan	3	24	3,567 (2,048)
Incheon	2	15	2,376 (1,388)
Daegu	1	11	2,542 (1,538)
Gwangju	1	22	1,584 (862)
Daejeon	1	8	1,599 (981)
Ulsan	0	4	1,012 (546)
Gyeonggi-do	1	55	10,424 (5,883)
Gangwon-do	1	14	1,377 (707)
Chungcheongbuk-do	1	10	1,488 (791)
Chungcheongnam-do	0	12	2,019 (1,013)
Jeollabuk-do	1	11	2,197 (1,110)
Jeollanam-do	0	22	2,048 (913)
Gyeongsangbuk-do	0	19	2,558 (1,206)
Gyeongsangnam-do	1	25	2,977 (1,521)
Jeju	0	7	575 (330)
Sejong-si	0	0	105 (57)
Total	23	307	50,868 (27,846)

http://dx.doi.org/10.4132/jptm.2016.03.04

Journal of Pathology and Translational Medicine 2016; 50: 211-216
http://dx.doi.org/10.4132/jptm.2016.02.01

■ ORIGINAL ARTICLE ■

Aberrant Blood Vessel Formation Connecting the Glomerular Capillary Tuft and the Interstitium Is a Characteristic Feature of Focal Segmental Glomerulosclerosis-like IgA Nephropathy

Beom Jin Lim[1,2] · Min Ju Kim[3]
Soon Won Hong[1] · Hyeon Joo Jeong[1]

[1]Department of Pathology, [2]Severance Institute for Vascular and Metabolic Research, Yonsei University College of Medicine, Seoul; [3]Department of Pathology, Gachon University Gil Medical Center, Incheon, Korea

Received: January 14, 2016
Revised: January 28, 2016
Accepted: February 1, 2016

Corresponding Author
Hyeon Joo Jeong, MD
Department of Pathology, Yonsei University College of Medicine, 50-1 Yonsei-ro, Seodaemun-gu, Seoul 03722, Korea
Tel: +82-2-2228-1766
Fax: +82-2-362-0860
E-mail: jeong10@yuhs.ac

Background: Segmental glomerulosclerosis without significant mesangial or endocapillary proliferation is rarely seen in IgA nephropathy (IgAN), which simulates idiopathic focal segmental glomerulosclerosis (FSGS). We recently recognized aberrant blood vessels running through the adhesion sites of sclerosed tufts and Bowman's capsule in IgAN cases with mild glomerular histologic change. **Methods:** To characterize aberrant blood vessels in relation to segmental sclerosis, we retrospectively reviewed the clinical and histologic features of 51 cases of FSGS-like IgAN and compared them with 51 age and gender-matched idiopathic FSGS cases. **Results:** In FSGS-like IgAN, aberrant blood vessel formation was observed in 15.7% of cases, 1.0% of the total glomeruli, and 7.3% of the segmentally sclerosed glomeruli, significantly more frequently than in the idiopathic FSGS cases (p = .009). Aberrant blood vessels occasionally accompanied mild cellular proliferation surrounding penetrating neovessels. Clinically, all FSGS-like IgAN cases had hematuria; however, nephrotic range proteinuria was significantly less frequent than idiopathic FSGS. **Conclusions:** Aberrant blood vessels in IgAN are related to glomerular capillary injury and may indicate abnormal repair processes in IgAN.

Key Words: Glomerulosclerosis, focal segmental; Glomerulonephritis, IgA; Kidney glomerulus; Neovascularization

IgA nephropathy (IgAN) is characterized by dominant or codominant IgA deposits in the mesangial matrix and is usually accompanied by focal or diffuse mesangial proliferation. However, IgAN has a variety of histologic features ranging from normal to minimal glomerular alterations to diffuse endocapillary and crescentic glomerulonephritis.

Glomerular segmental sclerosis is not unusual in biopsy samples that are diagnosed as IgAN, but it is usually associated with severe mesangial proliferation and/or advanced tubulointerstitial fibrosis.[1,2] Haas[3,4] reported a form of segmental sclerosis in IgAN that did not accompany mesangial proliferation and demonstrated clinical features that were indistinguishable from idiopathic focal segmental glomerulosclerosis (FSGS). Of the 18 cases presented in his study, 82% had nephrotic syndrome and all but one case had favorable prognoses. Another description of segmental sclerosis without significant mesangial proliferation was reported by Weber *et al*.[2] In their series of 26 cases, nephrotic syndrome was present in 24%, diffuse effacement of foot processes in only one case and the clinical outcomes were worse than in cases without FSGS. These two contrasting studies suggest that cases of mild IgAN with FSGS that are morphologically similar but have different pathogeneses may have different clinical outcomes. We recently recognized aberrant blood vessels running through the adhesion sites of sclerosed tufts and Bowman's capsule in IgAN with FSGS features. Since these vessels were present away from the glomerular hilum, they were regarded as related to previous glomerular capillary injury. Glomerular capillary necrosis[5] may be the forerunner of this lesion, but there have been no detailed descriptions of these vessels in IgAN.

To characterize segmental sclerosis in relation to abnormal vessels in early IgAN, we retrospectively reviewed clinical and histologic features of FSGS-like IgAN without accompanying severe glomerular cellular proliferation and/or advanced tubulointerstitial fibrosis. Idiopathic FSGS cases were used for comparison.

pISSN 2383-7837
eISSN 2383-7845

MATERIALS AND METHODS

Materials

A total of 565 cases with diagnoses of IgAN in native kidneys were retrieved from the renal biopsy registry of the Department of Pathology, Yonsei University Health System, between 1999 and 2008. Among these, 92 cases were diagnosed as IgAN, subclass II, according to the Haas classification. We selected 51 IgAN cases with focal and segmental sclerosis. The exclusion criteria included (1) significant glomerular mesangial proliferation of more than three cells in one mesangial area distant from the vascular hilum in 2–3-μm-thick periodic acid–Schiff (PAS)–stained sections; (2) endocapillary proliferation; (3) global glomerulosclerosis or tubular atrophy of 40% or more; or (4) insufficient sample size of less than six glomeruli on light microscopy. For comparison, age- and gender-matched idiopathic FSGS cases from the same period were collected from our renal biopsy registry. The same exclusion criteria were applied to these cases.

Tissue processing of renal biopsies

All biopsy samples were examined using light, immunofluorescent, and electron microscopy. For light microscopic examination, 2–3-μm-thick sections were stained with hematoxylin and eosin, PAS, aldehyde fuchsin orange G, and methenamine silver methods. Two to four tissue sections were mounted per glass slide, and two slides were prepared for each stain, resulting in eight slides for each biopsy. For immunofluorescence examination, snap-frozen 3-μm-thick sections were mounted in optimal cold temperature compound and stained with antibodies against IgG, IgA, IgM, C3, C4, C1q, and fibrinogen (Dako Cytomation, Glostrup, Denmark). For electron microscopy, fresh renal tissue was cut at the time of biopsy, and one to three blocks of 1 mm^3 renal tissue were double fixed with glutaraldehyde and osmium tetroxide, routinely processed, and stained with uranyl acetate and lead citrate.

Assessment of renal histology

An average of 26.7 consecutive sections (range, 18 to 32) were examined in each case. All glomeruli in each section were traced. The total glomeruli and glomeruli showing segmental sclerosis were counted. The segmental sclerosis was subtyped in each case as classic, perihilar, tip, cellular or collapsing variants and were numbered.[6] In segmental sclerosis, capillary adhesion to Bowman's capsule with or without aberrant vessel formation was also counted. To validate aberrant vessels, we followed afferent and efferent arterioles in the vascular poles and confirmed that there were no direct connections between vascular poles and presumed neovessels.

The other histologic parameters that we evaluated were type of glomerular crescent, percentage of global glomerulosclerosis, degree of tubular atrophy, interstitial fibrosis, and interstitial inflammation, and presence of arteriolar hyalinosis and arteriosclerosis. Crescents were defined as extracapillary proliferations of at least two layers that occupied at least 10% of the circumference. The degrees of tubular atrophy, interstitial fibrosis, interstitial inflammation, and arteriolar hyalinosis were semi-quantitatively scored according to the Banff 97 criteria.[7]

Clinical data

Patient age, gender, serum creatinine level, hematuria, and proteinuria level at the time of biopsy were obtained from the patient medical records and biopsy requisition forms. Proteinuria was evaluated in 49 FSGS-like IgAN patients and in 45 idiopathic FSGS patients by 24-hour urine collection or random urine protein to creatinine ratios.

Statistical analysis

Results are expressed as mean ± standard deviation. Comparisons of the frequencies of segmental sclerosis, tuft adhesion to Bowman's capsule, glomerular hyalinosis, and aberrant vessel formation between FSGS-like IgAN and idiopathic FSGS cases were performed using the Mann-Whitney U test. Tubulointerstitial and vascular changes were compared using Pearson's chi-square test combined with Fisher exact test. p-values less than .05 were considered significant.

RESULTS

Morphologic features of segmental sclerosis in FSGS-like IgAN

We observed an average of 16.3 glomeruli in each case of FSGS-like IgAN. Of the 829 total glomeruli, 110 (13.3%) showed segmental sclerosis. The most common subtype of segmental sclerosis was classic type, followed by tip and perihilar types. Hyalinosis was present in one glomerulus. Glomerular capillary tuft adhesion to Bowman's capsule was observed in 95 glomeruli (86.4% of the segmentally sclerosed glomeruli) in 49 cases. Among them, nine cases (8.2% of the total segmentally sclerosed glomeruli) demonstrated capillary-sized blood vessels connecting the segmentally sclerosed tuft and periglomerular interstitium. These vessels began in the sclerosed tufts, ran perpendicularly through the gap of Bowman's capsule, and merged

http://dx.doi.org/10.4132/jptm.2016.02.01

into the capillary networks of the interstitium. The vessels were surrounded by normal-looking glomerular capillary loops in five glomeruli, but accompanied endocapillary proliferations in four glomeruli (Fig. 1).

Comparison of segmental sclerosis between FSGS-like IgAN and idiopathic FSGS

In age and gender-matched idiopathic FSGS cases, segmental sclerosis was observed in 119 out of 746 glomeruli (16.0%). When segmental sclerosis of IgAN was compared with that of idiopathic FSGS, the mean percentages of glomeruli with tuft adhesion, aberrant vessel formation, and glomerular crescents were significantly higher in the FSGS-like IgAN group. Aberrant blood vessels found in FSGS were similar to those seen in IgAN in morphology but were identified in only one glomerulus (0.8% of the segmentally sclerosed glomeruli). The mean percentages of glomerular hyalinosis, the degrees of interstitial fibrosis, tubular atrophy, interstitial inflammation, and arteriolar hyalinosis were not significantly different between the two groups (Table 1).

Clinically, hematuria was present in 100% of the FSGS-like IgAN patients, whereas 51.0% of the idiopathic FSGS patients had hematuria. Proteinuria was more prevalent and severe in idiopathic FSGS: 91.1% of patients had proteinuria and 48.9% were in the nephrotic range, whereas proteinuria was present in

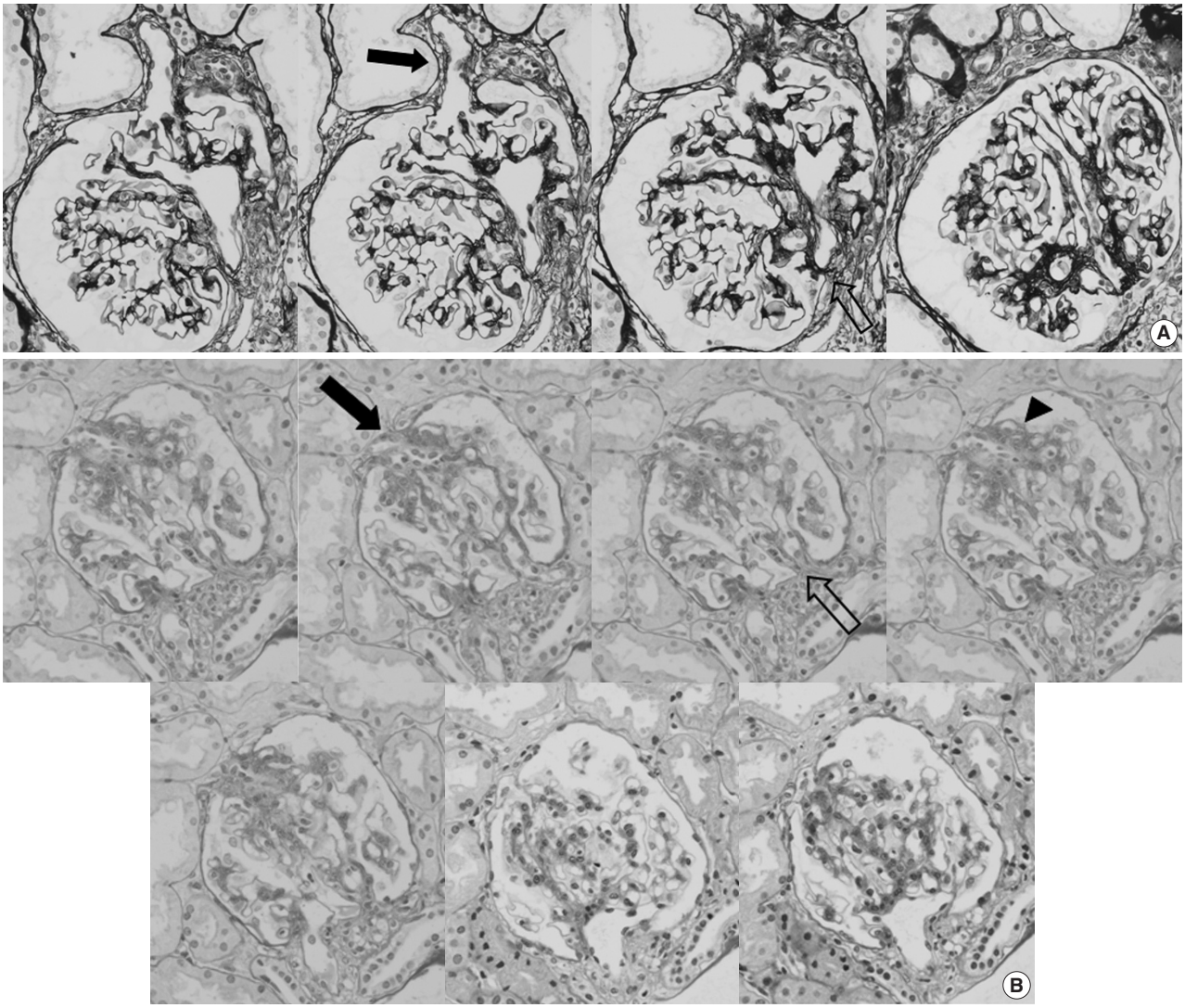

Fig. 1. Consecutive photos of two glomeruli showing extra-efferent vessel formation in focal segmental glomerulosclerosis-like IgA nephropathy. (A, B) Extra vessels connecting the segmentally sclerosed portions of glomerular tufts and the extraglomerular space through the gap of Bowman's capsule were observed when tracing the serial sections. These vessels were not connected to afferent or efferent arterioles in the vascular pole (solid arrows, extra vessels; open arrows, vascular poles). (B) Surrounding glomerular tufts showed capillary and endothelial proliferations in some cases (arrowhead) (periodic acid-Schiff, aldehyde fuchsin orange G, and methenamine silver stain).

Table 1. Histomorphologic characteristics of FSGS-like IgAN and idiopathic FSGS

Variable	FSGS-like IgAN	Idiopathic FSGS	p-value
No. of total glomeruli (per case)	829 (16.3)	746 (14.6)	-
Glomeruli with segmental sclerosis, n (%)	110 (13.3)	119 (16.0)	-
Classic/Perihilar/Tip/Cellular/Collapsing type	56/14/42/0/0	73/7/33/0/6	-
Segmental sclerosis in each case (%)	14.6±7.3	19.5±16.4	.451[a]
Glomerular hyalinosis in each case (%)	0.0±0.1	0.8±3.3	.177[a]
Capillary loop adhesion in each case (%)	13.2±7.8	6.5±8.7	<.001[a]
Neovessel formation in each case (%)	1.2±3.1	0.2±1.1	.009[a]
Glomerular crescents			<.001[b]
Absent	39	51	
Present	12	0	
Interstitial fibrosis			>.999[b]
Absent or mild	49	49	
Moderate to severe	2	2	
Tubular atrophy			.678[b]
Absent or mild	49	47	
Moderate to severe	2	4	
Interstitial inflammation			
Absent or mild	47	47	>.999[b]
Moderate to severe	4	4	
Arteriolar hyalinosis			.463[b]
Absent	39	42	
Present	12	9	

FSGS, focal segmental glomerulosclerosis; IgAN, IgA nephropathy.
[a]Mann-Whitney U test; [b]Pearson's chi-square test with Fisher exact test.

Table 2. Clinical characteristics of FSGS-like IgAN and idiopathic FSGS

Variable	FSGS-like IgAN	Idiopathic FSGS	p-value
No. of cases	51	51	
Male:Female	25:26	24:27	
Age, mean (range, yr)	35.1 (7–65)	35.6 (7-67)	
Proteinuria[a]	39 (79.9)	41 (91.1)	0.124[b]
Nephrotic range	1 (2.0)	22 (48.9)	0.000[b]
Hematuria[a]	51 (100)	26 (51.0)	0.000[b]
Serum creatinine level (mg/dL)	1.0±0.2	1.2±0.7	0.099[c]

Values are presented as number (%) or mean±standard deviation unless otherwise indicated.
FSGS, focal segmental glomerulosclerosis; IgAN, IgA nephropathy.
[a]Number of cases; [b]Pearson's chi-square test with Fisher exact test; [c]Mann-Whitney U test.

79.9% of FSGS-like IgAN patients with nephrotic range in 2.0%. Other clinical parameters including mean serum creatinine levels were similar in both groups (Table 2).

DISCUSSION

Aberrant vessels were more frequently observed in cases of FSGS-like IgAN than in idiopathic FSGS. Otherwise, the morphology of segmental sclerotic glomeruli was indistinguishable in two diseases, and the most common form was the classic type. Considering that more than 25 sections were examined, these features were rare and may be under-recognized or unnoticed in routine practice. Clinically, our cases were different from those reviewed by Haas[3,4] but similar to those reviewed by Weber *et al*.[2] The frequency of hematuria was higher and that of nephrotic range proteinuria was lower than observed by Haas.[3,4] Associations of nephrotic range proteinuria have been reported in IgAN with normal histology. However, it has not been resolved whether this entity is a subtype of IgAN or an overlap of IgAN and minimal change disease. Likewise, it is possible that the cases of FSGS-like IgAN described by Haas[3,4] were subtypes of IgAN or represented the overlap of IgAN and minimal change disease/FSGS. By contrast, consistent hematuria may suggest the involvement of capillary loop injury in FSGS-like IgAN.

Extra new vessel formation is rarely reported in animal models or in human diabetic nephropathy. Kriz *et al*.[8] proposed that "extraterritorial glomerular capillaries" that connect the glomerular space and periglomerular interstitium are responsible for the development of interstitial fibrosis in a hypertensive rat FSGS model. The extra vessels were located in the glomerular hilum in human diabetic nephropathy and did not cause rupture of the capillary loops, and most were connected to the second- and third-order branches of the afferent arteriole and drained into the peritubular capillaries.[9] The number of extra vessels ranged from

http://dx.doi.org/10.4132/jptm.2016.02.01

several to more than 10 per glomerulus. Rare extra vessels have been observed in a variety of cases, also localized within the glomerular hilum.[10,11] However, the aberrant vessels observed in our study differed from those in diabetic nephropathy in location and numbers. Extra vessels similar to our cases can be seen in glomerulonephritis characterizing small vessel vasculitis[5] such as Henoch-Schönlein purpura nephritis, antineutrophil cytoplasmic antibody–associated nephritis, and lupus nephritis. In these cases, new vessel formation was observed especially inside or near crescents.

Glomerular capillary loop sclerosis and adhesion were grouped together in a proposed Oxford classification of IgAN,[12] mainly to increase reproducibility between observers. However, not only are they morphologically distinct but they also differ in pathomechanisms. Glomerular capillary loop sclerosis is characterized by capillary loop collapse and accumulation of scleroprotein inside the glomerular capillary basement membrane. It can be caused by ischemia, toxins, or drugs, but the glomerular basement membrane integrity is essentially preserved. In contrast, glomerular capillary adhesion to Bowman's capsule produces a break in glomerular basement membrane integrity and may develop with or without glomerular capillary rupture. Therefore, adhesions and new vessels in IgAN might be signs of glomerular capillary injury and rupture. The presence of endocapillary proliferation and small glomerular crescents surrounding vessels supports this possibility. Glomerular capillary loop injury may be triggered by immune deposits along the capillary loops; however, our cases had localized mesangial deposits without peripheral capillary IgA deposits. Glomerular capillary basement membranes may be fragile and likely to break without deposits, since glomerular basement membrane thinning or attenuation is frequent in IgAN.[13] Mesangial cells have been shown to significantly down regulate vascular endothelial growth factor A mRNA and increase inducible nitric oxide synthase mRNA when incubated with aberrantly glycosylated IgA. Therefore, these molecules may be involved in the evolution of abnormal repair in IgAN.[14] It is unclear how aberrant vessels affect glomerular filtration and nearby structures, but they may contribute to interstitial inflammation and fibrosis by directly delivering pathogenic filtrate to the peritubular capillaries and interstitium.[8]

In conclusion, aberrant blood vessels were observed in segmentally sclerosed glomerular tufts in FSGS-like IgAN. Such structures indicate aberrant repair processes in glomerular capillaries. Further clinical and experimental studies may be needed to elucidate this faulty repair mechanism.

Conflicts of Interest

No potential conflict of interest relevant to this article was reported.

Acknowledgments

This study was supported by a grant from the Korean Society of Pathologists to Lim BJ.

REFERENCES

1. Packham DK, Yan HD, Hewitson TD, *et al*. The significance of focal and segmental hyalinosis and sclerosis (FSHS) and nephrotic range proteinuria in IgA nephropathy. Clin Nephrol 1996; 46: 225-9.
2. Weber CL, Rose CL, Magil AB. Focal segmental glomerulosclerosis in mild IgA nephropathy: a clinical-pathologic study. Nephrol Dial Transplant 2009; 24: 483-8.
3. Haas M. IgA nephropathy histologically resembling focal-segmental glomerulosclerosis: a clinicopathologic study of 18 cases. Am J Kidney Dis 1996; 28: 365-71.
4. Haas M. Histologic subclassification of IgA nephropathy: a clinicopathologic study of 244 cases. Am J Kidney Dis 1997; 29: 829-42.
5. D'Amico G, Napodano P, Ferrario F, Rastaldi MP, Arrigo G. Idiopathic IgA nephropathy with segmental necrotizing lesions of the capillary wall. Kidney Int 2001; 59: 682-92.
6. Thomas DB, Franceschini N, Hogan SL, *et al*. Clinical and pathologic characteristics of focal segmental glomerulosclerosis pathologic variants. Kidney Int 2006; 69: 920-6.
7. Solez K, Colvin RB, Racusen LC, *et al*. Banff 07 classification of renal allograft pathology: updates and future directions. Am J Transplant 2008; 8: 753-60.
8. Kriz W, Hosser H, Hähnel B, Gretz N, Provoost AP. From segmental glomerulosclerosis to total nephron degeneration and interstitial fibrosis: a histopathological study in rat models and human glomerulopathies. Nephrol Dial Transplant 1998; 13: 2781-98.
9. Min W, Yamanaka N. Three-dimensional analysis of increased vasculature around the glomerular vascular pole in diabetic nephropathy. Virchows Arch A Pathol Anat Histopathol 1993; 423: 201-7.
10. Smith JP. Anatomical features of the human renal glomerular efferent vessel. J Anat 1956; 90: 290-2.
11. Murakami T, Kikuta A, Akita S, Sano T. Multiple efferent arterioles of the human kidney glomerulus as observed by scanning electron microscopy of vascular casts. Arch Histol Jpn 1985; 48: 443-7.
12. Working Group of the International IgA Nephropathy Network and the Renal Pathology Society, Roberts IS, Cook HT, *et al*. The Oxford classification of IgA nephropathy: pathology definitions,

correlations, and reproducibility. Kidney Int 2009; 76: 546-56.
13. Yoshikawa N, Tanaka R, Iijima K. Pathophysiology and treatment of IgA nephropathy in children. Pediatr Nephrol 2001; 16: 446-57.
14. Amore A, Conti G, Cirina P, *et al*. Aberrantly glycosylated IgA molecules downregulate the synthesis and secretion of vascular endothelial growth factor in human mesangial cells. Am J Kidney Dis 2000; 36: 1242-52.

http://dx.doi.org/10.4132/jptm.2016.02.01

Journal of Pathology and Translational Medicine 2016; 50: 217-224
http://dx.doi.org/10.4132/jptm.2016.02.15

■ ORIGINAL ARTICLE ■

Core Needle Biopsy Is a More Conclusive Follow-up Method Than Repeat Fine Needle Aspiration for Thyroid Nodules with Initially Inconclusive Results: A Systematic Review and Meta-Analysis

Jung-Soo Pyo · Jin Hee Sohn
Guhyun Kang[1]

Department of Pathology, Kangbuk Samsung Hospital, Sungkyunkwan University School of Medicine, Seoul; [1]Department of Pathology, Inje University Sanggye Paik Hospital, Seoul, Korea

Received: January 25, 2016
Revised: February 12, 2016
Accepted: February 15, 2016

Corresponding Author
Jin Hee Sohn, MD
Department of Pathology, Kangbuk Samsung Hospital, Sungkyunkwan University School of Medicine, 29 Saemunan-ro, Jongno-gu, Seoul 03181, Korea
Tel: +82-2-2001-2391
Fax: +82-2-2001-2398
E-mail: jhpath.sohn@samsung.com

Background: This study investigated the appropriate management of thyroid nodules with prior non-diagnostic or atypia of undetermined significance/follicular lesion of undetermined significance (AUS/FLUS) through a systematic review and meta-analysis. **Methods:** This study included 4,235 thyroid nodules from 26 eligible studies. We investigated the conclusive rate of follow-up core needle biopsy (CNB) or repeat fine needle aspiration (rFNA) after initial fine needle aspiration (FNA) with non-diagnostic or AUS/FLUS results. A diagnostic test accuracy (DTA) review was performed to determine the diagnostic role of the follow-up CNB and to calculate the area under the curve (AUC) on the summary receiver operating characteristic (SROC) curve. **Results:** The conclusive rates of follow-up CNB and rFNA after initial FNA were 0.879 (95% confidence interval [CI], 0.801 to 0.929) and 0.684 (95% CI, 0.627 to 0.736), respectively. In comparison of the odds ratios of CNB and rFNA, CNB had more frequent conclusive results than rFNA (odds ratio, 5.707; 95% CI, 2.530 to 12.875). Upon subgroup analysis, follow-up CNB showed a higher conclusive rate than rFNA in both initial non-diagnostic and AUS/FLUS subgroups. In DTA review of follow-up CNB, the pooled sensitivity and specificity were 0.94 (95% CI, 0.88 to 0.97) and 0.88 (95% CI, 0.84 to 0.91), respectively. The AUC for the SROC curve was 0.981, nearing 1. **Conclusions:** Our results show that CNB has a higher conclusive rate than rFNA when the initial FNA produced inconclusive results. Further prospective studies with more detailed criteria are necessary before follow-up CNB can be applied in daily practice.

Key Words: Thyroid nodule; Non-diagnostic or atypia of undetermined significance/follicular lesion of undetermined significance; Follow-up core needle biopsy; Repeat fine-needle aspiration; Meta-analysis

Papillary thyroid carcinoma, which has recently increased in incidence, is the most common malignant tumor in endocrine system.[1] The cause for the increased incidence of papillary thyroid carcinoma is not fully understood.[1] One possible cause is the improvement in ultrasonography and computed tomography.[2,3] In daily practice, the treatment and follow-up for thyroid nodules are based on the results of initial fine needle aspiration (FNA). According to current guidelines,[4-6] FNA is recommended as the initially performed modality, and additional testing is suggested as indicated by the initial FNA results.

In daily practice, repeat FNA (rFNA) is recommended for thyroid nodules of non-diagnostic or atypia of undetermined significance/follicular lesion of undetermined significance (AUS/FLUS). In addition, for definite diagnosis of thyroid nodules, *BRAF*^{V600E} mutation test or diagnostic surgery can also be performed. In previous studies, the rates of non-diagnostic and AUS/FLUS were 5%–17% and 3%–18%, respectively.[7-9] For thyroid nodule with non-diagnostic result, the possibility of an inconclusive reading might also be higher with rFNA. Although rFNA is recommended for non-diagnostic or AUS/FLUS thyroid nodules in the current guidelines, other modalities, such as core needle biopsy (CNB) or combination of FNA and CNB, have been introduced in recent reports.[10,11] However, the effectiveness or diagnostic role of these follow-up modalities has not been fully elucidated.

In this study, follow-up CNB was defined as CNB performed after initial non-diagnostic or AUS/FLUS findings. We investigated the conclusive rates of the follow-up procedures of CNB and rFNA in thyroid nodule with initial non-diagnostic or AUS/FLUS finding through a systematic review and meta-analysis. Indeed, the diagnostic test accuracy (DTA) review was performed to determine the diagnostic accuracy of follow-up CNB in thy-

pISSN 2383-7837
eISSN 2383-7845

roid nodules with initial inconclusive results.

MATERIALS AND METHODS

Literature search and selection criteria

Relevant articles were obtained from a search of PubMed and MEDLINE databases through December 31, 2015. The search was performed using 'thyroid,' 'core needle biopsy,' and 'fine needle aspiration' as search terms. The titles and abstracts of all returned articles were screened for exclusion. To find additional eligible studies, review articles were also screened. Search results were then reviewed and included if (1) initial FNA for a thyroid nodule was performed, and (2) there was information about CNB or FNA as a follow-up study for thyroid nodules with initial non-diagnostic or AUS/FLUS results. Articles were excluded if they were (1) non-original articles or case reports or (2) non-English language publications.

Data extraction

The following information was collected from the full texts of eligible studies and verified: name of first author, publication year, study location, number of patients analyzed, and method and results of initial and follow-up studies. We did not define a minimal number of patients to be included in a study. Any disagreements were resolved by consensus.

Statistical analysis

Data were analyzed using the Comprehensive Meta-Analysis software package (Biostat, Englewood, NJ, USA). We evaluated the conclusive rates of follow-up studies with follow-up CNB or rFNA after initial FNA with non-diagnostic or AUS/FLUS results. The conclusive results included benign, follicular neoplasm or suspicious for follicular neoplasm, suspicious for malignancy, and malignancy categories. The conclusive rates were measured by dividing the number of conclusive results into the total number of cases with a follow-up study. The heterogeneity between eligible studies was assessed using Q and I^2 statistics and presented using p-values. A sensitivity analysis was performed to assess the impact of each study on the combined effect and the heterogeneity of eligible studies. To identify any publication bias, Egger's test and Begg's funnel plot were initially performed. When a significant publication bias was found, the fail-safe N and trim-fill tests were additionally conducted to confirm the degree of bias. The results were considered statistically significant at $p < 0.05$.

A DTA review was conducted using the Meta-Disc program ver. 1.4.[12] The forest plots of pooled sensitivity and specificity and the summary receiver operating characteristic (SROC) curve were determined as described previously.[13] The diagnostic odds ratio (OR) and the value of the area under the curve (AUC) on SROC were investigated.

RESULTS

Selection and characteristics of studies

In the current study, 356 reports were identified in the database search. Among the search results, 209 reports were excluded due to insufficient information. In addition, 121 reports were excluded for the following reasons: focusing on other diseases (n = 86), non-original articles (n = 17), duplicate articles (n = 13), and articles in a language other than English (n = 5). Twenty-six eli-

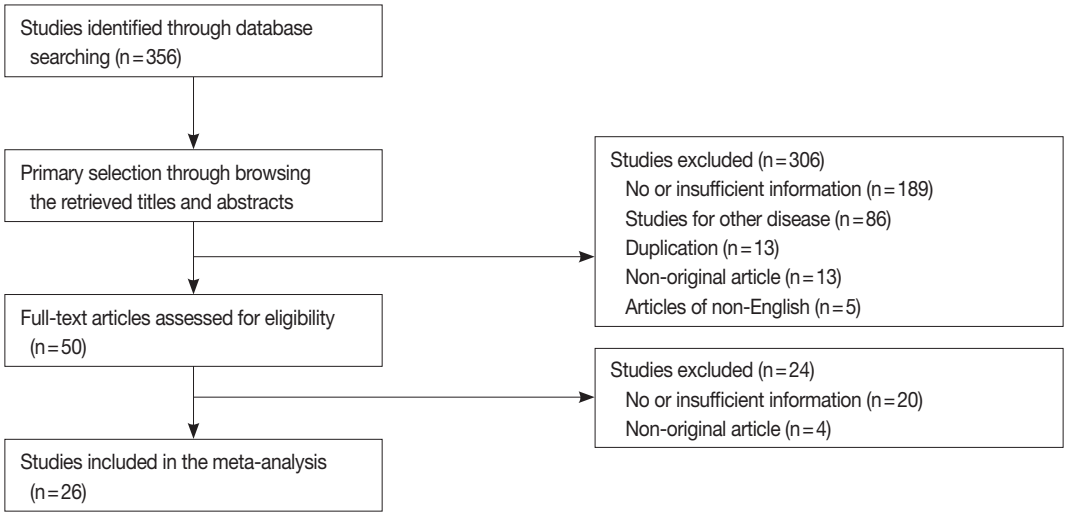

Fig. 1. Flow chart of study search and selection methods.

http://dx.doi.org/10.4132/jptm.2016.02.15

gible studies and 4,253 thyroid nodules were ultimately included in the current study (Table 1, Fig. 1).[14-39] The characteristics of the included studies are shown in Table 1.

Higher conclusive rate in follow-up CNB than in rFNA

For initial FNA with non-diagnostic or AUS/FLUS, follow-up studies using CNB or rFNA showed an overall conclusive

Table 1. Main characteristics of eligible studies

Study	Location	Diagnosis of initial FNA	Follow-up study	No.	Results of follow-up study	
					Conclusive	Inconclusive
Anderson *et al*.[14] (2014)	USA	Non-diagnostic	FNA	336	263	73
Baloch *et al*.[15] (2003)	USA	Non-diagnostic	FNA	123	92	31
Chen *et al*.[16] (2012)	USA	AUS/FLUS	FNA	26	17	9
Choi *et al*.[17] (2014)	Korea	Non-diagnostic	CNB	128	120	8
			FNA	140	40	100
Choi *et al*.[18] (2014)	Korea	AUS/FLUS	CNB	107	103	4
Dincer *et al*.[19] (2013)	Turkey	AUS/FLUS	FNA	74	51	23
Gocun *et al*.[20] (2014)	Turkey	AUS/FLUS	FNA	118	73	45
Gweon *et al*.[21] (2013)	Korea	AUS/FLUS	FNA	86	81	5
Ho *et al*.[22] (2014)	USA	AUS/FLUS	FNA	116	74	42
Hyeon *et al*.[23] (2014)	Korea	AUS/FLUS	FNA	274	214	60
Jo *et al*.[24] (2011)	USA	Non-diagnostic	FNA	363	267	96
Lee *et al*.[25] (2015)	Korea	AUS/FLUS	CNB	34	28	6
			FNA	118	74	44
Lee *et al*.[26] (2014)	Korea	Non-diagnostic	CNB	121	114	7
			FNA	357	239	118
Moon *et al*.[27] (2015)	Korea	AUS/FLUS	FNA	246	185	61
Moslavac *et al*.[28] (2012)	Croatia	Non-diagnostic	FNA	38	31	7
Na *et al*.[29] (2015)	Korea	AUS/FLUS	CNB	158	110	48
			FNA	158	75	83
Na *et al*.[30] (2012)	Korea	Non-diagnostic	CNB	45	43	2
			FNA	45	32	13
		AUS/FLUS	CNB	104	82	22
			FNA	104	75	29
Nagarkatti *et al*.[31] (2013)	USA	AUS/FLUS	FNA	51	28	23
Oertel *et al*.[32] (2007)	USA	Non-diagnostic	FNA	27	23	4
Park *et al*.[33] (2011)	Korea	Non-diagnostic	CNB	54	53	1
			FNA	142	73	69
Park *et al*.[34] (2015)	Korea	AUS/FLUS	FNA	236	155	81
Samir *et al*.[35] (2012)	USA	Non-diagnostic	CNB	69	51	18
			FNA	69	36	33
Sullivan *et al*.[36] (2014)	USA	AUS/FLUS	FNA	86	48	38
Trimboli *et al*.[37] (2015)	Italy	Indeterminate	CNB	198	125	73
Yeon *et al*.[38] (2013)	Korea	Non-diagnostic	CNB	116	108	8
Yoon *et al*.[39] (2011)	Korea	Non-diagnostic	FNA	99	91	8

FNA, fine needle aspiration; CNB, core needle biopsy; AUS/FLUS, atypia/follicular lesion of undetermined significance.

Table 2. Conclusive rates of second CNB and repeat FNA after prior FNA with non-diagnostic or AUS/FLUS significance in thyroid nodules

	No. of subsets	No. of patients	Fixed effect model (95% CI)	Heterogeneity (p-value)	Random effect model (95% CI)	Egger's test
Overall	35	4,566	0.690 (0.675–0.704)	<.001	0.748 (0.701–0.791)	.009
Second CNB	11	1,134	0.775 (0.745–0.802)	<.001	0.879 (0.801–0.929)	<.001
Non-diagnostic	6	533	0.897 (0.864–0.923)	<.001	0.927 (0.847–0.966)	.122
AUS/FLUS	5	601	0.712 (0.671–0.749)	<.001	0.794 (0.675–0.877)	.030
Repeat FNA	24	3,432	0.670 (0.653–0.686)	<.001	0.684 (0.627–0.736)	.651
Non-diagnostic	11	1,739	0.674 (0.650–0.697)	<.001	0.699 (0.596–0.785)	.773
AUS/FLUS	13	1,693	0.666 (0.642–0.689)	<.001	0.673 (0.608–0.732)	.719

CNB, core needle biopsy; FNA, fine needle aspiration; AUS/FLUS, atypia of undetermined significance/follicular lesion of undetermined significance; CI, confidence interval.

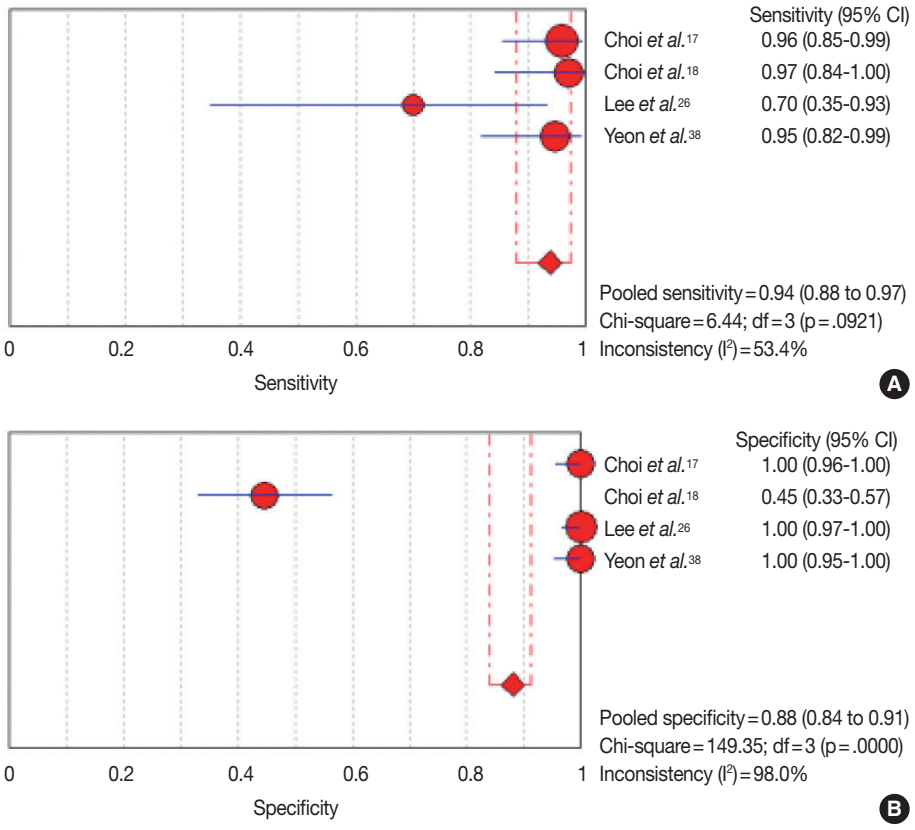

Fig. 2. The sensitivity (A) and specificity (B) of follow-up core needle biopsy for prediction of papillary thyroid carcinoma after prior fine needle aspiration with non-diagnostic or atypia/follicular lesion of undetermined significance in thyroid nodules.

rate of 0.690 (95% confidence interval [CI], 0.675 to 0.704) and 0.748 (95% CI, 0.701 to 0.791) with the fixed and random effect models, respectively. For follow-up CNB, the conclusive rate was 0.775 (95% CI, 0.745 to 0.802) and 0.879 (95% CI, 0.801 to 0.929) with the fixed and random effect models, respectively. In rFNA, the conclusive rate was 0.670 (95% CI, 0.653 to 0.686) and 0.684 (95% CI, 0.627 to 0.736) with the fixed and random effect models, respectively. The ranges of conclusive rates were 0.631–0.981 and 0.286–0.942 for follow-up CNB and rFNA, respectively. Follow-up CNB showed a higher conclusive rate compared with rFNA (OR, 5.707; 95% CI, 2.530 to 12.875). The heterogeneity of eligible studies was significant in both follow-up CNB and rFNA groups ($I^2 = 90.4\%$, $p < 0.001$ and $I^2 = 90.3\%$, $p < 0.001$, respectively). In sensitivity analysis, no study had an effect on the concordance rates for either follow-up CNB (range, 0.864 to 0.896) or rFNA (range, 0.670 to 0.697). Subgroup analysis revealed a significant difference in conclusive rate between follow-up CNB and rFNA in both non-diagnostic (0.927; 95% CI, 0.848 to 0.966 vs 0.699; 95% CI, 0.596 to 0.785) and AUSL/FLUS cases (0.794; 95% CI, 0.675 to 0.877 vs 0.673; 95% CI, 0.608 to 0.732) with the random effect model (Table 2).

Egger's test revealed that the follow-up CNB group showed a significant publication bias ($p = .009$). Additionally, fail-safe N and trim-fill tests were performed for confirmation of the degree of publication bias in the CNB group. The number of missing studies that would produce a p-value higher than alpha was 5,401 on the fail-safe N test. Because there were 11 observed studies, the publication bias was not large. In addition, the trim and fill test showed no significant difference between the observed and adjusted values. Therefore, we concluded that the publication bias in the follow-up CNB group was not significant through interpretation of Egger's test, Begg's funnel plot, the fail-safe N test, and the trim-fill test. In the rFNA group, there was no significant publication bias according to Egger's test ($p = .651$) or Begg's funnel plots.

DTA review of follow-up CNB as a follow-up study

For confirmation of the diagnostic accuracy of follow-up CNB, we conducted a DTA review. The pooled sensitivity and specificity values were 0.94 (95% CI, 0.88 to 0.97) and 0.88 (95% CI, 0.84 to 0.91), respectively (Fig. 2). The sensitivity and spe-

http://dx.doi.org/10.4132/jptm.2016.02.15

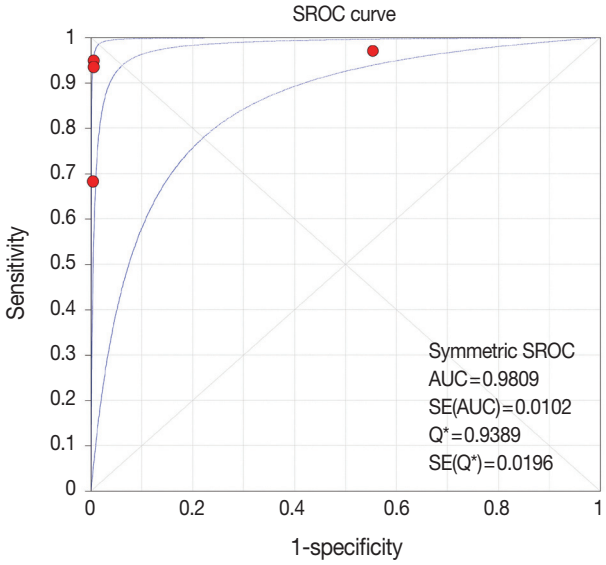

Fig. 3. The summary receiver operating characteristics (SROC) curve of follow-up core needle biopsy for prediction of papillary thyroid carcinoma after prior fine needle aspiration with non-diagnostic or atypia/follicular lesion of undetermined significance in thyroid nodules. AUC, area under the curve.

cificity of eligible studies ranged from 0.70 to 0.97 and from 0.45 to 1.00, respectively. On the SROC curve, the value of AUC was 0.981 (Fig. 3). In addition, the diagnostic OR was 448.73 (95% CI, 36.63 to 5,497.51).

DISCUSSION

The current guidelines recommend FNA as the initial test for thyroid nodules.[4-6] Although rFNA was applied to thyroid nodules with non-diagnostic and AUS/FLUS findings,[4-6] the effectiveness of rFNA has not been fully elucidated. The present study is the first meta-analysis and DTA review of published studies on the diagnostic role of follow-up CNB compared with rFNA after initial FNA with non-diagnostic or AUS/FLUS results.

In the assessment of thyroid nodule, FNA is the most cost-effective initial test. Recently, FNA using ultrasonography has produced a higher quality of specimens for more precise diagnosis.[10] However, some cases were non-diagnostic or AUS/FLUS, and the rates of inconclusive results ranged from 10%–33.6% in previous studies.[6,8,9,40] Although the current guidelines recommend rFNA as a follow-up study for thyroid nodules with initial inconclusive results,[4-6] rFNA does not ensure conclusive results. The inconclusive rates of rFNA in previous studies ranged from 9.9% to 72.0%.[18,29,34,36] In the current meta-analysis, the rate of inconclusive results for rFNA was 31.6%. If the cellularity of initial FNA is low, rFNA can also show low cellularity. In a previous study, rFNA was the most significant risk factor affecting repeat non-diagnostic results.[18] This situation might be caused by the nature of the thyroid nodule, including factors such as intratumoral calcification and cystic change.[41-43] In addition, the quality of the specimen might also be affected by the experience of the operator. Consequently, diagnostic surgery is recommended for thyroid nodule with repeat inconclusive results, and the incidence of diagnostic surgery has been reported as 22.2%–94.7%.[24,44-46] Therefore, to reduce the inconclusive rate, an alternative follow-up study, such as CNB, could be considered for thyroid nodules with inconclusive readings in initial FNA.

Considering the results of a previous meta-analysis, histologic examination using CNB as an initial test might be useful for obtaining conclusive results.[47] Other previous comparative studies of FNA and CNB as an initial test have reported that CNB has a suspected higher specificity, higher positive predictive value, and lower rate of inconclusive results.[11,48] However, definitive results for the sensitivity and specificity of CNB as a follow-up study have not yet been obtained.[10,11,47] CNB showed a lower sensitivity for thyroid glands than for other head and neck lesions.[49] However, the initial test might be more important for achieving higher sensitivity and patient safety. Furthermore, CNB has some limitations, including bleeding, tumor-cell displacement, and difficulty in approaching thyroid nodules in a posterior portion or close to critical structures, including the carotid artery or trachea; these factors limit its use as an initial test.[48,49] To obtain an adequate specimen for diagnosis, the experience of the operator may be more important for CNB than for FNA.[48] Whether CNB is appropriate as an initial test for thyroid nodules is not fully understood and could not be determined in the current systematic review. Despite a previous report that found follow-up CNB to have lower non-diagnostic and inconclusive rates than rFNA (7.2% vs 72.0%),[18] many previous studies have reported that CNB showed lower sensitivity than FNA. However, the diagnostic accuracy of follow-up CNB has not been fully elucidated. In the current DTA review, the pooled sensitivity and specificity of follow-up CNB were significantly high. For this reason, follow-up CNB after initial FNA might be useful for predicting malignancy and reducing the inconclusive rate in follow-up study.

There were some limitations in the current meta-analysis. First, most included studies were retrospective rather than prospective evaluations. Many thyroid nodules with initial inconclusive results only involved follow-up with ultrasonography. The conclusive and inconclusive rates of rFNA and follow-up CNB might have been affected by such cases. Therefore, cumu-

lative prospective studies are needed to determine the effectiveness of follow-up procedures. Second, the current study included both non-diagnostic and AUS/FLUS subgroups, and subgroup analysis was performed. However, the DTA review could be not conducted for the rFNA subgroup due to insufficient information from eligible studies. Thus, a comparison of diagnostic accuracy between follow-up CNB and rFNA could not be performed. Third, because the current guidelines recommend initial FNA test for thyroid nodules,[4-6] the current meta-analysis was performed only for studies with initial FNA. An investigation of the effectiveness of CNB as an initial test was therefore not conducted in the current study. Fourth, the current study was analyzed for initial non-diagnostic and AUS/FLUS categories. However, additional evaluations, including subgroup analysis for AUS and FLUS results, could not be performed due to lack of information on follow-up CNB from eligible studies.[23] Fifth, eligible studies used various criteria for nondiagnostic or indeterminate lesion. The rate of inconclusive results of CNB may have differed from the real value. Further studies are needed to establish guidelines of pathology reporting for thyroid CNB.

In conclusion, the current study showed that follow-up CNB had a higher conclusive rate than rFNA after initial FNA with inconclusive results. In addition, follow-up CNB had greater diagnostic accuracy for prediction of malignancy than rFNA. Additional prospective studies are required to determine standardized application criteria of follow-up CNB in daily practice.

Conflicts of Interest

No potential conflict of interest relevant to this article was reported.

REFERENCES

1. Sprague BL, Warren Andersen S, Trentham-Dietz A. Thyroid cancer incidence and socioeconomic indicators of health care access. Cancer Causes Control 2008; 19: 585-93.
2. Enewold L, Zhu K, Ron E, *et al*. Rising thyroid cancer incidence in the United States by demographic and tumor characteristics, 1980-2005. Cancer Epidemiol Biomarkers Prev 2009; 18: 784-91.
3. Mercante G, Frasoldati A, Pedroni C, *et al*. Prognostic factors affecting neck lymph node recurrence and distant metastasis in papillary microcarcinoma of the thyroid: results of a study in 445 patients. Thyroid 2009; 19: 707-16.
4. Cibas ES, Ali SZ. The Bethesda System for Reporting Thyroid Cytopathology. Thyroid 2009; 19: 1159-65.
5. American Thyroid Association (ATA) Guidelines Taskforce on Thyroid Nodules and Differentiated Thyroid Cancer, Cooper DS, Doherty GM, et al. Revised American Thyroid Association management guidelines for patients with thyroid nodules and differentiated thyroid cancer. Thyroid 2009; 19: 1167-214.
6. Gharib H, Papini E, Paschke R, *et al*. American Association of Clinical Endocrinologists, Associazione Medici Endocrinologi, and European Thyroid Association medical guidelines for clinical practice for the diagnosis and management of thyroid nodules: executive summary of recommendations. J Endocrinol Invest 2010; 33(5 suppl 1): 51-6.
7. Yang J, Schnadig V, Logrono R, Wasserman PG. Fine-needle aspiration of thyroid nodules: a study of 4703 patients with histologic and clinical correlations. Cancer 2007; 111: 306-15.
8. Yassa L, Cibas ES, Benson CB, *et al*. Long-term assessment of a multidisciplinary approach to thyroid nodule diagnostic evaluation. Cancer 2007; 111: 508-16.
9. Nayar R, Ivanovic M. The indeterminate thyroid fine-needle aspiration: experience from an academic center using terminology similar to that proposed in the 2007 National Cancer Institute Thyroid Fine Needle Aspiration State of the Science Conference. Cancer 2009; 117: 195-202.
10. Harvey JN, Parker D, De P, Shrimali RK, Otter M. Sonographically guided core biopsy in the assessment of thyroid nodules. J Clin Ultrasound 2005; 33: 57-62.
11. Renshaw AA, Pinnar N. Comparison of thyroid fine-needle aspiration and core needle biopsy. Am J Clin Pathol 2007; 128: 370-4.
12. Zamora J, Abraira V, Muriel A, Khan K, Coomarasamy A. Meta-DiSc: a software for meta-analysis of test accuracy data. BMC Med Res Methodol 2006; 6: 31.
13. Pyo JS, Sohn JH, Kang G. BRAF immunohistochemistry using clone VE1 is strongly soncordant with *BRAF*(V600E) mutation test in papillary thyroid carcinoma. Endocr Pathol 2015; 26: 211-7.
14. Anderson TJ, Atalay MK, Grand DJ, Baird GL, Cronan JJ, Beland MD. Management of nodules with initially nondiagnostic results of thyroid fine-needle aspiration: can we avoid repeat biopsy? Radiology 2014; 272: 777-84.
15. Baloch Z, LiVolsi VA, Jain P, *et al*. Role of repeat fine-needle aspiration biopsy (FNAB) in the management of thyroid nodules. Diagn Cytopathol 2003; 29: 203-6.
16. Chen JC, Pace SC, Chen BA, Khiyami A, McHenry CR. Yield of repeat fine-needle aspiration biopsy and rate of malignancy in patients with atypia or follicular lesion of undetermined significance: the impact of the Bethesda System for Reporting Thyroid Cytopathology. Surgery 2012; 152: 1037-44.
17. Choi YJ, Baek JH, Ha EJ, *et al*. Differences in risk of malignancy and

management recommendations in subcategories of thyroid nodules with atypia of undetermined significance or follicular lesion of undetermined significance: the role of ultrasound-guided core-needle biopsy. Thyroid 2014; 24: 494-501.
18. Choi SH, Baek JH, Lee JH, *et al*. Thyroid nodules with initially nondiagnostic, fine-needle aspiration results: comparison of core-needle biopsy and repeated fine-needle aspiration. Eur Radiol 2014; 24: 2819-26.
19. Dincer N, Balci S, Yazgan A, *et al*. Follow-up of atypia and follicular lesions of undetermined significance in thyroid fine needle aspiration cytology. Cytopathology 2013; 24: 385-90.
20. Gocun PU, Karakus E, Bulutay P, Akturk M, Akin M, Poyraz A. What is the malignancy risk for atypia of undetermined significance? Three years' experience at a university hospital in Turkey. Cancer Cytopathol 2014; 122: 604-10.
21. Gweon HM, Son EJ, Youk JH, Kim JA. Thyroid nodules with Bethesda system III cytology: can ultrasonography guide the next step? Ann Surg Oncol 2013; 20: 3083-8.
22. Ho AS, Sarti EE, Jain KS, *et al*. Malignancy rate in thyroid nodules classified as Bethesda category III (AUS/FLUS). Thyroid 2014; 24: 832-9.
23. Hyeon J, Ahn S, Shin JH, Oh YL. The prediction of malignant risk in the category "atypia of undetermined significance/follicular lesion of undetermined significance" of the Bethesda System for Reporting Thyroid Cytopathology using subcategorization and BRAF mutation results. Cancer Cytopathol 2014; 122: 368-76.
24. Jo VY, Vanderlaan PA, Marqusee E, Krane JF. Repeatedly nondiagnostic thyroid fine-needle aspirations do not modify malignancy risk. Acta Cytol 2011; 55: 539-43.
25. Lee SH, Oh HW, Fang Y, *et al*. Identification of plant compounds that disrupt the insect juvenile hormone receptor complex. Proc Natl Acad Sci U S A 2015; 112: 1733-8.
26. Lee SH, Kim MH, Bae JS, Lim DJ, Jung SL, Jung CK. Clinical outcomes in patients with non-diagnostic thyroid fine needle aspiration cytology: usefulness of the thyroid core needle biopsy. Ann Surg Oncol 2014; 21: 1870-7.
27. Moon HJ, Kim EK, Yoon JH, Kwak JY. Malignancy risk stratification in thyroid nodules with nondiagnostic results at cytologic examination: combination of thyroid imaging reporting and data system and the Bethesda System. Radiology 2015; 274: 287-95.
28. Moslavac S, Matesa-Anić D, Matesa N, Kusić Z. When to repeat thyroid fine needle aspiration cytology? Acta Clin Croat 2012; 51: 549-54.
29. Na DG, Min HS, Lee H, Won JK, Seo HB, Kim JH. Role of core needle biopsy in the management of atypia/follicular lesion of undetermined significance thyroid nodules: comparison with repeat fine-needle aspiration in subcategory nodules. Eur Thyroid J 2015; 4: 189-96.
30. Na DG, Kim JH, Sung JY, *et al*. Core-needle biopsy is more useful than repeat fine-needle aspiration in thyroid nodules read as nondiagnostic or atypia of undetermined significance by the Bethesda system for reporting thyroid cytopathology. Thyroid 2012; 22: 468-75.
31. Nagarkatti SS, Faquin WC, Lubitz CC, *et al*. Management of thyroid nodules with atypical cytology on fine-needle aspiration biopsy. Ann Surg Oncol 2013; 20: 60-5.
32. Oertel YC, Miyahara-Felipe L, Mendoza MG, Yu K. Value of repeated fine needle aspirations of the thyroid: an analysis of over ten thousand FNAs. Thyroid 2007; 17: 1061-6.
33. Park KT, Ahn SH, Mo JH, *et al*. Role of core needle biopsy and ultrasonographic finding in management of indeterminate thyroid nodules. Head Neck 2011; 33: 160-5.
34. Park VY, Kim EK, Kwak JY, Yoon JH, Moon HJ. Malignancy risk and characteristics of thyroid nodules with two consecutive results of atypia of undetermined significance or follicular lesion of undetermined significance on cytology. Eur Radiol 2015; 25: 2601-7.
35. Samir AE, Vij A, Seale MK, *et al*. Ultrasound-guided percutaneous thyroid nodule core biopsy: clinical utility in patients with prior nondiagnostic fine-needle aspirate. Thyroid 2012; 22: 461-7.
36. Sullivan PS, Hirschowitz SL, Fung PC, Apple SK. The impact of atypia/follicular lesion of undetermined significance and repeat fine-needle aspiration: 5 years before and after implementation of the Bethesda System. Cancer Cytopathol 2014; 122: 866-72.
37. Trimboli P, Nasrollah N, Amendola S, *et al*. A cost analysis of thyroid core needle biopsy vs. diagnostic surgery. Gland Surg 2015; 4: 307-11.
38. Yeon JS, Baek JH, Lim HK, *et al*. Thyroid nodules with initially nondiagnostic cytologic results: the role of core-needle biopsy. Radiology 2013; 268: 274-80.
39. Yoon JH, Moon HJ, Kim EK, Kwak JY. Inadequate cytology in thyroid nodules: should we repeat aspiration or follow-up? Ann Surg Oncol 2011; 18: 1282-9.
40. Degirmenci B, Haktanir A, Albayrak R, *et al*. Sonographically guided fine-needle biopsy of thyroid nodules: the effects of nodule characteristics, sampling technique, and needle size on the adequacy of cytological material. Clin Radiol 2007; 62: 798-803.
41. Choi YS, Hong SW, Kwak JY, Moon HJ, Kim EK. Clinical and ultrasonographic findings affecting nondiagnostic results upon the second fine needle aspiration for thyroid nodules. Ann Surg Oncol 2012; 19: 2304-9.
42. Choi SH, Han KH, Yoon JH, *et al*. Factors affecting inadequate sampling of ultrasound-guided fine-needle aspiration biopsy of thyroid nodules. Clin Endocrinol (Oxf) 2011; 74: 776-82.
43. Moon HJ, Kwak JY, Kim EK, Kim MJ. Ultrasonographic character-

istics predictive of nondiagnostic results for fine-needle aspiration biopsies of thyroid nodules. Ultrasound Med Biol 2011; 37: 549-55.
44. Orija IB, Piñeyro M, Biscotti C, Reddy SS, Hamrahian AH. Value of repeating a nondiagnostic thyroid fine-needle aspiration biopsy. Endocr Pract 2007; 13: 735-42.
45. Hryhorczuk AL, Stephens T, Bude RO, *et al*. Prevalence of malignancy in thyroid nodules with an initial nondiagnostic result after ultrasound guided fine needle aspiration. Ultrasound Med Biol 2012; 38: 561-7.
46. Lubitz CC, Nagarkatti SS, Faquin WC, *et al*. Diagnostic yield of nondiagnostic thyroid nodules is not altered by timing of repeat biopsy. Thyroid 2012; 22: 590-4.
47. Li L, Chen BD, Zhu HF, *et al*. Comparison of pre-operation diagnosis of thyroid cancer with fine needle aspiration and core-needle biopsy: a meta-analysis. Asian Pac J Cancer Prev 2014; 15: 7187-93.
48. Yoon JH, Kim EK, Kwak JY, Moon HJ. Effectiveness and limitations of core needle biopsy in the diagnosis of thyroid nodules: review of current literature. J Pathol Transl Med 2015; 49: 230-5.
49. Novoa E, Gürtler N, Arnoux A, Kraft M. Role of ultrasound-guided core-needle biopsy in the assessment of head and neck lesions: a meta-analysis and systematic review of the literature. Head Neck 2012; 34: 1497-503.

 http://dx.doi.org/10.4132/jptm.2016.02.15

Journal of Pathology and Translational Medicine 2016; 50: 225-230
http://dx.doi.org/10.4132/jptm.2016.03.08

■ ORIGINAL ARTICLE ■

Investigation of the Roles of Cyclooxygenase-2 and Galectin-3 Expression in the Pathogenesis of Premenopausal Endometrial Polyps

Esin Kasap · Serap Karaarslan[1]
Esra Bahar Gur · Mine Genc
Nur Sahin · Serkan Güclü

Departments of Obstetrics and Gynecology and [1]Pathology, Sifa University School of Medicine, Izmir, Turkey

Received: January 13, 2016
Revised: March 6, 2016
Accepted: March 8, 2016

Corresponding Author
Esin Kasap, MD
Department of Obstetrics and Gynecology,
Sifa University School of Medicine,
Fevzipasa Boulvard, No. 172/2, 35240,
Basmane/İzmir, Türkiye
Tel: +90-232-4460880
Fax: +90-232-4460770
E-mail: dresincelik@windowslive.com

Background: The pathogenesis and etiology of endometrial polyps has not been elucidated. In this study, we aimed to examine the pathogenic mechanisms of endometrial polyp development using immunohistochemistry. We evaluated the expression of galectin-3 and cyclooxgenase-2 (COX-2) during the menstrual cycle in premenopausal women with endometrial polyps or normal endometrium. **Methods:** Thirty-one patients with endometrial polyps and 50 healthy control patients were included in this study. The levels of expression of COX-2 and galectin-3 were studied by immunohistochemistry. **Results:** The percentage of COX-2–positive cells and the intensity of COX-2 staining in the endometrium did not vary during the menstrual cycle either in the control group or in patients with endometrial polyps. However, expression of galectin-3 was significantly lower in endometrial polyps and during the proliferative phase of the endometrium compared with the secretory phase. **Conclusions:** Our data suggests that the pathogenesis of endometrial polyps does not involve expression of COX-2 or galectin-3.

Key Words: Endometrial polyps; Cyclooxgenase-2; Galectin-3; Immunohistochemistry

Focal endometrial projections containing endometrial glands and stroma are termed endometrial polyps.[1] The reported prevalence of endometrial polyps in premenopausal women with abnormal uterine bleeding is 33%, but only 10% in asymptomatic women.[2] While endometrial polyps can occur in women of all ages, they are more common in women between the ages of 40 and 49.[3] Because endometrial polyps have not been reported to occur before the onset of menstruation, estrogenic stimulation is thought to be associated with endometrial polyp growth.[4] However, the pathogenesis and etiology of endometrial polyps has not been clearly determined. Endometrial polyps are believed to form due to hormonal factors, e.g., estrogen and progesterone, which mediate endometrial proliferation and differentiation via steroid receptors;[5] however, the mechanisms involved in the development of endometrial polyps are still unclear.

Cyclooxygenase (COX) is a key enzyme involved in the conversion of arachidonic acid to prostaglandins and other eicosanoids. Two isoforms of COX have been identified: COX-1 and COX-2. COX-1 is constitutively expressed in many tissues, whereas COX-2 is induced by a variety of factors including cytokines, growth factors, and tumor promoters. COX-2, which is involved in inflammatory responses and production of prostaglandins mediating uterine contractions, has been shown to induce excessive formation of some pro-angiogenic factors when overexpressed in colon cancer cell lines *in vitro*.[6] Furthermore, recent studies have shown the influence of COX-2 in neoplastic development.[5] However, the relationship between COX-2 and endometrial polyps has not been well established.

Galectin-3 is a β-galactoside–binding animal lectin that contains carbohydrate-recognition domains and is involved in a multitude of biological tasks,[7] including embryogenesis, growth, cell adhesion, proliferation, differentiation, cell-cycle progression, apoptosis, mRNA splicing, and immune system regulation. Galectin-3 is also involved in tumorigenesis, angiogenesis, and tumor metastasis, and is expressed in various cells and tissues including activated macrophages, eosinophils, neutrophils, mast cells, gastrointestinal and respiratory tract epithelial cells, kidneys cells, and some sensory neurons.[7,8] Interestingly, extracellular galectin-3 plays a role in inflammation, while intracellular galectin-3 participates in cell growth and anti-apoptotic processes

pISSN 2383-7837
eISSN 2383-7845

and modulates cell adhesion and migration.[7]

Polyps tend to occur when apoptosis is inhibited and there is unopposed growth.[9] However, the mechanisms mediating these endometrial alterations are unknown. Previous studies have suggested that endometrial polyps are a result of endometrial inflammation, i.e., endometritis, since the vessel axis of polyps has been shown to develop during endometritis.[10] This finding suggests that identification of markers of inflammation and tissue growth may help to elucidate the pathogenic mechanisms of endometrial polyps. Indeed, recent studies have shown that the levels of expression of COX-2 and galectin-3 are increased during the progression from hyperplasia to cancer in the endometrial tissue, suggesting that these proteins may play a role in tumor cell function. However, the association of COX-2 and galectin-3 expression with polyps has not yet been established.

Therefore, in this study, we analyzed the levels of expression of COX-2 and galectin-3 in endometrial polyps and normal endometrium using immunohistochemistry.

MATERIALS AND METHODS

Patients

We examined a total of 81 cases of endometrial tissues in patients who were treated in the Department of Obstetrics and Gynecology of our hospital. Tissues were sampled between 2012 and 2014. All procedures were approved by the İzmir Sifa University Human Ethics Committee and followed the principles of the Declaration of Helsinki.

All patients were premenopausal (mean age, 37 years; range, 27 to 52 years) and had a recent history of regular menstruation (cycle of 25–35 days). None of the women included in the study used nonsteroidal anti-inflammatory drugs, hormone replacement therapy, or any other estrogen-containing pills. Thirty-one of the 81 patients had endometrial polyps, including 10 who had undergone hysterectomy and 21 who had undergone polypectomy and endometrial curettage. None of the patients had identifiable leiomyoma or adenomyosis by ultrasonography and/or magnetic resonance imaging. The control group consisted of samples from a total of 50 additional patients with normal endometrium, and included 23 samples collected during the proliferative phase and 27 samples collected during the secretory phase. Control patients were recruited from patients with benign ovarian cysts or a uterine prolapse but no other pathology, and the endometrial samples in this group were collected during hysterectomy procedures. Endometrial samples were grouped according to menstrual cycle phases: proliferative (days 1–14 of the cycle) and secretory (days 15–28 of the cycle). The day of the menstrual cycle was established from the women's menstrual history and confirmed by endometrial dating using the criteria described by Noyes *et al*.[11]

Immunohistochemistry

All tissue samples were fixed in 10% formalin and sent to pathology for analysis. Routine hematoxylin and eosin staining was carried out in all samples either to confirm the diagnosis of polyps or to date the endometrium. Samples were embedded in paraffin blocks, cut into 4-μm-thick sections, and deparaffinized. The sections were then stained with primary monoclonal antibodies against COX-2 (1:100, clone CX-294, Dako, Glostrup, Denmark) and galectin-3 (1:100, NCL-GAL3, clone 9C4, NovaCastra, Hamburg, Germany) using a Dako Cytomation Autostainer (Dako). After staining, each sample was evaluated under a light microscope (200×, Olympus BX53, Olympus, Tokyo, Japan) to determine the percentage of COX-2–positive cells, the intensity of COX-2 staining, and the percentage of galectin-3–positive cells. For positive controls, staining of breast carcinoma tissue for COX-2 and papillary thyroid carcinoma tissue for galectin-3 were used. Primary monoclonal antibodies were omitted in negative controls.

Assessment of COX-2 and galectin-3 staining

Semi-quantitative analysis of immunostaining for COX-2 and galectin-3 was performed as follows based on the percentage of cells with positive cytoplasmic staining: 0%, 0; < 10%, 1; 10%–50%, 2; 51%–80%, 3; and ≥80%, 4. In addition, staining intensity was evaluated as either negative (0), weak (1+), moderate (2+), or strong (3+). Semi-quantitative and intensity scores were analyzed separately. Additionally, the positivity of cells was evaluated as positive or negative.[12] COX-2 and galectin-3 expression was evaluated in glandular epithelial cells and stromal cells. Assessment of staining results was performed by one observer in a blinded fashion.

Statistical analysis

Statistical analysis was performed using software (Rstudio software ver. 0.98.501 via R language, R Studio Inc., Boston, MA, USA). Data describing continuous variables are presented as the mean ± standard deviation. The Kruskal-Wallis and Pearson chi-square exact tests were used to compare continuous and categorical variables, respectively. Differences with p-values less than .05 were accepted as significant.

http://dx.doi.org/10.4132/jptm.2016.03.08

RESULTS

Patient demographics

There was no statistically significant difference between the ages of healthy control individuals and patients with endometrial polyps.

COX-2 expression

Immunoreactivity for COX-2 was observed in glandular epithelial cells and stromal cells. COX-2–positive cells were predominantly observed in the endometrial glandular epithelium, where expression peaked during the secretory phase. COX-2-positive cells were also observed in stromal cells, albeit to a lesser extent (Table 1, Fig. 1A). The percentage of COX-2–positive cells and the intensity of COX-2 staining in stromal cells and glandular epithelial cells did not vary during different periods of the menstrual cycle in the control group or in patients with endometrial polyps (Fig. 1B). Mean COX-2 scores in glandular epithelial cells and stromal cells were not significantly different between endometrial polyp specimens and normal endometrium specimens (Table 1).

Galectin-3 expression

Galectin-3 immunoreactivity was present in the endometrial glandular epithelial cells and stromal cells. Immunostaining was typically cytoplasmic. Galectin-3–positive cells were predominantly observed in the endometrial glandular epithelium, where expression levels peaked during the secretory phase. Galectin-3 expression was also observed to a lesser extent in stromal cells (Table 2). The mean percentage score of galectin-3 expression were lower both in endometrial polyps and the proliferative phase in normal endometrium than in the secretory phase in normal endometrium (Table 2, Fig. 1C). In glandular epithelial cells, no statistically significant differences in galectin-3 expression were found between endometrial polyps and normal endometrium during the proliferative phase. However, in patients with normal endometrium, galectin-3 expression was higher during the secretory phase (p = .349) (Fig. 1C). Finally, there

Table 1. Percentages of COX-2–positive cells and intensity of COX-2 staining

		Proliferative phase	Secretory phase	Endometrial polyps	p-value
Glandular epithelial tissues	COX-2 intensity	2.04 ± 1.02	2.07 ± 0.83	1.77 ± 1.11	.489[a]
	0–1	7	6	12	.398[b]
	2–3	16	21	19	
	COX-2 percentage score	2.35 ± 1.12	2.67 ± 1.04	2.35 ± 1.38	.614[a]
	0–1	4	3	8	.351[b]
	2–4	19	24	23	
Endometrial stroma	COX-2 intensity	0.65 ± 0.71	0.70 ± 0.67	0.53 ± 0.68	.564[a]
	0–1	20	24	27	.941[b]
	2–3	3	3	3	
	COX-2 percentage score	0.61 ± 0.65	0.81 ± 0.78	0.61 ± 0.76	.525[a]
	0–1	21	21	26	.430[b]
	2–4	2	6	5	

Values are presented as mean ± standard deviation.
COX, cyclooxgenase.
[a]p-value for Kruskal-Wallis tests, [b]p-value for Pearson chi-square test.

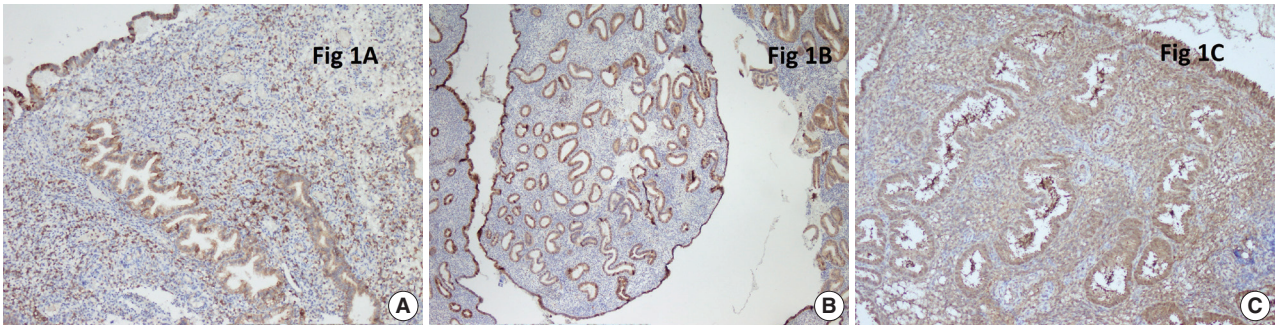

Fig. 1. Expression of cyclooxgenase 2 (COX-2) and galectin-3 in endometrium samples. (A) COX-2 expression in both the glandular epithelium and stroma during the secretory phase. (B) COX-2 expression in both the glandular epithelium and stroma of an endometrial polyp. (C) Galectin-3 expression in both the glandular epithelium and stroma during the secretory phase.

Table 2. Percentages of galectin-3–positive cells

	Proliferative phase	Secretory phase	Endometrial polyp	p-value
Galectin-3 glandular epithelial tissues (% score)	1.35±1.19	2.19±1.00	1.71±1.16	.039[a]
Galectin-3 endometrial stroma (% score)	1.43±1.12	1.63±1.15	1.19±0.87	.349[a]

Values are presented as mean±standard deviation.
[a]p-value for Kruskal-Wallis tests.

were no differences in galectin-3 expression in stromal cells of endometrial polyps and those of the endometrium at any phase of the menstrual cycle (Table 2).

DISCUSSION

In this study, we compared galectin-3 and COX-2 expression and staining patterns using immunohistochemistry in endometrial polyps and normal endometrium during the secretory and proliferative phases. Our data indicated that both galectin-3 and COX-2 were not associated with the formation of endometrial polyps.

Estrogen is known to play a pivotal role in the pathogenesis of endometrial malignant and benign cancers. However, the role of estrogen biosynthesis from stromal cells of the endometrium and its impact on malignancies has not been fully elucidated. Interestingly, estrogens are known to activate COX-2 in endometriosis, which increases levels of estradiol and prostaglandin above normal in women.[13] Therefore, the pathogenesis of peritoneal endometriosis may be a consequence of enhanced prostaglandins in the eutopic endometrium that stimulate COX-2 expression and activity.[14,15] This mechanism may also affect other endometrial pathologies, although no specific roles have been described.

COX-2 is expressed at higher levels in the glandular epithelial cells of the endometrium during the secretory phase of the menstrual cycle compared with the proliferative phase; however, its expression is similar during the secretory and proliferative phases in endometrial stromal cells.[16] In the present study, we observed that COX-2 expression tended to be higher during the secretory phase than in either the proliferative phase or endometrial polyps in glandular epithelial cells.

Some studies have suggested that endometrial polyps may originate from endometrial inflammation.[17] After demonstrating that COX-2 is expressed in the epithelial lining of postmenopausal polyps, Maia *et al*.[18] concluded that COX-2 may be involved in the regulation of polyp growth. Nevertheless, COX-2 expression has not been shown to differ significantly between normal endometrial tissue and endometrial polyps.[19]

In 2006, Maia and colleagues compared COX-2 expression between endometrial polyps and normal endometrium in women with a regular menstrual cycle and found no significant difference in COX-2 expression between polyps and the normal endometrium.[19] In addition, Pinheiro *et al*.[20] observed higher COX-2 expression in the glandular epithelium of obese women than in women of normal weight. This finding indicates that expression of COX-2 expression may be influenced by metabolic changes and growth factors associated with obesity.[20] Here, we also demonstrated that COX-2 expression in the glandular epithelium and stromal cells in endometrial polyps did not differ significantly from that of normal endometrium. Thus, our data suggest that COX-2 expression may not be associated with the formation of endometrial polyps.

We previously reported that expression of galectin-3 is augmented during the formation of the receptive endometrium and the mid-secretory phase of the menstrual cycle.[21] In addition, there is mounting evidence for a strong relationship between embryo implantation and tumor invasion and metastasis. Interestingly, galectin-3 has been reported to have anti-apoptotic potential in tumor cells, although there is no evidence for the role of galectin-3 in endometrial cell apoptosis. Thus, we hypothesize that galectin-3 functions as an anti-apoptotic factor in the endometrium and may facilitate the development of endometrial polyps.

Chiu *et al*.[22] found that immunohistochemical analysis of galectin-3 protein expression is a sensitive, specific, and accurate marker for the diagnosis of thyroid cancer and certain other cancers.[23] In endometriosis, Noel *et al*.[24] found that galectin-3 protein expression, as measured using immunohistochemistry, is higher in endometriosis samples compared to eutopic endometrium, and also higher in the eutopic endometrium of women with endometriosis compared to those without endometriosis. Together, these data suggest that galectin-3 may have a potential role in the development of endometriosis.[24] In a study by Brustmann *et al*.,[25] galectin-3 expression was assessed by immunohistochemistry in patients with normal endometrium, simple hyperplasia, complex hyperplasia without atypia, atypical hyperplasia, endometrioid carcinoma, serous papillary carcinoma, and clear cell carcinoma. They showed that in normal endometrium, simple hyperplasia, and complex hyperplasia without atyp-

 http://dx.doi.org/10.4132/jptm.2016.03.08

ia, the galectin-3 expression did not differ significantly among these groups. Immunohistochemical expression of galectin-3 for atypical hyperplasia and endometrioid carcinoma were significantly higher than those in the aforementioned groups. Serous papillary carcinoma and clear cell carcinoma, which are known to have a poorer prognosis than endometrioid carcinoma,[26] also demonstrated significantly elevated galectin-3 expression levels in this study. On the basis of these findings, we assumed that galectin-3 expression may be related to the different biological behaviors of endometrialcarcinomas.[25] Importantly, while there was no difference in galectin-3 expression in glandular epithelium and stromal cells of endometrial polyps and normal endometrium, our data demonstrated that galectin-3 expression was significantly lower in both endometrial polyps and the proliferative phase of the endometrium than in the secretory phase of the endometrium. This finding suggests that larger-scale studies are needed to measure galectin-3 levels in secretory adenocarcinomas, a subgroup of endometrioid adenocarcinomas, and in other endometrial cancers.

In analyzing our results, we wondered whether galectin-3 expression may be regulated by estrogen and progesterone. Although previous reports have shown that estrogen and/or progesterone increases galectin-3 expression in endometrial cells at all concentrations,[27] we did not observe any direct effect of these hormones on galectin-3 expression, suggesting that the relationship may be indirect. Thus, further studies are needed to determine the exact nature of the relationship of estrogen and progesterone on galectin-3 expression.

The small sample size was a limitation of the present study. Therefore, the results of this study must be confirmed in larger longitudinal population studies.

In summary, our data suggested that endometrial polyps may form through certain common pathways that do not involve COX-2 and galectin-3. While COX-2 and galectin-3, in addition to angiogenesis, are known to be involved in different steps of carcinogenesis,[28] these two target proteins may not be involved in the formation of endometrial polyps. Further large scale studies comparing adjacent endometrial tissue and healthy women at specific phases of the menstrual cycle should be performed.

Conflicts of Interest

No potential conflict of interest relevant to this article was reported.

REFERENCES

1. Neto LC, Soares JM Jr, Giusa-Chiferi MG, Gonçalves WJ, Baracat EC. Expression of p53 protein in the endometrial polyp in postmenopausal women. Eur J Gynaecol Oncol 2013; 34: 509-12.
2. Clevenger-Hoeft M, Syrop CH, Stovall DW, Van Voorhis BJ. Sonohysterography in premenopausal women with and without abnormal bleeding. Obstet Gynecol 1999; 94: 516-20.
3. Droegemueller W. Benign gynecologic lesions. In: Stenchever MA, Droegemueller W, Herbst AL, Mishell DR Jr, eds. Comprehensive gynecology. 5th ed. St. Louis: Mosby Inc., 2001; 440-92.
4. Inceboz US, Nese N, Uyar Y, *et al*. Hormone receptor expressions and proliferation markers in postmenopausal endometrial polyps. Gynecol Obstet Invest 2006; 61: 24-8.
5. Sant'Ana de Almeida EC, Nogueira AA, Candido dos Reis FJ, Zambelli Ramalho LN, Zucoloto S. Immunohistochemical expression of estrogen and progesterone receptors in endometrial polyps and adjacent endometrium in postmenopausal women. Maturitas 2004; 49: 229-33.
6. Kendall RL, Wang G, Thomas KA. Identification of a natural soluble form of the vascular endothelial growth factor receptor, FLT-1, and its heterodimerization with KDR. Biochem Biophys Res Commun 1996; 226: 324-8.
7. Lee J, Moon C, Kim J, *et al*. Immunohistochemical localization of galectin-3 in the granulomatous lesions of paratuberculosis-infected bovine intestine. J Vet Sci 2009; 10: 177-80.
8. Sakaki M, Fukumori T, Fukawa T, *et al*. Clinical significance of galectin-3 in clear cell renal cell carcinoma. J Med Invest 2010; 57: 152-7.
9. Topcu HO, Erkaya S, Guzel AI, *et al*. Risk factors for endometrial hyperplasia concomitant endometrial polyps in pre- and postmenopausal women. Asian Pac J Cancer Prev 2014; 15: 5423-5.
10. Costa-Paiva L, Godoy CE Jr, Antunes A Jr, Caseiro JD, Arthuso M, Pinto-Neto AM. Risk of malignancy in endometrial polyps in premenopausal and postmenopausal women according to clinicopathologic characteristics. Menopause 2011; 18: 1278-82.
11. Noyes RW, Hertig AT, Rock J. Dating the endometrial biopsy. Fertil Steril 1950; 1: 3-25.
12. Harrington DJ, Lessey BA, Rai V, *et al*. Tenascin is differentially expressed in endometrium and endometriosis. J Pathol 1999; 187: 242-8.
13. Maia H Jr, Maltez A, Studard E, Zausner B, Athayde C, Coutinho E. Effect of the menstrual cycle and oral contraceptives on cyclooxygenase-2 expression in the endometrium. Gynecol Endocrinol 2005; 21: 57-61.
14. Erdemoglu E, Güney M, Karahan N, Mungan T. Expression of cyclooxygenase-2, matrix metalloproteinase-2 and matrix metallo-

proteinase-9 in premenopausal and postmenopausal endometrial polyps. Maturitas 2008; 59: 268-74.
15. Bulun SE, Zeitoun KM, Takayama K, Sasano H. Estrogen biosynthesis in endometriosis: molecular basis and clinical relevance. J Mol Endocrinol 2000; 25: 35-42.
16. Wang D, Chen Q, Zhang C, Ren F, Li T. DNA hypomethylation of the COX-2 gene promoter is associated with up-regulation of its mRNA expression in eutopic endometrium of endometriosis. Eur J Med Res 2012; 17: 12.
17. Carvalho FM, Aguiar FN, Tomioka R, de Oliveira RM, Frantz N, Ueno J. Functional endometrial polyps in infertile asymptomatic patients: a possible evolution of vascular changes secondary to endometritis. Eur J Obstet Gynecol Reprod Biol 2013; 170: 152-6.
18. Maia H Jr, Correia T, Freitas LA, Athayde C, Coutinho E. Cyclooxygenase-2 expression in endometrial polyps during menopause. Gynecol Endocrinol 2005; 21: 336-9.
19. Maia H Jr, Pimentel K, Silva TM, *et al*. Aromatase and cyclooxygenase-2 expression in endometrial polyps during the menstrual cycle. Gynecol Endocrinol 2006; 22: 219-24.
20. Pinheiro A, Antunes A Jr, Andrade L, De Brot L, Pinto-Neto AM, Costa-Paiva L. Expression of hormone receptors, Bcl2, Cox2 and Ki67 in benign endometrial polyps and their association with obesity. Mol Med Rep 2014; 9: 2335-41.
21. Du GP, Zhang W, Wang L, Liu YK, Zhou JP. Expression of galectin-3 in human endometrium. Fudan Univ J Med Sci 2006; 2: 143-6.
22. Chiu CG, Strugnell SS, Griffith OL, *et al*. Diagnostic utility of galectin-3 in thyroid cancer. Am J Pathol 2010; 176: 2067-81.
23. Cay T. Immunhistochemical expression of galectin-3 in cancer: a review of the literature. Turk Patoloji Derg 2012; 28: 1-10.
24. Nöel JC, Chapron C, Borghese B, Fayt I, Anaf V. Galectin-3 is overexpressed in various forms of endometriosis. Appl Immunohistochem Mol Morphol 2011; 19: 253-7.
25. Brustmann H, Riss D, Naudé S. Galectin-3 expression in normal, hyperplastic, and neoplastic endometrial tissues. Pathol Res Pract 2003; 199: 151-8.
26. Silverberg SG, Kurman RJ. Atlas of tumor pathology, 3rd series. Fascicle 3. Tumors of the uterine corpus and gestational trophoblastic disease. Washington, DC: Armed Forces Institute of Pathology, 1992.
27. Yang H, Lei C, Cheng C, *et al*. The antiapoptotic effect of galectin-3 in human endometrial cells under the regulation of estrogen and progesterone. Biol Reprod 2012; 87: 39.
28. Kumar V, Abbas AK, Fausto N. Robbins and Cotran: pathologic basis of disease. 7th ed. Philadelphia: Elsevier Saunders, 2005; 269-342.

 http://dx.doi.org/10.4132/jptm.2016.03.08

Journal of Pathology and Translational Medicine 2016; 50: 231-237
http://dx.doi.org/10.4132/jptm.2015.08.08

■ CASE STUDY ■

Rare Case of Anal Canal Signet Ring Cell Carcinoma Associated with Perianal and Vulvar Pagetoid Spread

Na Rae Kim · Hyun Yee Cho
Jeong-Heum Baek[1] · Juhyeon Jeong
Seung Yeon Ha · Jae Yeon Seok
Sung Won Park[1] · Sun Jin Sym[2]
Kyu Chan Lee[3] · Dong Hae Chung

Departments of Pathology and [1]General Surgery, [2]Division of Hematology and Oncology, Department of Internal Medicine, [3]Department of Radiation Oncology, Gachon University Gil Medical Center, Incheon, Korea

Received: June 19, 2015
Revised: July 27, 2015
Accepted: August 7, 2015

Corresponding Author
Dong Hae Chung, MD
Department of Pathology, Gachon University Gil Medical Center, 21 Namdong-daero 774beon-gil, Namdong-gu, Incheon 21565, Korea
Tel: +82-32-460-3866
Fax: +82-32-460-2394
E-mail: dhchung@gilhospital.com

A 61-year-old woman was referred to surgery for incidentally found colonic polyps during a health examination. Physical examination revealed widespread eczematous skin lesion without pruritus in the perianal and vulvar area. Abdominopelvic computed tomography showed an approximately 4-cm-sized, soft tissue lesion in the right perianal area. Inguinal lymph node dissection and Mils' operation extended to perianal and perivulvar skin was performed. Histologically, the anal canal lesion was composed of mucin-containing signet ring cells, which were similar to those found in Pagetoid skin lesions. It was diagnosed as an anal canal signet ring cell carcinoma (SRCC) with perianal and vulvar Pagetoid spread and bilateral inguinal lymph node metastasis. Anal canal SRCC is rare, and the current case is the third reported case in the English literature. Seven additional cases were retrieved from the world literature. Here, we describe this rare case of anal canal SRCC with perianal Pagetoid spread and provide a literature review.

Key Words: Carcinoma, signet ring cell; Anal canal; Paget disease, extramammary

According to the recent World Health Organization classification of the digestive system, patients with mucinous adenocarcinoma have a significantly high survival rate compared to those with signet ring cell carcinoma (SRCC).[1] By definition, SRCC has more than 50% intracellular mucin and mucinous carcinoma has more than 50% extracellular mucin. SRCC can arise from virtually all organs, including stomach, colon, breasts, gallbladder, or even urinary bladder.[2] When an extragastric SRCC is found in an unusual site, metastasis from other primary sites should be excluded. Among colorectal SRCCs of the digestive tract, anal canal SRCCs are even rarer.[3] Only two cases of anal canal SRCC have been described in the English literature.[4,5]

We recently encountered a rare case of anal canal SRCC and extramammary Paget's disease. Extramammary Paget's disease commonly appears in the vulvar area, followed by the perianal region, scrotum, penis, and axillae.[6] In most cases, Paget's disease is not accompanied by cancer; however, cancer hidden in the adjacent organs, including the vulva, vagina, uterus, ovary, bladder, and colorectal area, should be kept in mind.

Here, we report on a case of anal canal SRCC and Pagetoid spread, and provide a literature review.

CASE REPORT

A 61-year-old woman visited our hospital for alleged colon polyps found during a colonoscopy examination as part of a routine health examination. Endoscopic submucosal dissection was performed. Four polyps were diagnosed as tubular adenoma. Abdominopelvic computed tomography (CT) showed an approximately 4-cm-sized, well-enhancing soft tissue lesion in the right perianal area (Fig. 1A) and a well-enhancing enlarged lymph node in both inguinal areas, suggesting hypervascular tumor metastasis such as melanoma in those lymph nodes (Fig. 1B). Upon physical examination, however, a widespread ery-

pISSN 2383-7837
eISSN 2383-7845

thematous lichenified skin lesion, measuring 12 × 9.7 cm, was noted in the perianal and vulvar area (Fig. 2A), which had developed over the previous 3 years according to the patient. She did not complain of pruritus. She had no history of anal fissure, fistula, or change in bowel habit. Skin biopsy was taken from the perianal and vulvar area, which showed infiltrating Pagetoid cells and SRCC cells. There was neither abnormal bowel wall thickening nor masses in the sigmoid colon. No other lesion was observed on upper esophagogastroscopy. The preoperative carcinoembryonic antigen (CEA) level was elevated to 39.75 ng/mL (reference, 0 to 5 ng/mL). Carbohydrate antigen 19-9 was within normal ranges. Inguinal lymph node dissection with an extended Miles' operation was performed; traditional Miles' operation with extended resection around bilateral labium majora, followed by skin reconstruction with gluteal flap, was performed. The resected specimen was composed of the anal canal and rectum with skin and soft tissue of the perianal region and vulva (Fig. 2B). Upon sectioning, the anal canal showed an ulcerative firm mass measuring 4.0 × 3.0 × 2.7 cm, which invaded the perianal sphincter muscle and subcutaneous fat of the anal skin (Fig. 2C). Light microscopy showed that the anal canal was totally replaced by singly scattered intracytoplasmic mucin-containing signet ring cells and some extracellular mucin (Fig. 3A, B). Focally, well-formed glands were also found in less than 5% of the tumor. Most of the surface epithelium was denuded. The focal residual transformation zone showed a focus of adenocarcinoma *in situ* (Fig. 3C), and was not contiguous with the anal glands. Anal canal SRCC was diagnosed. The erythematous skin around the anus and labium majora showed linear infiltration of Pagetoid cells as well as infiltration of signet ring cells in the dermis and subcutis (Fig. 3D). Involved skin area measured 8.2 × 8.0 × 0.5 cm. Lymphatic permeation was noted in the dermis. Enlarged bilateral inguinal lymph nodes also showed infiltration of the signet ring cells.

Immunohistochemically, both signet ring cells and Pagetoid cells were positive for cytokeratin (CK) 20, CEA, MOC-31, and CK19. Intracellular and extracellular mucin was eosinophilically stained with mucicarmine. Both signet ring cells and Paget's

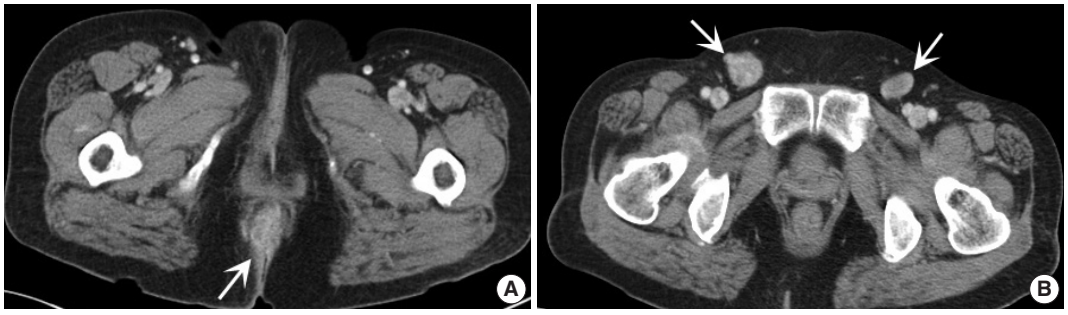

Fig. 1. Radiologic findings. (A) Abdominal computed tomography reveals a well-enhancing lesion (arrow) at the right perianal portion. (B) Enlarged bilateral inguinal lymph nodes (arrows) are found.

Fig. 2. Gross pictures. (A) Perianal and vulvar skin shows elevated erythematous changes. (B) Extended Miles' operation specimen consists of distal rectal segment and excision of perianal region and vulva. (C) Cross-section of the resected specimen shows a firm anal canal mass infiltrating to the perianal skin and levator ani muscle.

http://dx.doi.org/10.4132/jptm.2015.08.08

cells were positive for epidermal growth factor receptor and weakly positive for CK5/6. They were negative for CK7, human melanoma black 45, S-100 protein, caudal-related homeobox gene nuclear transcription factor (CDX2), p53, synaptophysin, chromogranin, and CD56. These results are shown in Table 1.

A mutation study of the KRAS gene (codon 12 and codon 13) was performed by means of the peptide nucleic acid-mediated real-time polymerase chain reaction clamping method using genomic DNA isolated from formalin fixed paraffin-embedded tissue. Mutations in codon 12 and 13 were not detected in anal canal SRCC.

Microsatellite instability (MSI) was tested using five Bethesda markers (D2S123, D5S346, D17S250, BAT25, and BAT26). MSI-high (MSI-H) was defined if they differed in at least two of the five markers and MSI-low was defined if they differed in only one of the five markers. Anal canal mass was microsatellite stable (MSS).

Positron emission tomography CT and chest CT showed no evidence of systemic metastases. The case was diagnosed as anal canal SRCC with Pagetoid spread in perianal and vulva skin, stage IIIB according to the TNM staging system of the Ameri-

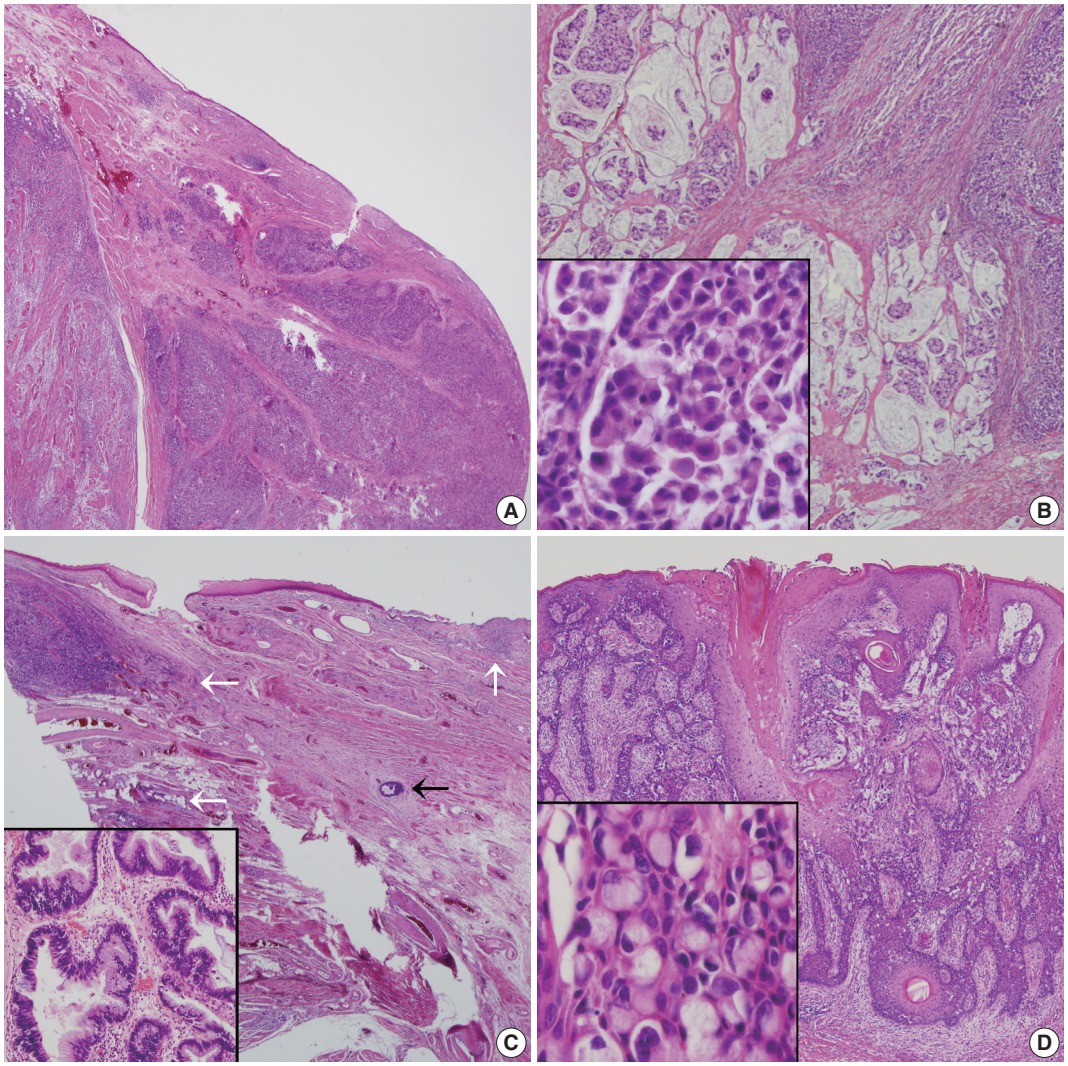

Fig. 3. (A) A transmural, yellowish gray firm mass is composed of singly scattered signet ring cells and some extracellular mucin. Note the surface mucosal erosion. (B) The majority of the mass is infiltrated by signet ring carcinoma cells, and poorly differentiated mucinous glands are floating in the mucin pool. Inset indicates high magnification of signet ring cells showing intracytoplasmic mucin compressing the hyperchromatic nuclei to the periphery. (C) The transformation zone of the anal canal shows infiltration of multifocal signet ring cell carcinoma (white arrows) and a focus of atypical gland beneath the mucosa (black arrow). Inset shows adenocarcinoma *in situ* with a gland having enlarged hyperchromatic nuclei with coarse chromatin and increased nuclear/cytoplasmic ratio. (D) Large Paget cells showing clear cytoplasm with eccentric hyperchromic nuclei are located along the basal layer of the squamous epithelium. Inset indicates Paget cells in the epidermis.

Table 1. Immunohistochemical results of anal canal signet ring cell carcinoma and Paget's disease

	Clone, dilution, company	Anal canal signet ring cell carcinoma	Pagetoid spread of vulvar and perianal skin
CK7	OV-TL 12/30; 1:100 dilution; Dako, Glostrup, Denmark	–	–
CK20	Ks20.8; 1:100 dilution; Dako, Glostrup, Denmark	+	+
CK19	A53-B/A2.26; 1:200 dilution; Thermo Scientific, Fremont, USA	+	+
CK5/6	D5/16 B4; prediluted; Dako, Glostrup, Denmark	+ weak	–
EGFR	SP84; 1:30 dilution; Novocastra, Newcastle upon Tyne, UK	+	+
CEA	Polyclonal; prediluted; Dako, Glostrup, Denmark	+	+
MOC-31	MOC-31; 1:70 dilution; Novocastra, Newcastle upon Tyne, UK	+	+
CDX2	AMT28; 1:50 dilution; Novocastra, Newcastle upon Tyne, UK	–	–
S-100 protein	Polyclonal; 1:1,200 dilution; Dako, Glostrup, Denmark	–	–
Synaptophysin	DAK-SYNAP; prediluted; Dako, Glostrup, Denmark	–	–
Chromogranin	polyclonal; prediluted; Dako, Glostrup, Denmark	–	–
CD56	123C3; prediluted; Dako, Glostrup, Denmark	–	–
HMB45	HMB45; prediluted; Dako, Glostrup, Denmark	–	–
p53	DO-7; 1:100 dilution; Dako, Glostrup, Denmark	+	+

CK, cytokeratin; EGFR, epidermal growth factor receptor; CEA, carcinoembryonic antigen; CDX2, caudal-related homeobox gene nuclear transcription factor; HMB45, human melanoma black 45.

can Joint Committee on Cancer.

The patient was scheduled to undergo chemotherapy with mitomycin-C and 5-fluorouracil (5-FU) and subsequent radiotherapy. The patient's postoperative course was unremarkable.

Institutional review board (IRB) approval was obtained for this case report.

DISCUSSION

Colorectal SRCC is a rare histologic subtype of adenocarcinoma, accounting for 0.1% to 2.4% of all colorectal malignancies.[1] Anal canal SRCC is even rarer; only two cases of anal canal SRCCs have been reported in the English literature.[4,5] Seven additional cases have been retrieved from the Japanese literature.[3,7-12]

The current case showed anal canal SRCC. Anal canal carcinoma is histologically and pathogenetically divided into squamous cell carcinoma, cloacogenic (basaloid or transitional cell) carcinoma and adenocarcinoma.[13] Anal canal squamous cell carcinoma originates from the non-keratinizing squamous epithelium below the dentate line of the anal canal, while anal canal adenocarcinoma is regarded as arising from the upper part lined by the columnar epithelium. Anal canal adenocarcinomas are rare. According to the World Health Organization classification, anal canal adenocarcinomas are subclassified according to adenocarcinoma arising from anal mucosa and extramucosa, and adenocarcinoma arising from anorectal fistula or adenocarcinoma of anal glands.[14] No description of in situ lesion was found in the previously reported cases of anal canal SRCCs. Based on the findings of the overlying ulcerated anal surface mucosa, remnants of anal gland adenocarcinoma *in situ* without continuity to SRCC portion, the present anal canal SRCC belongs to extramucosal perianal adenocarcinoma with wide Pagetoid spread along the perianal soft tissues and skin.

We have summarized the clinicopathologic characteristics in Table 2. Similar to the current case, eight out of 10 anal canal SRCCs (80%) were accompanied by perianal or vulvar Pagetoid spread.[3-5,7-12] Extramammary perianal Paget's disease is a rare and heterogeneous neoplasm, which is frequently combined with underlying hidden adenocarcinoma.[6] Immunohistochemical panels such as CK7, CK20, CEA, gross cystic disease fluid protein-15 (GCDFP-15), MUC1, MUC2, MUC5AC, and CDX2 have been used to distinguish primary from secondary Paget's disease.[15] In anal SRCCs with Pagetoid spread, i.e., not primary extramammary Paget's disease, the tumor cells were positive for CK20, MUC1, or MOC-31, while they were negative for GCDFP-15, and negative for CK7, whereas primary Paget's disease is commonly positive for CK7.[16] However, none of these were a specific and confirmative diagnostic clue; further accumulative data may be needed. SRCC is most commonly encountered in the stomach, but it can also arise in various organs, such as breast, urinary bladder, or colon. Immunohistochemical profiles for CK7 and CK20 have also been used to differentiate the sites of origin for SRCCs; CK20 is normally expressed in the gastrointestinal epithelium, urothelium, and in Merkel's cells. While CK7 is uncommonly expressed in the lower gastrointestinal tract, it is commonly expressed in lung, ovary, endometrium, and breast.[15]

http://dx.doi.org/10.4132/jptm.2015.08.08

Table 2. Clinicopathologic summary of the reported cases of primary anal canal signet ring cell carcinomas with or without Paget's disease

Case No.	Author	Age (yr)/ Sex	Presenting symptom	Gross and histopathology	Immunohistochemistry	TNM at the initial evaluation	Treatment	Clinical outcome (follow-up period)
1	Uchigasaki *et al*. (1992)[3]	52/F	Anal ulcer and pruritus for 2 yr[a]	Anal canal SRCC progressed from adenocarcinoma *in situ* of anal glands or mucinous glands (1.5 cm), Pagetoid spread (7 cm)	pCEA+ mCEA+ mucicarmine+ PAS+ D-PAS-resistant	T1N3M0, stage IIIB	Topical 5-FU cream, EB, ASR	Recurrence with systemic metastasis and died (7 mo)
2	Morihisa *et al.* (1999)[7,b]	75/F	Perianal erythema and erosion for 7 mo	Anal canal SRCC (size not described), Pagetoid spread (5 cm)	CEA+ mucicarmine+ PAS+	N3M1, stage IV	Nephrostomy for ARF due to systemic metastasis	Systemic metastasis and died (4 mo)
3	Nagano *et al.* (1999)[8]	46/F	Inguinal LN enlargement	Anal canal and rectal SRCC (3.5 cm), Pagetoid spread (7.5 cm)	Alcian blue+ PAS+	T2N3M0, stage IIIB	APR, CTX (5-FU, LV)	NR (3 mo)
4	Naganuma *et al.* (2004)[9]	85/F	Anal bleeding for 3 yr	Anal canal SRCC (unknown size of polyp, residual anal canal mass, 5 mm), Pagetoid spread (size not described)	CEA+ CA19-9+ CK20+ CK7– GCDFP-15–	N3M1, stage IV	Anal polypectomy with CTX (5-FU), RT	Systemic metastasis and died (25 mo)
5	Nishimura *et al.* (2004)[10, b]	76/F	Anal erosion and erythema for 2 yr	Anal canal SRCC (size not described), Pagetoid spread (6 cm)	CK20+ GCDFP-15–	Not available[b]	APR, CTX (5-FU, cisplatin)	NR (5 mo)
6	Yoshitani *et al.* (2009)[11]	50/M	Axillary and inguinal LN enlargement for 1 mo, erythematous perianal skin	Anal canal SRCC (size not precisely described; anal verge to dentate line), Pagetoid spread (size not described)	CK20+ MUC-1+ CK7–	N3M1, stage IV	CTX (bevacizumab/ mFOLFOX6, FOLFIRI)	Alive with CR evaluated by PET-CT (6 mo)
7	Ikezawa *et al.* (2010)[12]	53/M	Anal pruritus for 22 mo	Anal canal SRCC (1 cm), Pagetoid spread (2 cm)	pCEA+ CK20+ CK7– GCDFP-15–	T1N2M0, stage IIIB	APR, CTX (uracil-tegafur, LV, mFOLFOX6)	Recurrence with systemic metastasis and died (9 mo)
8	Ioannidis *et al.* (2012)[4]	87/F	Anal discomfortness and pain for 8 mo	Anal canal SRCC (3 cm)	Not done	T2N0M0, stage II	Wide excision with chemotherapy (5-FU) and RT	NR (6 yr)
9	Terada (2014)[5]	49/M	Anal bleeding	Anal canal SRCC (<2 cm)	AE1/3+ CK8+ CK19+ CEA+ CA19-9+ synaptophysin+ CDX2+ MUC1+ MUC2+ EMA+ CK7– CK20– CK5/6– MUC5AC– MUC6– CD56– NSE– chromogranin– vimentin–	T1N1M0, stage IIIA	Miles' operation with LN dissection	Metastatic carcinomatosis and died (5 mo)
10	Kim *et al.* (2016)	61/F	Erythematous perianal and vulvar skin for 3 yr, synchronous colon adenocarcinoma (0.2 cm)	Anal canal SRCC (4 cm), Pagetoid spread (8.2 cm)	pCEA+ CK20+ CK19+ MOC-31+ CDX2– CK7– HMB45– mucicarmine+	T2N3M0, stage IIIB	Extended Miles' operation and inguinal LN dissection, CTX (5-FU, MTC), RT (planned)	NR (2 mo)

F, female; SRCC, signet ring cell carcinoma; pCEA, polyclonal carcinoembryonic antigen; mCEA, monoclonal carcinoembryonic antigen; PAS, periodic acid-Schiff; D-PAS, PAS diastase stain; 5-FU, 5-fluorouracil; EB, electron beam therapy; ASR, abdominosacral resection; CEA, carcinoembryonic antigen; ARF, acute renal failure; LN, lymph node; APR, abdominoperineal resection; CTX, chemotherapy; LV, leucovorin; NR, no recurrence; CA19-9, carbohydrate antigen 19-9; CK, cytokeratin; GCDFP-15, gross cystic disease fluid protein-15; RT, radiotherapy; M, male; mFOLFOX6, leucovorin, 5-FU, and oxaliplatin; FOLFIRI, irinotecan, 5-FU, and leucovorin; CR, complete remission; PET-CT, positron emission tomography-computed tomography; EMA, epithelial membrane antigen; NSE, neuron specific enolase; HMB-45, human melanoma black 45; MTC, mitomycin-C.

[a]This case was diagnosed as Paget's disease 15 years before the anal canal SRCC; [b]These articles were not available.

As the term "signetring cells" implies, the tumor cells have intracellular mucin vacuoles displacing the nucleus to one side of the cells scattered as single cells or in loose clusters. This is caused by disrupted cell-to-cell adhesion and diffuse spreading, and results in more frequent lymphovascular invasion and node metastasis of SRCC as compared with other mucinous adenocarcinoma.

In view of the clinical aspects, colorectal SRCC has a very high mortality rate compared to mucinous carcinoma and non-mucinous colorectal adenocarcinomas. Even a minor signet-ring cell component, i.e., 50% or less, in colorectal carcinomas was independently associated with a high mortality rate, regardless of molecular or other clinicopathological factors.[17] Anal canal SRCC grows insidiously underneath the mucosa, and thus it may not be found before the late advanced stage. It is uncertain whether anal SRCCs have an adverse prognosis like that of colorectal SRCC.[18] Inguinal nodes should be examined for anal cancer staging. In a review of 10 cases of anal canal SRCCs, the ages ranged from 46 to 87 years (mean, 63.4 years).[3-5,7-12] Two cases were proven as primary anal canal SRCCs by autopsy.[7,9] SRCC has a shorter patient survival. During the follow-up period, ranging from 4 to 25 months, death caused by lymphatic or peritoneal carcinomatosis or distant metastases occurred in 50% of cases (5/10).[3,5,7,9,12] The five remaining cases were alive with a follow-up period ranging from 2 months to 6 years. None of the previous cases underwent moleculocytogenetic application. For the past decade, molecular prognostic markers in colorectal carcinoma have been studied; MSI-H is a well-established reliable predictive marker for chemotherapeutic efficacy in colorectal carcinoma. However, contrary to colorectal SRCCs that take an aggressive course, colorectal mucinous carcinoma takes a favorable course, although both are associated with MSI-H.[1] Data on anal canal SRCC concerning MSI-H as a predictive factor is lacking. The current case showed MSS, albeit it is only one case. Due to the rarity of anal canal SRCCs, the MSI status of anal canal SRCC relating to prognosis has not been determined. Further accumulative investigation is required.

Traditional treatment of anal canal carcinoma is surgery including abdominopelvic resection with or without chemoradiotherapy.[19] Radiation therapy for anal canal carcinoma reaches a cure rate of up to 70% in selected low-stage patients. However, there is no general agreement regarding the treatment of anal canal SRCC due to the extremely rare incidence and limited data on cancer treatment, as shown in Table 2. In a case reported by Yoshitani *et al.*,[11] a patient with distant metastatic foci achieved complete remission after chemotherapy using bevacizumab/mFOLFOX6, FOLFIRI. Ioannidis *et al.*[4] reported on a long-survived stage II patient with no recurrent tumor who underwent chemoradiotherapy using 5-FU for a 6-year follow-up period.

In summary, anal canal SRCC is extremely rare. If there is perianal Paget's disease raising the possibility of underlying hidden adenocarcinoma, careful evaluation is necessary for early diagnosis of anal canal SRCC.

Conflicts of Interest

No potential conflict of interest relevant to this article was reported.

REFERENCES

1. Inamura K, Yamauchi M, Nishihara R, *et al*. Prognostic significance and molecular features of signet-ring cell and mucinous components in colorectal carcinoma. Ann Surg Oncol 2015; 22: 1226-35.
2. Chu PG, Weiss LM. Immunohistochemical characterization of signet-ring cell carcinomas of the stomach, breast, and colon. Am J Clin Pathol 2004; 121: 884-92.
3. Uchigasaki S, Ochiai T, Miyakawa K, Suzuki H, Morishima T. Circumanal Paget's disease which was complicated by anus cancers after 15 years. Skin Cancer 1992; 7: 254-8.
4. Ioannidis O, Papaemmanouil S, Paraskevas G, *et al*. Primary signet ring cell anal adenocarcinoma. J Gastrointest Cancer 2012; 43 Suppl 1: 168-70.
5. Terada T. Primary pure signet-ring cell carcinoma of the anus: a case report with immunohistochemical study. Endoscopy 2014; 46 Suppl 1 UCTN: E347.
6. Lopes Filho LL, Lopes IM, Lopes LR, Enokihara MM, Michalany AO, Matsunaga N. Mammary and extramammary Paget's disease. An Bras Dermatol 2015; 90: 225-31.
7. Morihisa A, Nobutoh T, Kohda M, Ueki H. An autopsy case of anal canal cancer showing Paget's disease as the first sign. Jpn J Clin Dermatol 1999; 53: 758-60.
8. Nagano Y, Nanko M, Nagahori Y. Rectal signet ring cell carcinoma associated with perianal Paget's disease: report of a case. J Jpn Surg Assoc 1999; 60: 473-6.
9. Naganuma H, Ottomo S, Takaya K, Sakai N, Tamahashi N, Takahashi T. An autopsy case of anal canal cancer (signet ring cell carcinoma) accompanied with perianal Pagetoid spread. Jpn J Diagn Pathol 2004; 21: 129-32.
10. Nishimura H, Kaneko T, Mizuki D, *et al.* A case of anal canal cancer presenting a pagetoid phenomenon in the perianal lesion. Jpn J

 http://dx.doi.org/10.4132/jptm.2015.08.08

Clin Dermatol 2004; 58: 674-7.
11. Yoshitani S, Hosokawa K, Yokoi M, *et al*. A case of anal canal carcinoma with systemic lymph node metastases successfully treated by bevacizumab+mFOLFOX6 therapy. Gan To Kagaku Ryoho 2009; 36: 2229-31.
12. Ikezawa F, Miura K, Shibata C, *et al*. Pagetoid spread with anal canal poorly differentiated adenocarcinoma: a case report. Jpn J Gastroenterol Surg 2010; 43: 678-84.
13. Moritani Y, Tomioka N, Izumi A, Takiue T, Kobayashi N, Shirakawa Y. A case of anal gland carcinoma accompanied by Pagetoid spread. Nippon Daicho Komonbyo Gakkai Zasshi 2009; 62: 121-6.
14. Welton ML, Lambert R, Bosman FT. Tumours of the anal canal. In: Bosman, FT, Carneiro F, Hruban RH, Theise ND, eds. WHO classification of tumours of the digestive system. 4th ed. Lyon: IARC Press, 2010; 183-93.
15. Grelck KW, Nowak MA, Doval M. Signet ring cell perianal paget disease: loss of MUC2 expression and loss of signet ring cell morphology associated with invasive disease. Am J Dermatopathol 2011; 33: 616-20.
16. Ohnishi T, Watanabe S. The use of cytokeratins 7 and 20 in the diagnosis of primary and secondary extramammary Paget's disease. Br J Dermatol 2000; 142: 243-7.
17. Ogino S, Nosho K, Kirkner GJ, *et al*. CpG island methylator phenotype, microsatellite instability, *BRAF* mutation and clinical outcome in colon cancer. Gut 2009; 58: 90-6.
18. Kang H, O'Connell JB, Maggard MA, Sack J, Ko CY. A 10-year outcomes evaluation of mucinous and signet-ring cell carcinoma of the colon and rectum. Dis Colon Rectum 2005; 48: 1161-8.
19. Shridhar R, Shibata D, Chan E, Thomas CR. Anal cancer: current standards in care and recent changes in practice. CA Cancer J Clin 2015; 65: 139-62.

Journal of Pathology and Translational Medicine 2016; 50: 238-242
http://dx.doi.org/10.4132/jptm.2016.02.19

■ CASE STUDY ■

Sclerosing Perivascular Epithelioid Cell Tumor of the Lung: A Case Report with Cytologic Findings

Ha Yeon Kim · Jin Hyuk Choi
Hye Seung Lee · Yoo Jin Choi
Aeree Kim · Han Kyeom Kim

Department of Pathology, Korea University Guro Hospital, Seoul, Korea

Received: January 21, 2016
Revised: February 11, 2016
Accepted: February 19, 2016

Corresponding Author
Han Kyeom Kim, MD, PhD
Department of Pathology, Korea University Guro Hospital, 148 Gurodong-ro, Guro-gu, Seoul 08308, Korea
Tel: +82-2-2626-3251
Fax: +82-2-2626-1481
E-mail: sswords@naver.com

Benign perivascular epithelioid cell tumor (PEComa) of the lung is a rare benign neoplasm, a sclerosing variant of which is even rarer. We present a case of 51-year-old man who was diagnosed with benign sclerosing PEComa by percutaneous fine needle aspiration cytology and biopsy. The aspirate revealed a few cell clusters composed of bland-looking polygonal or spindle cells with fine granular or clear cytoplasm. Occasional fine vessel-like structures with surrounding hyalinized materials were seen. The patient later underwent wedge resection of the lung. The histopathological study of the resected specimen revealed sheets of polygonal cells with clear vacuolated cytoplasm, variably sized thin blood vessels, and densely hyalinized stroma. In immunohistochemical studies, reactivity of tumor cells for human melanoma black 45 and Melan-A further supported the diagnosis of benign sclerosing PEComa. To the best of our knowledge, this is the first case of benign sclerosing PEComa described in lung.

Key Words: Lung neoplasms; Solitary pulmonary nodule; Perivascular epithelioid cell neoplasms

Benign perivascular epithelioid cell tumor (PEComa) of the lung is a rare benign neoplasm. It is also called benign clear cell "sugar" tumor due to its glycogen content in cytoplasm. Since initially described by Liebow and Castleman in 1963,[1] about 50 cases have been reported so far in the English literature. Histologically, benign PEComa is composed of sheets of epithelioid or spindle cells with clear cytoplasm and thin walled vascular spaces. Cytological findings of benign PEComa include loosely cohesive clusters of polygonal or spindle cells with fine granular or clear cytoplasm. To our knowledge, the cytologic findings of benign PEComa of the lung have been described in only three reports to date, and benign sclerosing PEComa was not mentioned in those reports.[2-4] In 2008, a distinctive variant of benign PEComa with > 50% stromal hyalinization was designated as benign "sclerosing" PEComa by Hornick and Fletcher.[5] We present cytologic findings of a benign sclerosing PEComa of the lung.

CASE REPORT

We report a case of a 51-year-old male patient diagnosed with benign PEComa by percutaneous fine needle aspiration of the lung. He had hypertension, diabetes mellitus and history of smoking (30 pack-years). He complained no specific symptoms. On chest X-ray, a well-demarcated mass was incidentally found in the periphery of the right upper lobe. It measured 1 cm and was confined to lung parenchyma.

Computed tomography-guided percutaneous aspiration and gun biopsy was simultaneously performed. The lesion was diagnosed as benign sclerosing PEComa on the basis of cytologic and histologic findings. After the diagnosis, the patient underwent subsequent wedge resection of the lung. The histologic and immunohistochemical findings of the resected specimen confirmed the diagnosis of benign sclerosing PEComa.

Cytologic findings

Alcohol-fixed liquid-based preparation (ThinPrep, Cytyc Corporation, Boxborough, MA, USA) was performed after percutaneous fine needle aspiration. The cytologic preparation was hypocellular with a few cell clusters in a clean background. These clusters consisted of polygonal to spindle cells with oval nuclei and small distinct nucleoli. Most of the cells showed abundant basophilic and granular cytoplasm or clear intracytoplasmic vac-

pISSN 2383-7837
eISSN 2383-7845

uoles (Fig. 1A). Nuclear pleomorphism was minimal. Neither necrosis nor mitotic figures was observed. Some of the clusters had thin vessel-like structures within (Fig. 1B). Semitranslucent hyalinizing material was noted around the vascular structures (Fig. 1C).

Histologic findings of biopsied specimen

Gun-biopsied specimen was also composed of bland-looking polygonal cells with vacuolated cytoplasm and minimal atypia. Variable-sized vascular spaces were observed among sheets of tumor cells. Dilated vessels were surrounded by hyalinized stroma. Focal microcalcification was noted. Tumor cells were positive for human melanoma black 45 (HMB-45). Intracytoplasmic vacuoles were confirmed as glycogen by periodic acid–Schiff stain and diastase periodic acid–Schiff stain.

Gross findings of resected specimen

Wedge resected specimen of the right upper lobe revealed a 1.0-cm-sized, well-demarcated, non-encapsulated, and round mass. It was well confined within the pulmonary parenchyma. The mass was tan-colored and had a firm texture. The cut surface of the mass showed multiple tiny cyst-like spaces at the periphery.

Histologic findings of resected specimen

On light microscopy, the histologic findings of the surgical specimen were similar to those of the gun-biopsied specimen. The tumor was mainly composed of sheets of polygonal cells with distinct cell borders. Tumor cells showed clear cytoplasmic vacuoles and round to oval nuclei with granular chromatin and distinct nucleoli (Fig. 2A). Numerous dilated, thin walled blood vessels were present throughout the tumor. Those vessels were surrounded by pinkish hyalinized stroma (Fig. 2B). A few microcalcifications were seen. The cytoplasmic vacuoles were revealed to be glycogen on periodic acid–Schiff stain and diastase periodic acid–Schiff stain (Fig. 3A, B). Those vacuoles were not

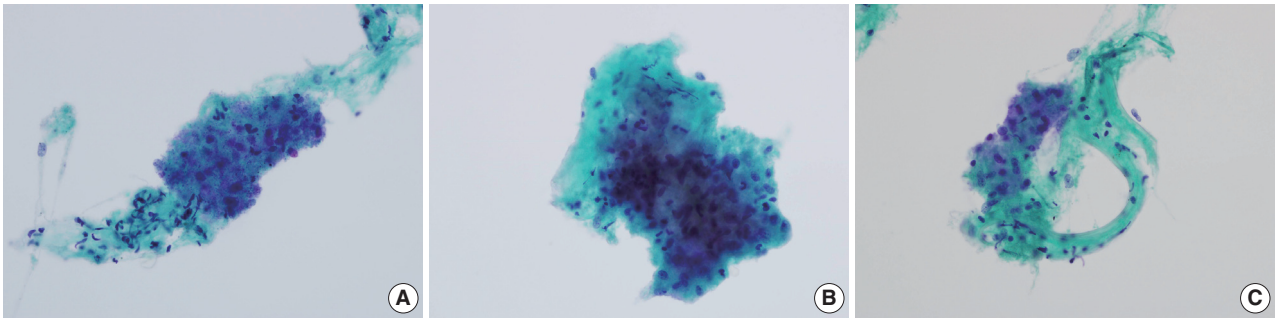

Fig. 1. Liquid-based aspiration cytology of benign sclerosing perivascular epithelioid cell tumor. (A) A few cohesive clusters of polygonal to spindle-shaped bland cells in a clean background (Papanicolaou staining). (B) The tumor cells show oval nuclei, small distinct nucleoli and abundant basophilic and granular cytoplasm. Most cells contain clear intracytoplasmic vacuoles (Papanicolaou staining). (C) Thin-walled blood vessels are occasionally seen. Semitranslucent hyalinizing material was noted around the vascular structure (Papanicolaou staining).

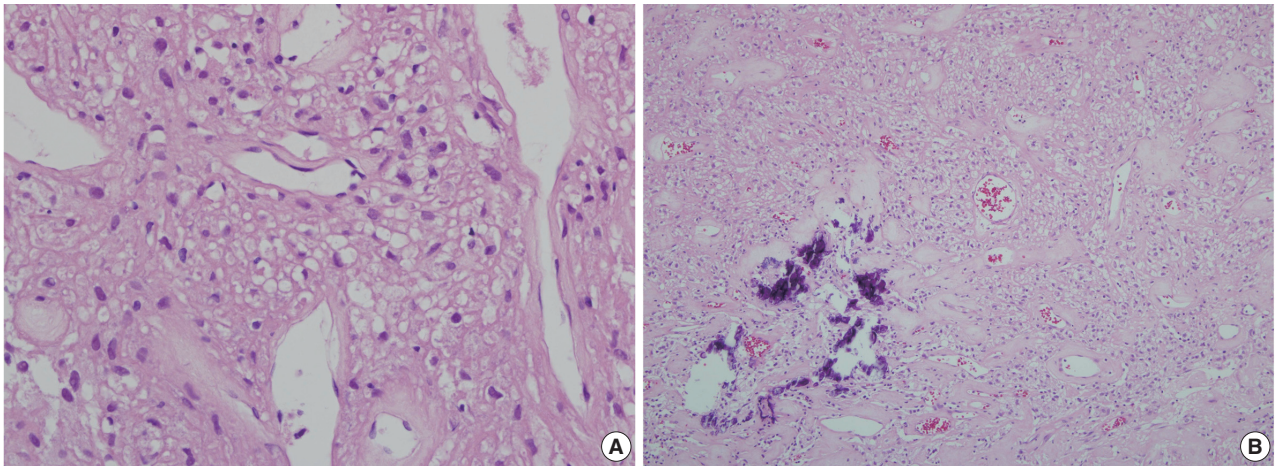

Fig. 2. Histologic section of benign sclerosing perivascular epithelioid tumor. (A) Dilated vessels surrounded by collagenous stroma and polygonal cells with clear cytoplasm. (B) Sheet-like arrangement of tumor cells around various-sized blood vessels and a focus of microcalcification.

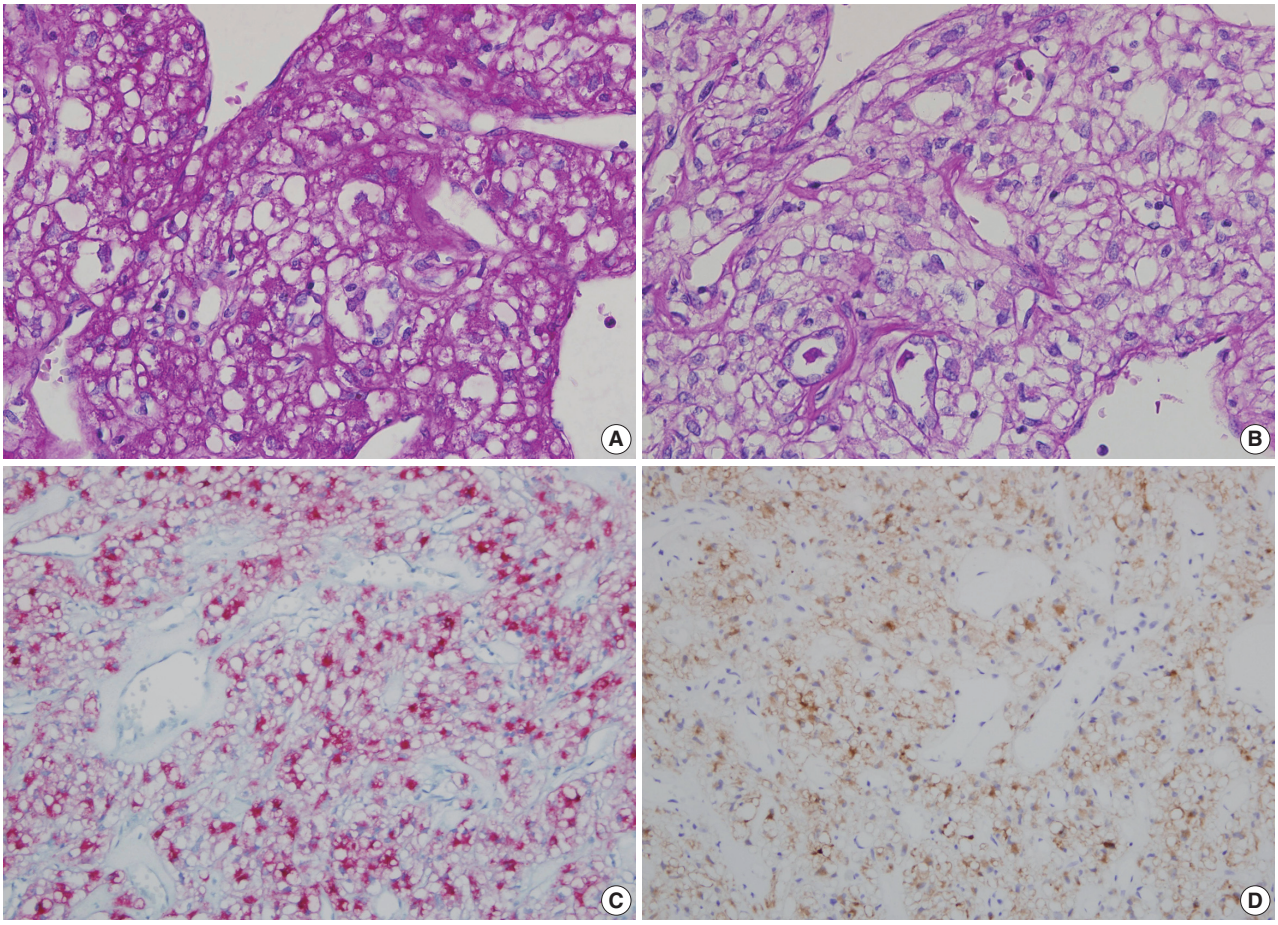

Fig. 3. Special stain and immunohistochemical stains (A, B) Periodic acid–Schiff (PAS) (A) stain and diastase-PAS (B) stain show positive reaction of the clear intracytoplasmic vacuoles in tumor cells. (C, D) Tumor cells show positive reaction to human melanoma black 45 (C) and to Melan-A (D).

reactive in mucicarmine and alcian blue stainings.

Immunohistochemical findings

Various immunohistochemical studies were performed. The results are summarized in Table 1. Tumor cells showed positivity for HMB-45 and Melan-A (Fig. 3C, D). They were negative for S-100 protein, neuroendocrine markers (CD56, synaptophysin, and chromogranin), pulmonary adenocarcinoma markers (thyroid transcription factor 1 [TTF-1], surfactant, and napsin), and cytokeratins. Ki-67 labeling index was low (< 2%).

DISCUSSION

Benign PEComa of the lung was first described in 1963 by Leiwbow and Castleman.[1] It was termed "sugar tumor" due to the intracytoplasmic glycogen content. It is a rare benign neoplasm and about 50 cases have been reported in the English literature so far.

Table 1. Results of immunohistochemical studies of the benign sclerosing perivascular epithelioid cell tumor

Test	Result
HMB-45	Positive
Melan-A	Positive
S-100	Negative
CD56	Negative
Synaptophysin	Negative
Chromogranin	Negative
Vimentin	Positive
TTF-1	Negative
Surfactant	Negative
Napsin	Negative
Cytokeratin	Negative
p63	Negative
Ki-67	Positivity in < 2%
CD68	Negative
SMA	Positive of intratumoral vasculature
CD34	Positive of intratumoral vasculature

HMB-45, human melanoma black 45; TTF-1, thyroid transcription factor 1; SMA, smooth muscle antigen.

http://dx.doi.org/10.4132/jptm.2016.02.19

Patients with benign PEComas of the lung are generally asymptomatic.[6] Our case was similar to most other cases in that the patient had no symptoms and the tumor was detected incidentally. A few cases presented with hemoptysis.[7,8] One case presented with thrombocytosis which resolved after the removal of the tumor.[9]

Typical aspirate specimens of benign PEComas show loosely cohesive clusters of bland-looking cells of various sizes. The cells are mostly epithelioid or spindle and have round-to-oval nuclei, indistinct nucleoli, and vacuolated cytoplasm. Nuclear atypia is rare and necrosis is not observed. Our findings were generally similar to the previous cytologic reports of Nguyen in 1989,[2] Edelweiss *et al*. in 2007[4] and Policarpio-Nicolas *et al*. in 2008.[3] Two exceptional findings include small distinct nucleoli and fine granular basophilic cytoplasm, while others reported indistinct or inconspicuous nucleoli and clear, vacuolated cytoplasm. Different preparation methods might have contributed to these differences. In our case, the aspiration specimen was fixed in alcohol and prepared according to the liquid-based method. Other reports on cytologic findings of benign PEComa all used conventional smear method.

Histologically, benign PEComas are composed mainly of sheets of polygonal cells and occasional spindle cells. Those polygonal cells have round to oval nuclei with granular chromatin and clear cytoplasm with distinct cell borders. The cells look bland and show low proliferative index. Multiple thin-walled and dilated vessels throughout the tumor are a characteristic feature.[10] Tumor cells generally show immunoreactivity with HMB-45, Melan-A, and vimentin.[11] They are negative for cytokeratin, TTF-1, and neuroendocrine markers. Reactivity for S-100 protein is variable.[6,11,12]

Our case was generally similar to the typical findings of benign PEComas of the lung. However, it was different from other cases in that the thin-walled vessels were surrounded by densely hyalinized stroma.

In 2008, Hornick and Fletcher[5] reported an analysis on sclerosing PEComa as a distinctive variant. PEComas showing more than 50% stromal hyalinization were designated as sclerosing PEComa. Among the total 70 cases collected from 1996 to 2006, only 13 cases fulfilled the criterion. Similar to conventional PEComas, those tumors were composed of bland-looking round to oval cells with clear or eosinophilic cytoplasm. The most distinguishable feature that differed from the conventional PEComa was excessive hyalinization of the stroma. On the basis of this report, we diagnosed our case as benign sclerosing PEComa.

In the collected cases, stromal hyalinization showed cord-like, trabecular or rarely, nested growth pattern. Eight out of 13 benign sclerosing PEComas arose in retroperitoneum, while remainders were found in the abdominal wall or pelvis.[5] Other reports described several cases in female genital tract and pararenal area.[12,13] There has been no case depicted as benign sclerosing PEComa of the lung. In addition, no reports on cytologic findings of benign sclerosing PEComa of any organs exist to our knowledge.

When considering sclerosing variant of benign PEComa in the aspiration cytology specimen from the lung, sclerosing pneumocytoma should be included in differential diagnosis. Sclerosing pneumocytoma is usually found incidentally on chest X-ray as a single round mass. Typical cytologic findings of sclerosing pneumocytoma include blood spaces surrounded by epithelial cell-like tumor cell aggregates. Tumor cells have round to oval nuclei, finely distributed chromatin, and small nucleoli. Tumor cells may aggregate around sclerotic stromal cores.[14] These findings might be confusing with those of benign sclerosing PEComa of the lung, which may show small blood vessels with surrounding neoplastic cells and hyalinizing material.

Differential diagnosis for typical benign PEComa of the lung includes primary clear cell adenocarcinoma of the lung and metastatic clear cell renal cell carcinoma. Primary clear cell adenocarcinoma of the lung shows clusters or single cells with ill-defined cell borders and pale cytoplasm. Nuclei are pleomorphic and have prominent nucleoli. Metastatic clear cell renal cell carcinoma shows round to polygonal cells which make loosely cohesive clusters. Tumor cells have abundant pale cytoplasm and round to oval nuclei. While nuclear atypia is mild in low-grade clear cell renal cell carcinoma, high-grade tumors show marked pleomorphism with occasional macronucleoli.

It is difficult to diagnose benign PEComa of the lung by fine needle aspiration only. If an asymptomatic patient has a coin-shaped mass in the lung periphery, cytologic features mentioned above are helpful for the differential diagnosis of other pulmonary tumors with clear cell features. Before diagnosing sclerosing variant of benign PEComa, the possibility of sclerosing pneumocytoma should always be considered.

Conflicts of Interest

No potential conflict of interest relevant to this article was reported.

REFERENCES

1. Liebow AA, Castleman B. Benign "clear cell tumors" of the lung.

Am J Pathol 1963; 43: 13-4.
2. Nguyen GK. Aspiration biopsy cytology of benign clear cell ("sugar") tumor of the lung. Acta Cytol 1989; 33: 511-5.
3. Policarpio-Nicolas ML, Covell J, Bregman S, Atkins K. Fine needle aspiration cytology of clear cell "sugar" tumor (PEComa) of the lung: report of a case. Diagn Cytopathol 2008; 36: 89-93.
4. Edelweiss M, Gupta N, Resetkova E. Preoperative diagnosis of clear cell "sugar" tumor of the lung by computed tomography-guided fine-needle biopsy and core-needle biopsy. Ann Diagn Pathol 2007; 11: 421-6.
5. Hornick JL, Fletcher CD. Sclerosing PEComa: clinicopathologic analysis of a distinctive variant with a predilection for the retroperitoneum. Am J Surg Pathol 2008; 32: 493-501.
6. Wang GX, Zhang D, Diao XW, Wen L. Clear cell tumor of the lung: a case report and literature review. World J Surg Oncol 2013; 11: 247.
7. Gora-Gebka M, Liberek A, Bako W, Szumera M, Korzon M, Jaskiewicz K. The "sugar" clear cell tumor of the lung-clinical presentation and diagnostic difficulties of an unusual lung tumor in youth. J Pediatr Surg 2006; 41: e27-9.
8. Santana AN, Nunes FS, Ho N, Takagaki TY. A rare cause of hemoptysis: benign sugar (clear) cell tumor of the lung. Eur J Cardiothorac Surg 2004; 25: 652-4.
9. Sen S, Senturk E, Kuman NK, Pabuscu E, Kacar F. PEComa (clear cell "sugar" tumor) of the lung: a benign tumor that presented with thrombocytosis. Ann Thorac Surg 2009; 88: 2013-5.
10. Kim WJ, Kim SR, Choe YH, *et al*. Clear cell "sugar" tumor of the lung: a well-enhanced mass with an early washout pattern on dynamic contrast-enhanced computed tomography. J Korean Med Sci 2008; 23: 1121-4.
11. Mizobuchi T, Masahiro N, Iwai N, Kohno H, Okada N, Nakada S. Clear cell tumor of the lung: surgical and immunohistochemical findings. Gen Thorac Cardiovasc Surg 2010; 58: 243-7.
12. Yamada Y, Yamamoto H, Ohishi Y, *et al*. Sclerosing variant of perivascular epithelioid cell tumor in the female genital organs. Pathol Int 2011; 61: 768-72.
13. Leão RR, Pereira BJ, Grenha V, Coelho H. Pararenal sclerosing PEComa. BMJ Case Rep 2013; 2013: bcr2013009097.
14. Wojcik EM, Sneige N, Lawrence DD, Ordóñez NG. Fine-needle aspiration cytology of sclerosing hemangioma of the lung: case report with immunohistochemical study. Diagn Cytopathol 1993; 9: 304-9.

 http://dx.doi.org/10.4132/jptm.2016.02.19

Journal of Pathology and Translational Medicine 2016; 50: 243-245
http://dx.doi.org/10.4132/jptm.2015.10.15

A Rare Case of Pulmonary Arteriovenous Hemangioma Presenting as a Peribronchial Mass

Soomin Ahn · Sejin Jung · Jong Ho Cho[1] · Tae Sung Kim[2] · Joungho Han

Departments of Pathology and Translational Genomics, [1]Thoracic Surgery, and [2]Radiology, Samsung Medical Center, Sungkyunkwan University School of Medicine, Seoul, Korea

Vascular tumors in the lung are unusual. The majority of previous reports described cases of multiple or solitary lymphangiomas or capillary and cavernous hemangiomas.[1-4] To date, there has been only one report describing arteriovenous malformation/hemangioma (AVMH) in the middle mediastinum.[5] Herein, we report an unusual case of pulmonary AVMH presenting as a peribronchial mass.

CASE REPORT

A 62-year-old man presented with a 1-month history of sputum and fatigue. He was afebrile, and routine physical examinations were within normal limits. He is an ex-smoker with a 40-pack years smoking history and denied any other medical history. Routine laboratory tests showed no abnormality. Chest computed tomography (CT) identified a 45-mm-sized mass-like lesion located centrally in the apical segment of the left upper lobe (Fig. 1A). Although the CT findings were not diagnostic, the possibility of infectious condition was favored rather than neoplastic. The patient took antibiotics for 45 days, but experienced no symptom relief, and follow-up chest CT showed no interval change of the lesion. Additional positron emission tomography was performed to characterize the lesion. A 55 × 24-mm-sized soft tissue mass showed mild heterogeneous fludeoxyglucose uptake in the lesion, suggesting malignancy (Fig. 1A). Under the clinical impression of lung cancer, left upper lobectomy was planned. Although video-assisted thoracoscopic surgery was initially attempted during the operation, it was converted to thoracotomy due to mediastinal pleural adhesion.

On the cut section of the lobectomy specimen, the dilated lumen of the lobar bronchus was packed with necrotic and mucoid material (Fig. 1B). Bronchiectasis was noted along the bronchial tree. There was no definite endobronchial lesion. Interestingly, serial cut sections of the peribronchial area revealed an ill-defined white-yellow rubbery mass-like lesion that measured approximately 2.8 cm in total extent and had pinpoint-sized spaces (Fig. 1B). Microscopically, the lesion consisted of multiple thick and prominent vessels with intervening connective tissue, and it grew between bronchial mucosa and hyaline cartilage plates (Fig. 1C). The vessels were variably sized, up to 4 mm in diameter with a thickness of up to 0.8 mm (Fig. 1D). Elastic stain visualized no definite elastic lamina, which implied the lesion to be composed of arterialized vein (Fig. 1E). These histologic findings were characteristic of AVMH. The patient was discharged without any postoperative complication. This study was approved by the Institutional Review Board of Samsung Medical Center (IRB File No. SMC 2015-07-194).

DISCUSSION

Vascular tumors of the lung are extremely rare. We presented an unusual case of pulmonary AVMH clinically mimicking lung cancer. This hemangioma presented as a peribronchial mass leading to post-obstructive bronchiectasis with mucin impaction.

The recent World Health Organization classification intro-

Corresponding Author
Joungho Han, MD
Department of Pathology and Translational Genomics, Samsung Medical Center, Sungkyunkwan University School of Medicine, 81 Irwon-ro, Gangnam-gu, Seoul 06351, Korea
Tel: +82-2-3410-2765, Fax: +82-2-3410-0025, E-mail: hanjho@skku.edu

Received: July 29, 2015 **Revised:** September 16, 2015
Accepted: October 15, 2015

pISSN 2383-7837
eISSN 2383-7845

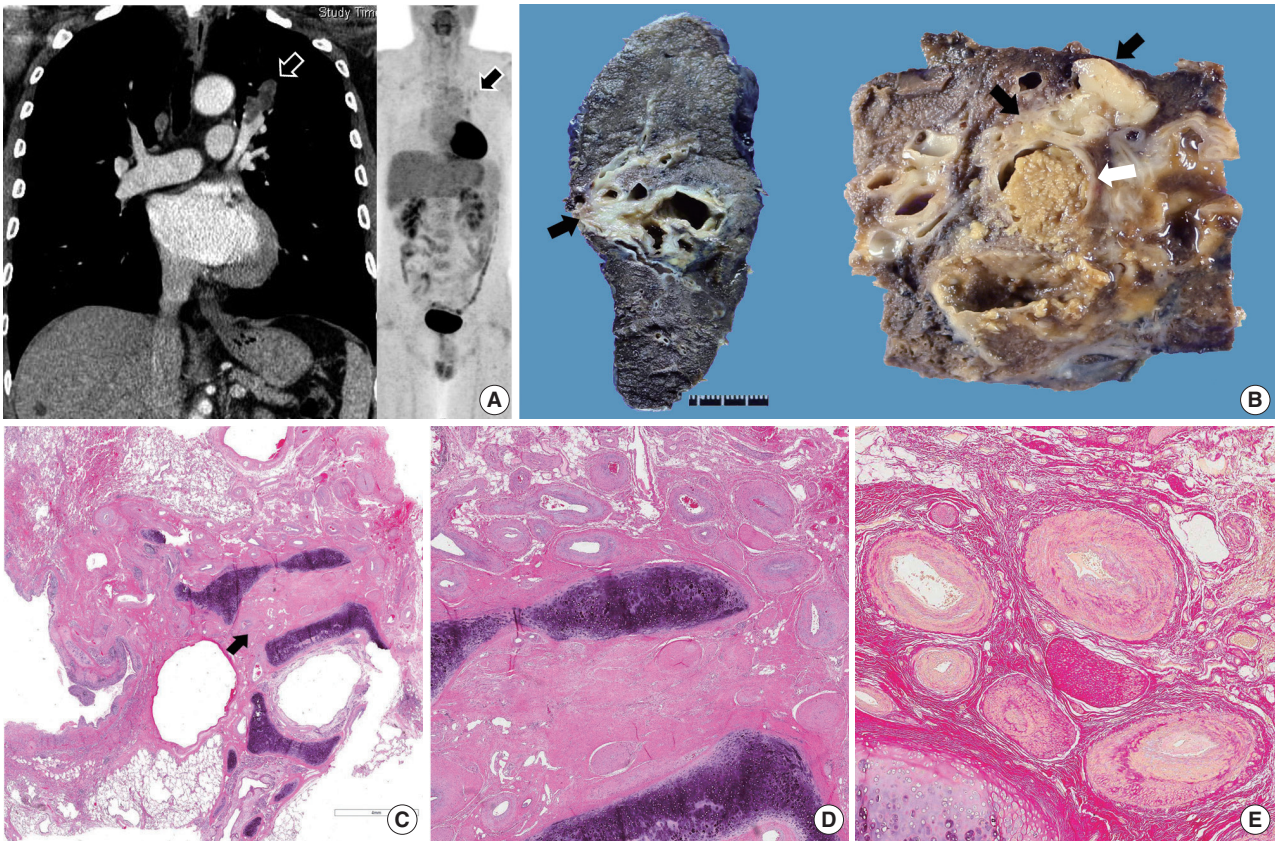

Fig. 1. Arteriovenous malformation/hemangioma (AVMH) of the lung. (A) Chest computed tomography reveals a mass-like lesion measuring 45 mm, and the lesion shows mild heterogeneous fludeoxyglucose uptake on positron emission tomography scan. (B) On the cut section of the lobectomy specimen, an ill-defined rubbery mass-like lesion (black arrows) is noted adjacent to dilated bronchial lumen with mucin impaction (white arrow). Microscopically, the lesion grows between the bronchial mucosa and cartilage plate (C) and consists of multiple thick and prominent vessels of various sizes, consistent with the diagnosis of AVMH (D). (E) Elastic stain visualizes no definite elastic lamina.

duces four entities of vascular neoplasm in the mediastinum: lymphangioma, hemangioma, epithelioid hemangioendothelioma, and angiosarcoma.[6] Of the benign entities, lymphangioma is composed of medium- or small-sized lymphatic channels filled with lymphatic fluid, and hemangioma can be cavernous or capillary. To date, there have been only a few reports of multiple or solitary lymphangiomas and hemangiomas in the lung.[1-4] The present tumor had histologic features of AVMH characterized by complex thick-walled vessels. To the best of our knowledge, this is the first report describing AVMH arising in the peribronchial soft tissue. Deep-seated AVMH usually arises in the limbs or head and neck. Mizutani *et al*.[5] previously reported arteriovenous hemangioma in the middle mediastinum.

The literature review showed that abnormal communications between pulmonary arteries and pulmonary veins have been given various names including pulmonary arteriovenous fistulae, arteriovenous aneurysm, and AVMH.[7,8] Among these, pulmonary arteriovenous fistulae refer to abnormally dilated vessels that provide a right-to-left shunt between the pulmonary artery and pulmonary vein, thereby bypassing the pulmonary capillary bed.[8] Pulmonary arteriovenous fistulae are mostly congenital, and the majority of patients have hereditary hemorrhagic telangiectasia.[8] These lesions have been described as pulmonary AVMH in several reports.[7,8] On the other hand, AVMH is different from arteriovenous fistulae in that AVMH is an acquired tumor-like condition characterized by complex thick-walled vessels with no evidence of fistula formation. In the present case, there was no evidence of obvious fistula or shunt formation on chest CT. To avoid misunderstanding and confusion, clarification of terminology for pulmonary vascular lesion is warranted.

Conflicts of Interest

No potential conflict of interest relevant to this article was reported.

http://dx.doi.org/10.4132/jptm.2015.10.15

REFERENCES

1. Fugo K, Matsuno Y, Okamoto K, *et al*. Solitary capillary hemangioma of the lung: report of 2 resected cases detected by high-resolution CT. Am J Surg Pathol 2006; 30: 750-3.
2. Song HJ, Han J, Kim K, Lee KS, Seo J. Solitary pulmonary lymphangioma in an adult: a brief case report. Korean J Pathol 2008; 42: 125-7.
3. Maeda R, Isowa N, Sumitomo S, Matsuoka K. Pulmonary cavernous hemangioma. Gen Thorac Cardiovasc Surg 2007; 55: 177-9.
4. Weissferdt A, Moran CA. Primary vascular tumors of the lungs: a review. Ann Diagn Pathol 2010; 14: 296-308.
5. Mizutani E, Morita R, Kitamura S. Arteriovenous hemangioma in the middle mediastinum: report of a case. Surg Today 2011; 41: 846-8.
6. Travis WD, Brambilla E, Burke AP, Marx A, Nicholson AG. WHO classification of tumours of the lung, pleura, thymus and heart. Lyon: IARC Press, 2015.
7. Gossage JR, Kanj G. Pulmonary arteriovenous malformations: a state of the art review. Am J Respir Crit Care Med 1998; 158: 643-61.
8. Gill SS, Roddie ME, Shovlin CL, Jackson JE. Pulmonary arteriovenous malformations and their mimics. Clin Radiol 2015; 70: 96-110.

Journal of Pathology and Translational Medicine 2016; 50: 246-249
http://dx.doi.org/10.4132/jptm.2015.10.08

■ BRIEF CASE REPORT ■

Soft Tissue Roasi-Dorfman Disease with Features of IgG4-Related Disease in a Patient with a History of Acute Myeloid Leukemia

Cheol Keun Park · Eun Kyung Kim · Ji-Ye Kim · Hayoung Woo · Mi Jang · Hyang Sook Jeong · Woo Ick Yang · Sang Kyum Kim

Department of Pathology, Yonsei University College of Medicine, Seoul, Korea

Rosai-Dorfman disease (RDD), also known as sinus histiocytosis with massive lymphadenopathy, was first described by Rosai and Dorfman in 1969.[1] A subtype of this disease shows overlapping features with IgG4-related disease.[2] Soft tissue involvement of RDD is very rare, and there has been no report of RDD associated with acute myeloid leukemia to date. Here, we describe a case of soft tissue RDD (STRDD) with features of IgG4-related disease in a patient with a history of acute myeloid leukemia.

CASE REPORT

Authorization for the use of the case information and materials was obtained from the Institutional Review Board of the Yonsei University College of Medicine (4-2015-0612).

A 12-year-old male patient presented with a recently developed, hard, non-tender mass in the right thigh. He had been diagnosed with acute leukemia 4 years earlier and has been in complete remission after receiving standard chemotherapy and bone marrow transplantation. Magnetic resonance imaging showed a 3.8 × 2.8 cm enhanced soft tissue mass in the subcutaneous layer on the posteromedial side of the right mid-thigh that was suggestive of leukemic infiltration (Fig. 1A). Grossly, the excised lesion showed an irregular, tan-white appearance with sclerotic areas (Fig. 1B). Microscopic examination revealed dense lymphoplasmacytic and histiocytic infiltration into sclerotic stroma involving the subcutaneous layer and deep dermis (Fig. 2A, B). Dilated sinuses were filled with large histiocytes containing intact lymphocytes (emperipolesis) (Fig. 2C, D), and these histiocytes were positive for CD68 and S100 protein (Fig. 3A, B). CD117- and CD34-positive atypical blastic cell infiltration was not identified in any of the submitted sections (data not shown). Up to 70 IgG4-positive plasma cells per high power field were noted, and the IgG4/IgG ratio was 25% in the most IgG4-positive area (Fig. 3C, D). No evidence of recurrence has been found in imaging workups during a 12-month follow-up.

Corresponding Author
Sang Kyum Kim, MD, PhD
Department of Pathology, Yonsei University College of Medicine, 50-1 Yonsei-ro, Seodaemun-gu, Seoul 03722, Korea
Tel: +82-2-2228-6751, Fax: +82-2-362-0860, E-mail: nicekyumi@yuhs.ac

Received: August 25, 2015 **Revised:** September 24, 2015
Accepted: October 8, 2015

DISCUSSION

RDD frequently involves extranodal sites, observed in 43% of cases. However, isolated extranodal involvement is unusual, and soft tissue involvement is even more rare.[3] Aside from a few case reports, only a few large-scale studies have assessed STRDD. In a previous study, most STRDD presented as a rapidly growing mass and was frequently found in trunk and proximal extremities.[4] Multicentricity was occasionally demonstrated in STRDD; however, associated lymphadenopathy was not common. Other studies have reported female predominance for STRDD over a wide range of ages with variable-sized masses.[5,6] A higher recurrence rate has been suggested for STRDD with multicentric lesions compared to solitary lesions.[7] The present case was a solitary lesion at diagnosis, and the patient is receiving regular follow-up.

Various degrees of sclerosis and IgG4-positive plasma cells have been noted in the RDD literature.[8] A recent study reported that about 30% of RDD cases showed stromal sclerosis and increased number of IgG4-positive plasma cells, sharing similar

pISSN 2383-7837
eISSN 2383-7845

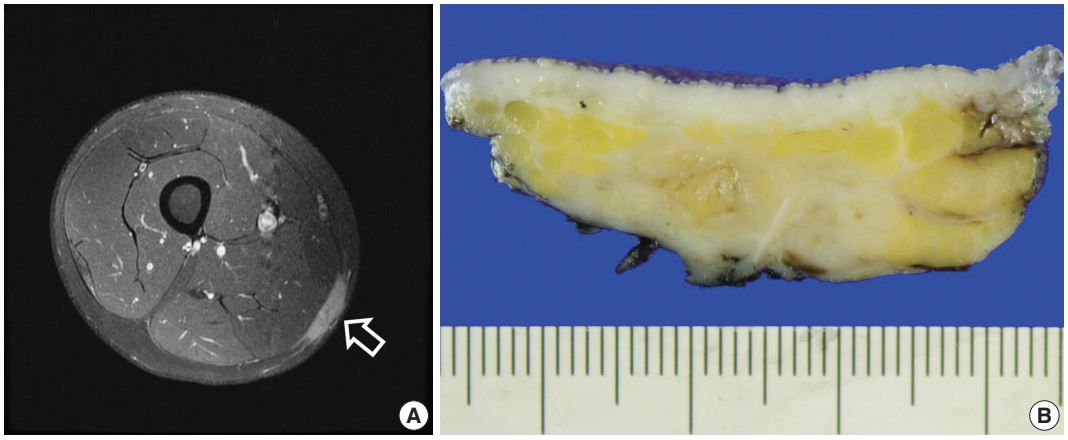

Fig. 1. Imaging and macroscopic findings of soft tissue Rosai-Dorfman disease with features of IgG4-related disease. (A) Magnetic resonance imaging shows a 3.8×2.8 cm enhanced soft tissue mass (arrow) in the subcutaneous layer on the posteromedial side of the right mid-thigh, suggestive of leukemic infiltration. (B) In the excised specimen, a 3.0-cm irregular tan-white mass-like lesion is observed in the subcutis.

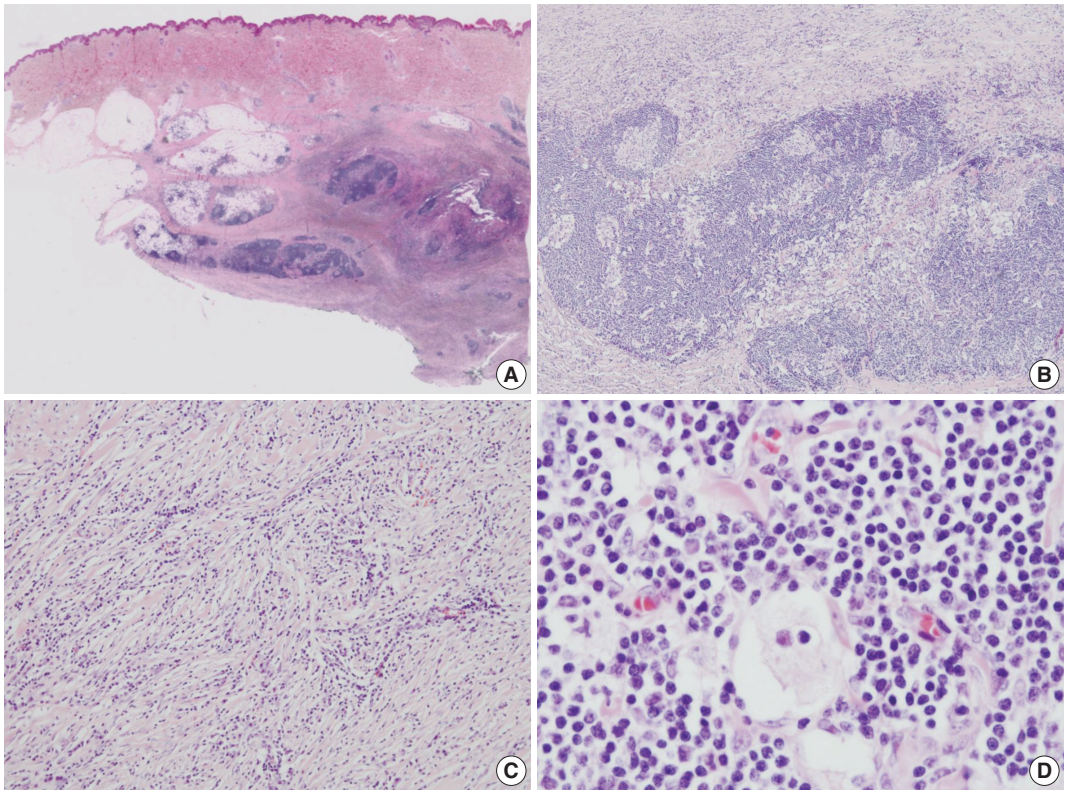

Fig. 2. Microscopic findings of soft tissue Rosai-Dorfman disease with features of IgG4-related disease. (A) In the scanning view, the infiltrative lesion involving the deep dermis and subcutaneous layer is noted. (B) In the low-power view, dense lymphoplasmacytic infiltration with scattered histiocytes is noted. (C) Diffuse lymphoplasmacytic infiltration is noted in the sclerotic stroma. (D) Dilated sinuses are filled with histiocytes containing intact lymphocytes (emperipolesis).

histologic features to IgG4-related disease.[2] These results assumed that RDD with features of IgG4-related disease could possibly be on the spectrum of IgG4-related disease or the certain phase of RDD.[2,8] However, a general consensus regarding cut-off values for IgG4-positive plasma cells and the IgG4/IgG ratio has not been established for patients with RDD.[2,9] The patient described here had dense lymphoplasmacytic infiltrations in a sclerotic stroma with increased number of IgG4-positive plasma cells.

The differential diagnoses showing similar histologic features

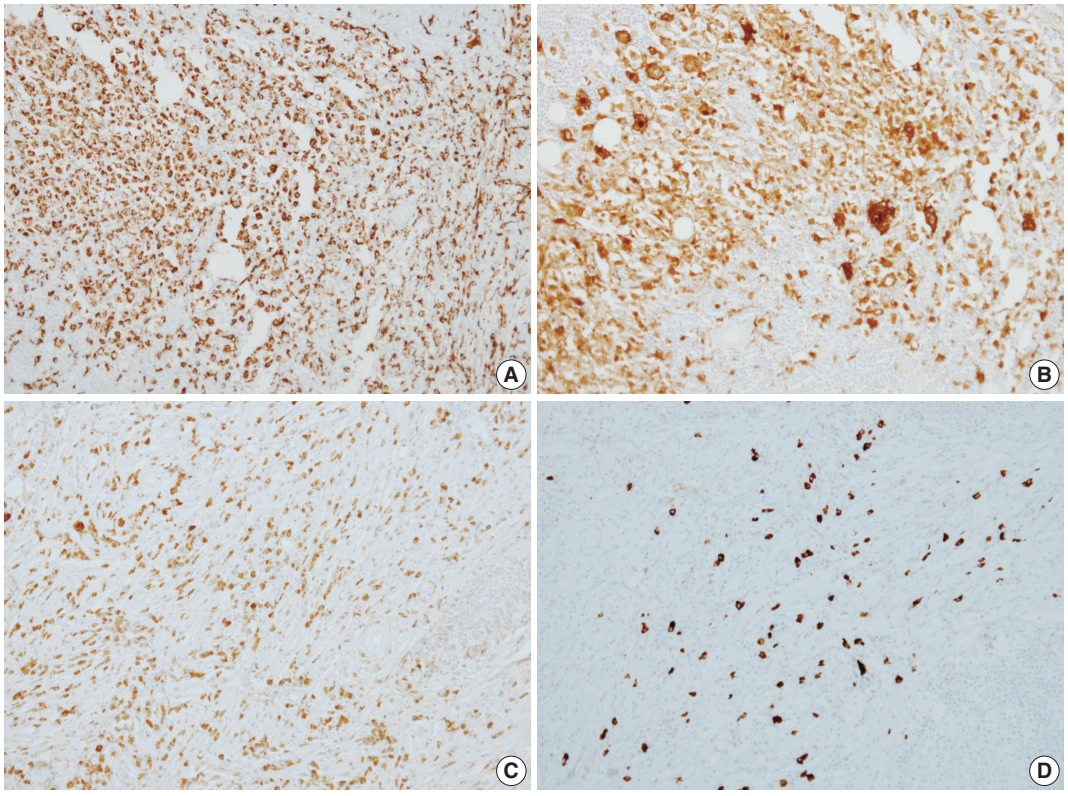

Fig. 3. Immunohistochemical staining results of soft tissue Rosai-Dorfman disease with features of IgG4-related disease. (A) Immunohistochemical staining for CD68 demonstrates histiocytes. (B) Immunohistochemical staining for S100 protein demonstrates emperipolesis. (C) Plasma cell IgG immunoreactivity. (D) Frequently identified IgG4-positive cells.

to RDD include inflammatory myofibroblastic tumor (IMT), Langerhans cell histiocytosis (LCH), and leukemic infiltration.[3] Some IMTs show compact spindle cell proliferation with fibrosis and diffuse inflammatory cell infiltration, similar histologic features to RDD. IMTs show membranous expression of anaplastic lymphoma kinase (ALK) in immunohistochemistry. We could not find ALK reactivity in this case (data not shown) and excluded the possibility of IMT.

LCH shows histiocytic aggregation in the background of mixed inflammatory cells, a similar morphologic feature to RDD. However, we could not identify the histologic characteristics of LCH exhibiting Langerhans cells with elongated nuclei and occasional nuclear grooves positive for S100 protein and CD1a.

Considering our patient's clinical history of acute myeloid leukemia, leukemic infiltration can also be considered as a differential diagnosis. Leukemic infiltration shows infiltration of atypical blastic cells in the fibrotic background, with frequent subcutaneous involvement.[10] We assessed the possibility of leukemic involvement via immunohistochemical staining for CD117 and CD34, but did not observe immunoreactive atypical blastic cells.

RDD is a rare disease entity and can have overlapping histologic features with IgG4-related disease. STRDD is even more rare and presents as a rapidly growing mass, making it difficult to be differentiated from other malignancies. In this case report, we described a case of STRDD with characteristic histologic features of IgG4-related disease in a patient with a history of acute myeloid leukemia.

Conflicts of Interest

No potential conflict of interest relevant to this article was reported.

REFERENCES

1. Rosai J, Dorfman RF. Sinus histiocytosis with massive lymphadenopathy: a newly recognized benign clinicopathological entity. Arch Pathol 1969; 87: 63-70.
2. Zhang X, Hyjek E, Vardiman J. A subset of Rosai-Dorfman disease exhibits features of IgG4-related disease. Am J Clin Pathol 2013;

 http://dx.doi.org/10.4132/jptm.2015.10.08

139: 622-32.
3. Bi Y, Huo Z, Meng Y, *et al*. Extranodal Rosai-Dorfman disease involving the right atrium in a 60-year-old male. Diagn Pathol 2014; 9: 115.
4. Al-Daraji W, Anandan A, Klassen-Fischer M, Auerbach A, Marwaha JS, Fanburg-Smith JC. Soft tissue Rosai-Dorfman disease: 29 new lesions in 18 patients, with detection of polyomavirus antigen in 3 abdominal cases. Ann Diagn Pathol 2010; 14: 309-16.
5. Montgomery EA, Meis JM, Frizzera G. Rosai-Dorfman disease of soft tissue. Am J Surg Pathol 1992; 16: 122-9.
6. Kong YY, Kong JC, Shi DR, *et al*. Cutaneous rosai-dorfman disease: a clinical and histopathologic study of 25 cases in China. Am J Surg Pathol 2007; 31: 341-50.
7. Young PM, Kransdorf MJ, Temple HT, Mousavi F, Robinson PG. Rosai-Dorfman disease presenting as multiple soft tissue masses. Skeletal Radiol 2005; 34: 665-9.
8. Kuo TT, Chen TC, Lee LY, Lu PH. IgG4-positive plasma cells in cutaneous Rosai-Dorfman disease: an additional immunohistochemical feature and possible relationship to IgG4-related sclerosing disease. J Cutan Pathol 2009; 36: 1069-73.
9. Deshpande V, Zen Y, Chan JK, *et al*. Consensus statement on the pathology of IgG4-related disease. Mod Pathol 2012; 25: 1181-92.
10. Thomas CG, Patel RM, Bergfeld WF. Cytophagic and S-100 protein immunoreactive myeloid leukemia cutis. J Cutan Pathol 2010; 37: 390-5.